STEWART, William Samuel. DYNAMICS OF HEAT REMOVAL FROM A JACKETED, AGITATED VESSEL.

The University of Oklahoma, Ph.D., 1960
Engineering, chemical

THE UNIVERSITY OF OKLAHOMA

GRADUATE COLLEGE

DYNAMICS OF HEAT REMOVAL FROM A JACKETED, AGITATED VESSEL

A DISSERTATION

SUBMITTED TO THE GRADUATE FACULTY

in partial fulfillment of the requirements for the

degree of

DOCTOR OF PHILOSOPHY

BY

WILLIAM S. STEWART

Norman, Oklahoma

1960

DYNAMICS OF HEAT REMOVAL FROM A JACKETED,

AGITATED VESSEL

APPROVED BY

C. M. Sliepcevich

Wm. L. [illegible]

Robert H. [illegible]

Gerald [illegible]

William Viavant

DISSERTATION COMMITTEE

ACKNOWLEDGMENT

The author wishes to express his sincere gratitude to the many individuals from whom assistance has been obtained in the preparation of this thesis. In particular, appreciation is extended to Dr. C. M. Sliepcevich, Professor of Chemical Engineering and Associate Dean of the College of Engineering at the University of Oklahoma, for the inspiration, advice, and invaluable assistance rendered during his direction of the project. Also, Dr. R. J. Fanning of the Continental Oil Company is to be thanked for suggesting the project.

The advice and suggestions of Professor Thomas Puckett, Professor Gerald Tuma, and Mr. Dale Young of the Electrical Engineering Department of the University of Oklahoma, in certain of the theoretical phases of the project, are sincerely appreciated. Thanks are also extended to the various members of the Doctoral Advisory Committee for their interest in the project.

Mr. Paul Gallier has assisted with the IBM 650 computations. Mr. Frank Magannis has given numerous suggestions on the design of certain parts of the equipment. Mr. Bob Howard has assisted greatly in the construction of the apparatus.

Finally, thanks are to be extended to the Phillips Petroleum Company for their financial support in the form of a fellowship and to the National Science Foundation whose Research Grant made this work possible.

TABLE OF CONTENTS

LIST OF TABLES

Table		Page

LIST OF ILLUSTRATIONS

Figure | Page

DYNAMICS OF HEAT REMOVAL FROM A JACKETED, AGITATED VESSEL

CHAPTER I

INTRODUCTION

In the past, chemical engineering process designs were carried out on the basis of steady state operating conditions, and the unsteady state conditions received little or no attention in the design calculations. Even today the majority of all chemical engineering process designs are carried out on a steady state basis. After the design and construction of a process, it was customary to install standardized controllers on the pieces of process equipment in the hope that by originally over designing the equipment and with a wide range of flexibility in the controllers, a satisfactory control of the process could be attained.

In reality, however, chemical processes do not operate under conditions of steady state. Instead, chemical processes operate under fluctuating conditions about some steady state value and hopefully within certain allowable limits of variations. The economic success of a process depends upon the control and maintenance of the operation within an allowable range of variation about some desired steady state value. The adequacy of the control attained depends much more on the dynamic or unsteady state behavior of a process than on the static or steady state behavior. Therefore, a knowledge of the dynamic behavior of a process is of the utmost importance.

The importance of applying dynamic analysis or systems engineering to process design can hardly be over-emphasized. All too frequently the steady state design of process equipment results in: (a) the over design of equipment, (b) a degraded product specification or a lower product yield than is theoretically possible, and (c) a poor selection of control variables, control instruments, and sensing element locations. These cases are perhaps best illustrated by examples of instances which have actually occurred in practice and which have been reported in the literature. The number of such examples that have been reported in the literature is quite small. However, the number of instances that have actually occurred in practice and that have not been reported in the literature must undoubtedly be much larger.

One example was discussed by Aikman (45). The piece of equipment involved was a spray drier. The drier--as a drier--was well designed but as a control system it was entirely unsatisfactory because poor temperature control spoiled the product. A frequency response study was made on the system. The results of the frequency response study showed that the poor temperature control was caused by excessive hold-up time, and a relocation of the control valves solved the problem. The study also revealed an over design in the size of certain auxiliary equipment connected to the spray drier.

A second example was given by Boyd (45). This example was concerned with the control of a fractionating column. The column was one that had been in existence and in operation for quite some time, but was giving poor performance because of inadequate control. It was felt that the column was well designed and should have been very stable. A dynamic analysis of the problem indicated that the poor control of the tower was due to improper controllers. The old controllers were replaced by the proper controllers, and the tower was stabilized. The result was an increase in tray efficiency of eight percent.

A third and very excellent example was given by Woods (45). This example was a mixing tank with pH control. The mixing tank was a piece of installed equipment located in a new plant that was being placed on-stream. The tank was considered to be well designed but was completely uncontrollable. A dynamic analysis of the system showed that dead time was responsible for the instability; however, due to other factors, a mere relocation of control valves and sensing elements would not solve the problem. The solution to the problem was to replace the old tank with a larger tank. This is an excellent example of how systems design actually affected the sizing of the equipment itself.

The above examples all illustrate how economic benefits can be reaped by applying systems engineering to process design. In Aikman's case an economic benefit could have been realized by the elimination of a certain amount of down time and by the purchase of smaller, but entirely suitable, auxiliary equipment. How long the fractionating column in Boyd's example had been in operation was not stated, but whatever the time was, it represented a period in which an inferior product had to be accepted. Also, an increase in efficiency of eight percent could represent a fairly large sum of money. Boyd's case is also clearly an example of how systems engineering can improve processes already in existence. However, it must be remembered that once a plant is built, the really big opportunity for saving money is forever lost. In the example discussed by Wood, aside from any increase in down time which may have resulted, it was necessary to remove and replace an unused piece of installed equipment which quite obviously represents wasted money.

The application of frequency response techniques to the control of processes is well known to mechanical, electrical, and instrumentation engineers, and the general theory of frequency response analysis has, of course, long been developed. A large amount of work has been done in systems engineering on problems related to aircraft, guided missiles, and weapons fire control systems. Only since 1953 has any interest been shown in applying systems engineering to chemical processes, as evidenced by a sudden increase in published papers and expanded research activity by industrial organizations. Because there was very little research being performed in the laboratory, the control characteristics of chemical processes were first encountered either in the pilot plant or in the field.

The first step in a systems engineering problem is, of course, a theoretical analysis of the process in question from the standpoint of its unsteady state behavior. A very important part of dynamic analysis is transfer function theory. Transfer function theory implies a linear system by definition. Therefore, if transfer function theory is to be used in the analysis, certain assumptions (aside from any assumption made for the sake of simplicity) must be made in order to linearize the equations describing the process in question. The validity of these assumptions will, of course, be open to question. <u>The experimental data will</u>

then either confirm or refute the assumptions.

The experimental technique used perhaps most often in dynamic studies involves the application of frequency response. In the collection of the frequency response data, the input sinusoid can be generated by a mechanical unit constructed from a linear diaphragm control valve. The fluctuation with time of the output variable can be recorded continuously by a suitable recorder. From the frequency response data, amplitude and phase angle information is obtained and the familiar Bode diagrams are constructed. From the Bode diagram, the system time constants and hence the transfer function are obtained. Both theoretical and experimental transfer functions should, of course, be compared.

This study was motivated by the fact that processes designed on the basis of steady state operations may sometimes prove inadequate for automatic control. The present investigation is a continuation of the work of Fanning (24) and involves a study of the dynamic heat transfer characteristics of a continuous, agitated vessel. A considerable number of chemical reactions are exothermic; hence the dynamics of heat removal is of interest. Many reactors are of the agitated tank type, equipped with a jacket and utilizing the inner tank wall as a heat exchange surface. Alternately agitated tank reactors are equipped with internal cooling coils or tubes and baffled to provide effective heat transfer. The present equipment is provided with a removable jacket. The heat of vaporization of a boiling liquid located in the jacket can be utilized to remove heat.

The purpose of this investigation is to study the dynamic heat transfer characteristic of an agitated vessel from which the heat is removed by utilizing the heat of vaporization of a volatile coolant.

CHAPTER II

STATEMENT OF THE PROBLEM AND REVIEW OF PREVIOUS WORK

Objectives of Process Dynamic Studies

The term "systems engineering" denotes the application of process dynamics to the design of process equipment. The expression "process dynamics" refers to the characteristics displayed by a piece of equipment during conditions which change with time. Therefore, the object in any process dynamic study is to investigate the manner in which a piece of equipment responds with time. Hence, the study involves obtaining relationships between two or more pertinent process variables and time. These relationships may be obtained either theoretically or experimentally.

In the purely theoretical approach, these relationships usually take the form of a set of non linear, ordinary or partial, differential equations. These equations are then simplified to the point where they can be solved analytically, or the equations are simulated and solved on an analog or a digital computer.

In the experimental approach, it is necessary to impose a change of some kind upon the piece of process equipment and to observe its response with time. One means of doing this is to vary sinusodially one of the process variables and to note the effect upon a related variable.

This method is known as frequency response.

Frequency response techniques have been used as far back as the middle of the last century in studies of system properties and process behavior. Angstrom (14) in 1861 used periodic forcing to measure the thermal conductivity of a metal rod. The use of frequency response techniques in process dynamics is, of course, as old as the field of servomechanisms. The subject of frequency response is adequately covered by Brown and Campbell (11), Thaler and Brown (53), and numerous other text books on servomechanisms.

If experimental frequency response techniques are used, the desired relationships are obtained in the form of transfer functions which can be used to relate the input forcing variable, the output forced variable, and time.

Previous Investigations

The subject of process dynamics has been characterized in recent years by a rapid expansion of interest both on the academic level and on the part of the chemical and petroleum industry. The number of articles on chemical process dynamics appearing in the literature are becoming rather numerous in recent years. However, the extent of the increased activity in this field has not yet become fully evident in the chemical engineering literature because of the inevitable time lag of several years between the time a problem is initiated and the time the results appear in print.

From the standpoint of the advancement of process control theory, the most important work has been done outside the field of chemical engineering. However, from the viewpoint of application, a number of very interesting papers have appeared on chemical process dynamics. Perhaps the most important of these and the ones which will have the greatest effect upon future progress has been on the subject of computer control of chemical processes. Although most of this effort has come from companies engaged in the manufacture of analog and digital computers, notable effort has been shown by some of the chemical and petroleum companies. The reader is referred to the articles by Lewis (35), Woods (60), and Tolin and Fleugel (55).

The major deterrent to a rapid growth of the chemical process control field lies in a critical lack of personnel with a background in both chemistry or chemical engineering and the servomechanism, mathematical, and computer techniques necessary for advanced process control studies. While this shortage is acute at present, it shows signs of easing in the not-too-distant future. Some companies have set up company sponsored training programs, either internally or in cooperation with a university (19). The American Institute of Chemical Engineers has recently issued a special publication (59) presenting several proposed outlines of courses and associated laboratory work for such courses at both the undergraduate and the graduate level. Finally, the Instrument Society of America has urged high schools to present basic courses in instrumentation and control (5).

A second deterrent to progress in this field has been due to the distinct shortage of suitable textbooks. This situation has been improved somewhat by the recent appearance of two excellent new textbooks (12,20).

Although on any particular phase of process dynamics the literature is not too extensive, the literature on the field as a whole has become quite extensive. It is not the purpose here to review the literature of the entire field of process dynamics, but rather only that part of it concerned with the dynamics of an agitated vessel. Most of the dynamic studies of agitated vessels have been done in connection with chemical reactions. For an extensive review of the entire field, the reader is referred to the bibliographies given by Higgins (29), Stout (52), Roberts and others (46), and Industrial and Engineering Chemistry (15,44). For an introduction to the theory of process control, the reader is referred to Truxal (56), Savant (49), or any other standard text on servomechanisms.

Although most of the work on reactor dynamics is relatively recent, one might date its beginning as far back as 1908. At that time the chemist Hirnick (30) demonstrated mathematically the possibility of damped concentration oscillations in an autocatalytic reaction. In 1910, Lotka (36, 37) examined sustained oscillations in such systems. More work in connection with sustained oscillation and with autoregulated reactions has been done in the intervening years, but it will not be quoted here as it is not directly concerned with reactor dynamics. The two references mentioned above are quoted only because they probably served as a stimulant for some very important work of recent times.

The transient response of chemical reactors has received some attention in the past. The unsteady state equations governing the response of chemical reactors have been solved under various limiting conditions by Ham and Coe (27), MacMullin and Weber (28), Kandiner (33), Johnson and Edwards (32), Mason and Piret (40, 41), and Acton and Lapidus (1). The papers by Mason and Piret are particularly good. All of these works are of a theoretical nature.

In 1955, Bilous and Amundson (8) published the first of a number of articles (8, 9, 10, 2, 3) on reactor dynamics by these authors or their co-workers. These articles are all noteworthy. Our present knowledge of reactor dynamics has been considerably enhanced by these papers.

Bilous and Amundson (8) and later Ehrenfeld (22) treated mathematically a well agitated continuous reactor from the standpoint of stability of the steady state and presented methods of developing criteria for the quantitative determination of stability or instability. With somewhat the same type of treatment, Cannon and Denbigh (13) describe two distinct forms of thermal instability which can arise in gas-solid reactions. Also, the character of the steady state of an exothermic reaction has been described by von Heerden (57).

In a later article, Bilous and Amundson (9) treat the cases of stability of a quasi-isothermal reactor and a reactor with a recycle stream. Aris and Amundson (2) have examined the conditions for stability of an agitated continuous reactor operating under proportional control alone. Some methods of non linear mechanics are applied and phase plane plots of the complete non linear reactor equations are constructed. This paper is a preview of a later paper published by Aris and Amundson (3).

The use of frequency response analysis to develop the theory of control of continuous-flow reactors is discussed by Bilous, Block, and Piret (10). In this paper, cascades of continuous-flow reactors are also discussed, and how automatic control requirements can influence proper reactor design is illustrated. Ellingsen and Ceaglske (23) have presented a paper on the applications of the root-locus method in the design of a control system for a theoretical stirred-tank reactor. The modes of control studied were proportional, proportional-integral, and proportional-integral-rate. Aris and Amundson (4) applied statistical techniques to a continuous-flow, stirred tank reactor.

The stability of a fixed-bed catalytic reactor has been investigated by Hoelscher (31) under various conditions. Oncutt and Lamb (42) considered the case of stability of a fixed-bed catalytic reactor system with feed-effluent heat exchange. Shinskey (50) gave a paper on the temperature control of gas phase reactions.

Some very interesting articles have been presented concerning the on-stream control of a chemical reactor by a high speed computer by Eckman and Lefkowitz (21), Roberts and Laspe (47), Tierney and others (54), and Tolin and Fleugel (55). Some other interesting cases of applications of computers to reactor dynamic problems are given by Beutler and Roberts (7) and Bathe, Franks, and James (6).

A novel method of obtaining high accuracy in a process control loop by using a minor feedback loop around the controller to prevent dead-time oscillations has been proposed by Smith (51). He presents an example where this method is applied to a catalytic cracker.

Fanning (24, 25) obtained frequency response data on the heat transfer characteristic of a stirred-pot reactor and compared the theoretically derived transfer functions with those obtained experimentally.

The problem of mixing in an agitated vessel has been studied by Marr and Johnson (39). Mixing in a vertical tube reactor has been investigated by Head (28). A transfer function relating input to output concentration was obtained. The resulting transfer function was that of a first order system exhibiting time delay.

A number of papers have been presented on the dynamic measurements that have been made on packed and fluidized beds with no chemical reaction occurring, primarily to study the nature of fluid mixing in chemical reactors. The reader is referred to the works of Danckwerts (16), Danckwerts, Jenkins, and Place (17), Deisler and Wilhelm (18), Kramers and Alberda (34), Prausnitz and Wilhelm (43), and Romano (48).

The work of the past has placed considerable stress on a theoretical analysis followed by a solution on an analog or a digital computer. Very little experimental work has been done.

Specific Objectives of the Present Investigation

The continuous, agitated vessel is widely used in the chemical industry for mixing and for carrying out chemical reactions. The majority of reactions carried out in these vessels are exothermic, and the removal of heat is therefore of importance. Also, the reaction temperature must be controlled if a quality product is to be produced.

There are a number of different methods now in use for the continuous removal of heat from a stirred-pot reactor. The method studied here is the utilization of the heat of vaporization of a volatile coolant located either within internal cooling coils, within an external jacket, or both. In this case, temperature control can be achieved either by varying an input fluid flow rate or by controlling the back pressure on the volatile coolant and therefore the temperature. The latter is perhaps the most important.

The present investigation was directed towards the determination of the dynamics of the two temperature control methods just described. Other methods have been investigated by Fanning (24). It was planned to make both experimental and theoretical studies. Only the open loop system was considered either experimentally or theoretically, as information can be obtained on the closed loop once the dynamics of the individual components are known.

Finally, it was hoped that this study would contribute some measure of knowledge on the dynamic behavior of agitated vessels.

CHAPTER III

DESCRIPTION OF THE EXPERIMENTAL APPARATUS

The experimental apparatus consisted primarily of the following: (a) a test section (a continuous-flow, agitated autoclave reactor), (b) a preheater and recycle system, (c) a refrigeration unit, (d) various measuring, controlling, and recording instruments, and (e) a valve equipped with a sine wave generating device. A flow sheet for the experimental apparatus is shown in Figure 6.

Test Section

The test section consisted of a continuous-flow, agitated autoclave reactor, equipped with baffles. The reactor had a one liter capacity. Heat was removed from the reactor by means of an external jacket. The heat transfer area and other physical parameters of the test section are presented in Table 21, Appendix C.

The fluid was introduced into the bottom of the reactor. The fluid flowed out of the system through an overflow tube located in the top of the reactor.

The agitator was driven by a V-belt and pulley arrangement connected to a 1/4-horsepower electric motor. The motor speed was 1725 revolutions per minute. The agitator speed could be varied by using different sized pulleys.

The test section was equipped with a flexible copper-constantan thermocouple for measuring temperatures at various points within the reactor.

A photograph of the test section is shown in Figures 1 and 2.

Preheater and Recycle System

This system consists of a preheating vessel, a feed pump, a recycle accumulator, and a recycle pump.

Preheater. The preheating vessel was constructed from a fourteen-inch section of ten-inch pipe. The bottom of the vessel was made of 1/4-inch sheet iron and was welded in place. The top of the vessel was made of wood and could be removed. The vessel was fitted with a one-inch over-flow line located two inches from the top of the vessel. Hot liquid was withdrawn from an opening in the bottom of the vessel. The vessel was insulated by two inches of ten-inch magnesia pipe insulation.

The feed to the preheater was water from the recycle accumulator. Cold tap water was used for make-up. The liquid in the preheater was heated by live steam introduced into the bottom of the vessel. The steam flow rate was controlled by a 1/2-inch control valve. The valve position was regulated by a temperature recorder and controller. The preheater temperature was measured in the hot water exit line. In addition to heating the fluid, the preheater also served as a feed tank.

Recycle Accumulator. The recycle accumulator and the preheater are identical in construction with the exception that the recycle accumulator was not provided with a means for heating the liquid.

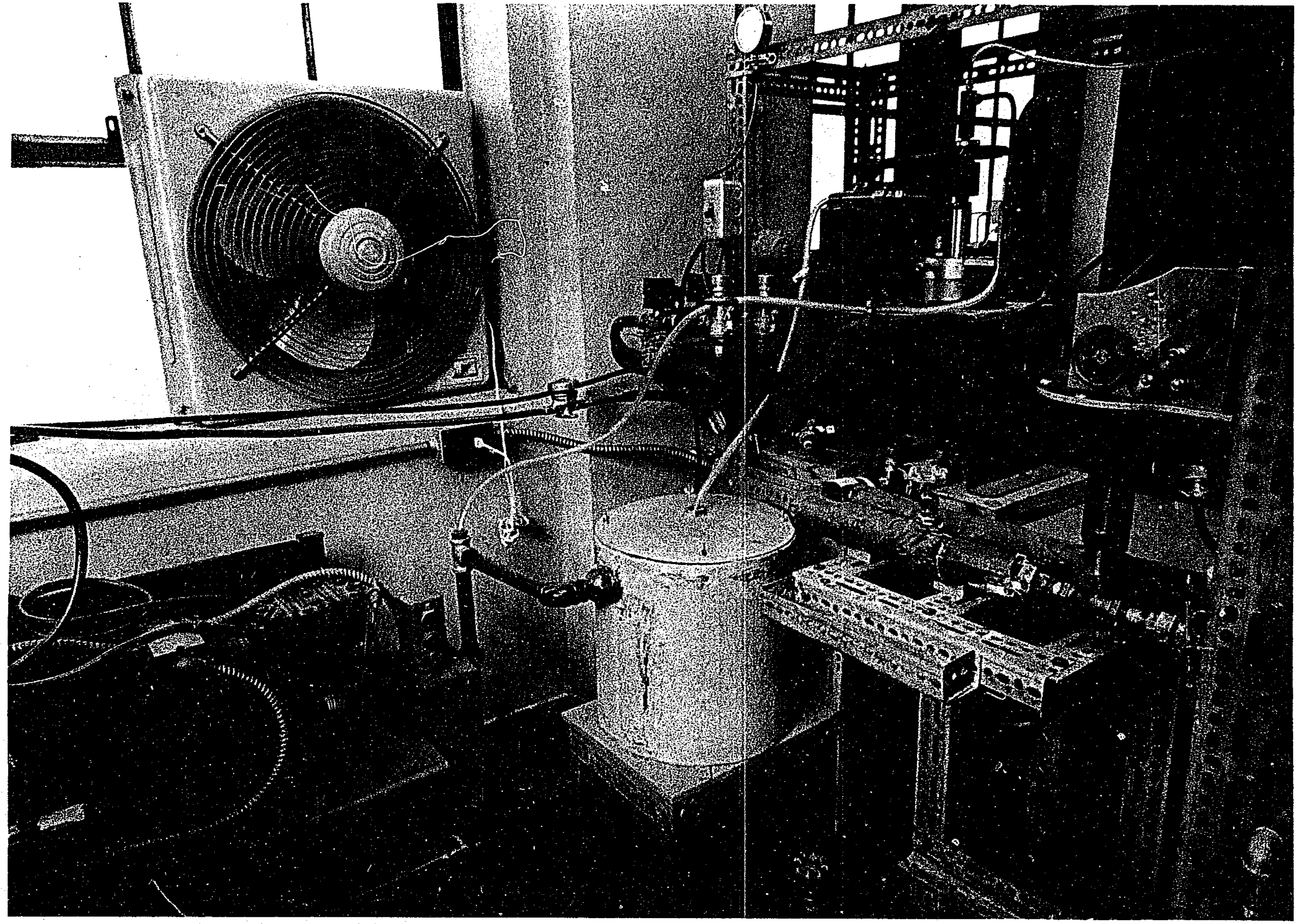

Figure 1. View of Test Section and Refrigeration Unit

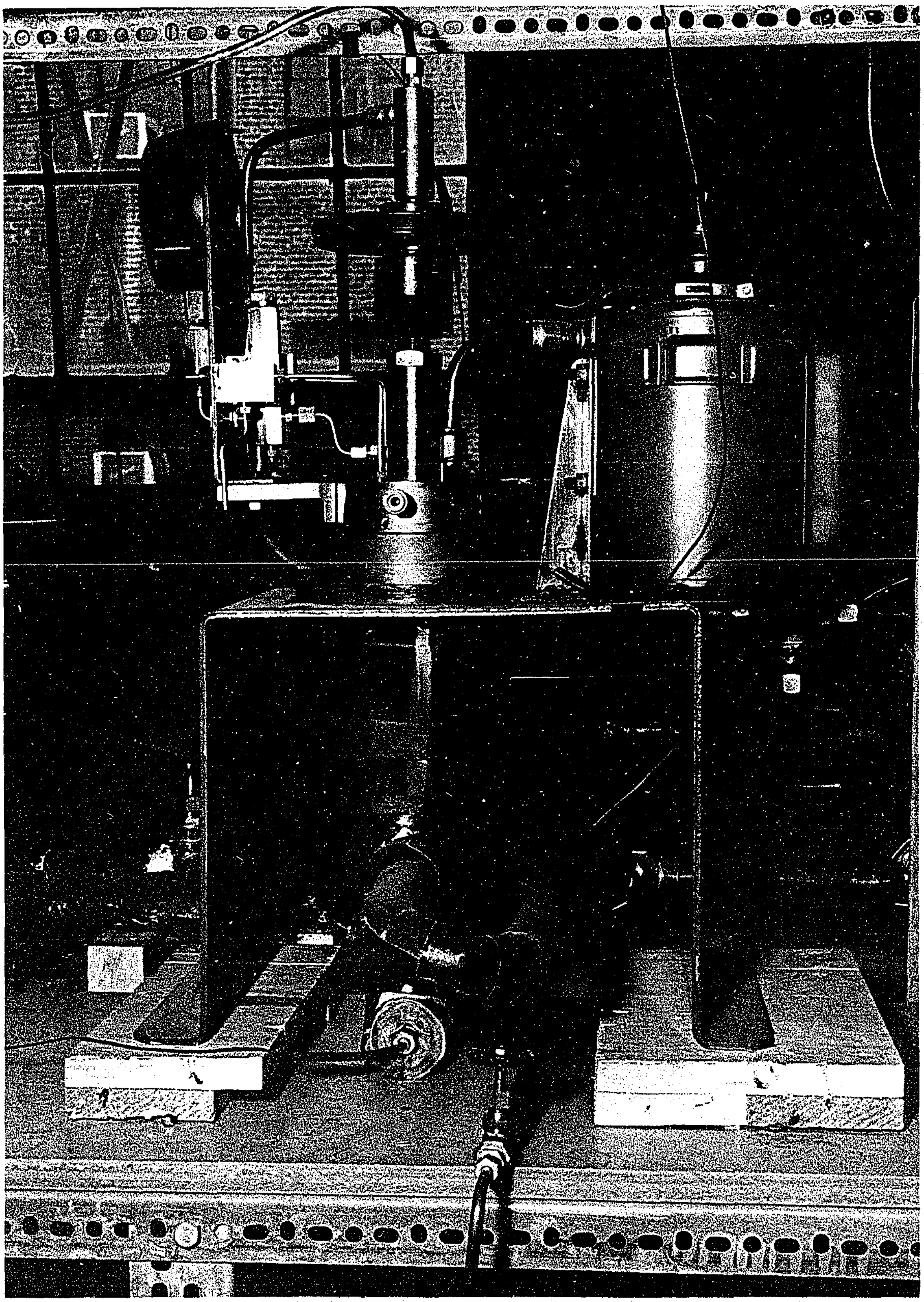

Figure 2. Rear View of Test Section

Feed Pump. The feed pump was a 1/2-horsepower positive displacement pump delivering a 25-foot head with a maximum capacity of three gallons per minute.

Recycle Pump. The recycle pump was a 1/4-horsepower centrifugal pump. The head and capacity of this pump were not known; however, the pump was found to be satisfactory for the purpose.

Refrigeration Cycle

The refrigeration cycle consisted of a Copeland refrigeration unit complete with compressor, condenser, accumulator, and throttle valve. The jacket of the reactor served as the evaporator portion of the refrigeration cycle. The condenser was water cooled and the refrigerant was Freon-12. The compressor was driven by a 1 1/2-horsepower motor. A view of the refrigeration cycle is shown in Figure 1.

Measuring Instruments, Controllers, and Recording Devices

Flow Rate. The only flow rate metered was that of the reactor inlet water stream. When the flow rate was recorded, it was measured by a Model 10 C 1505 Fischer and Porter turbine flowmeter. The range of flow of this meter was 0.13 to 1.1 gallons per minute. The potential generated by the flowmeter was indicated by a Model FR-111 Waugh pulse rate converter, and was recorded on one channel of a two-channel Sanborn recorder. A view of the turbine flowmeter is also shown in Figure 1.

For those runs in which it was not necessary to record the flow rate, a Fischer and Porter flowrator (rotameter) was used to indicate the flow. The maximum capacity of this meter was about one gallon per minute. The rotameter was used on runs, regardless of whether the flow rate was to be recorded, to establish the initial steady state operating conditions.

Temperatures. A total of four different temperatures were measured: (a) preheater temperature, (b) inlet reactor fluid temperature, (c) temperature inside reactor, and (d) reactor coolant temperature. All temperatures were measured with copper-constantan thermocouples. The preheater temperature was indicated and controlled by a Minneapolis-Honeywell temperature recorder and controller. The reactor inlet fluid temperature and the reactor coolant temperature were indicated by a Model 156X15P-X-C Brown temperature indicator. The reactor temperature was recorded on one channel of a Sanborn recorder. A Model 1 PH 560-51-T46-T66X-T82 Bristol Dynamaster recorder was used as an amplifier for the Sanborn recorder.

Pressure. The pressure on the coolant in the reactor was the only pressure measured. This pressure was indicated with a pressure gage. The pressure was regulated by a back pressure regulator. An arrangement of two solenoid valves and two back pressure regulators was used for varying the pressure. This arrangement is shown in Figure 1.

Controller. The only piece of equipment being controlled was the preheater. The preheater temperature was controlled by a Model 152P14P-93-18 Minneapolis-Honeywell temperature recorder and controller. The modes of control were proportional band and reset.

Recording Device. To record continuously the forcing variable and the forced variable, a Model 60-1300 Sanborn Twin-Viso recorder was used.

The recorder was equipped with one preamplifier and two amplifiers.

A view of the panel board on which the Minneapolis-Honeywell temperature recorder and controller, the Brown temperature indicator, the Bristol recorder, and the Waugh pulse rate convertor were mounted is depicted in Figure 3. The Sanborn recorder is also shown in Figure 3.

Sine Wave Generator

The sine wave generator consisted in part of a 1/2-inch Research Control Valve. The valve has a stainless steel stem and a bronze valve body tested to 150 psig. The valve was linear throughout the lower 80 percent of the stem travel. The top half of the diaphragm body together with the diaphragm and the spring were removed. The lower half of the diaphragm body was used to support the device which imparted the harmonic-translational motion to the valve stem. This device consisted of a driver, a Scotch yoke, and a connecting gear train. The driver was a Model SG-10 Merkle-Korff induction motor. Various sets of gears were available. The range of frequency that could be obtained varied from 0.6 to 60 radians per minute (two decades). Figures 4 and 5 are front and rear views of the sine wave generator.

Flow Sheet

Two different systems were studied. Both systems are depicted in Figure 6.

System No. 1. In the first system studied the input forcing variable was the reactor inlet fluid flow rate and the output forced variable was the reactor fluid temperature. In the experimental apparatus there were two different streams: (a) a water stream, and (b) a coolant stream.

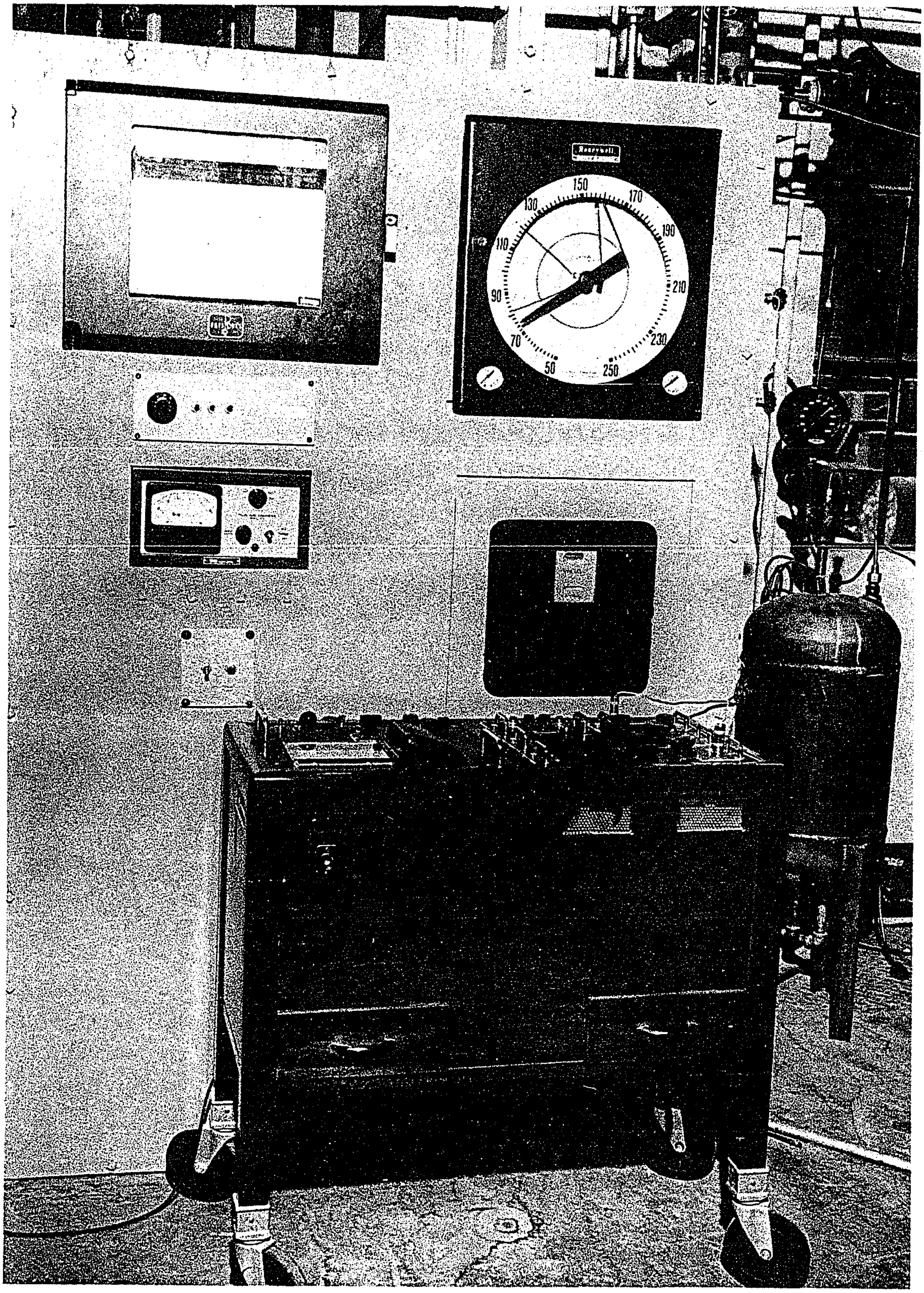

Figure 3. View of Panel Board and Sanborn Recorder

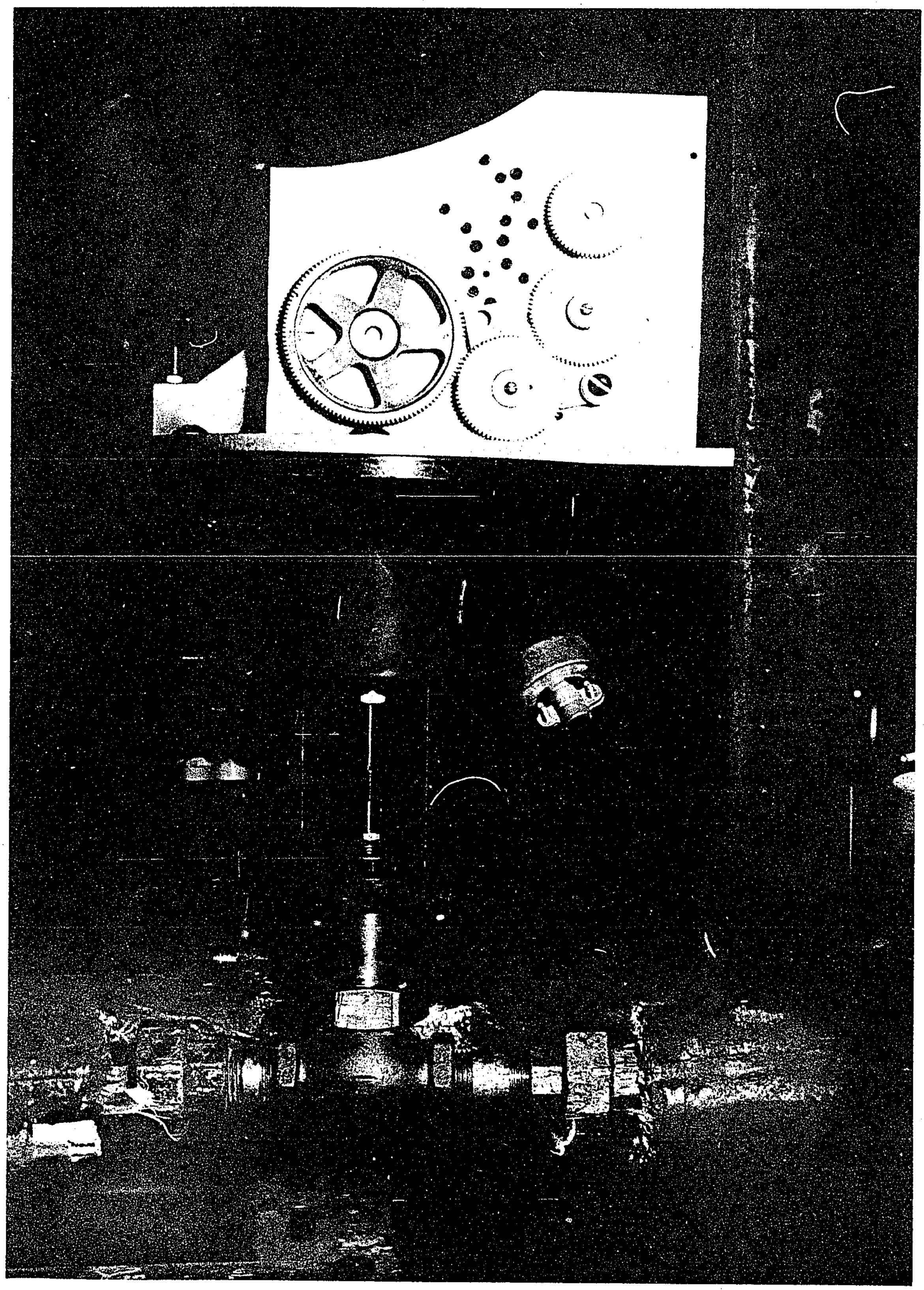

Figure 4. Front View of Sine Wave Generator

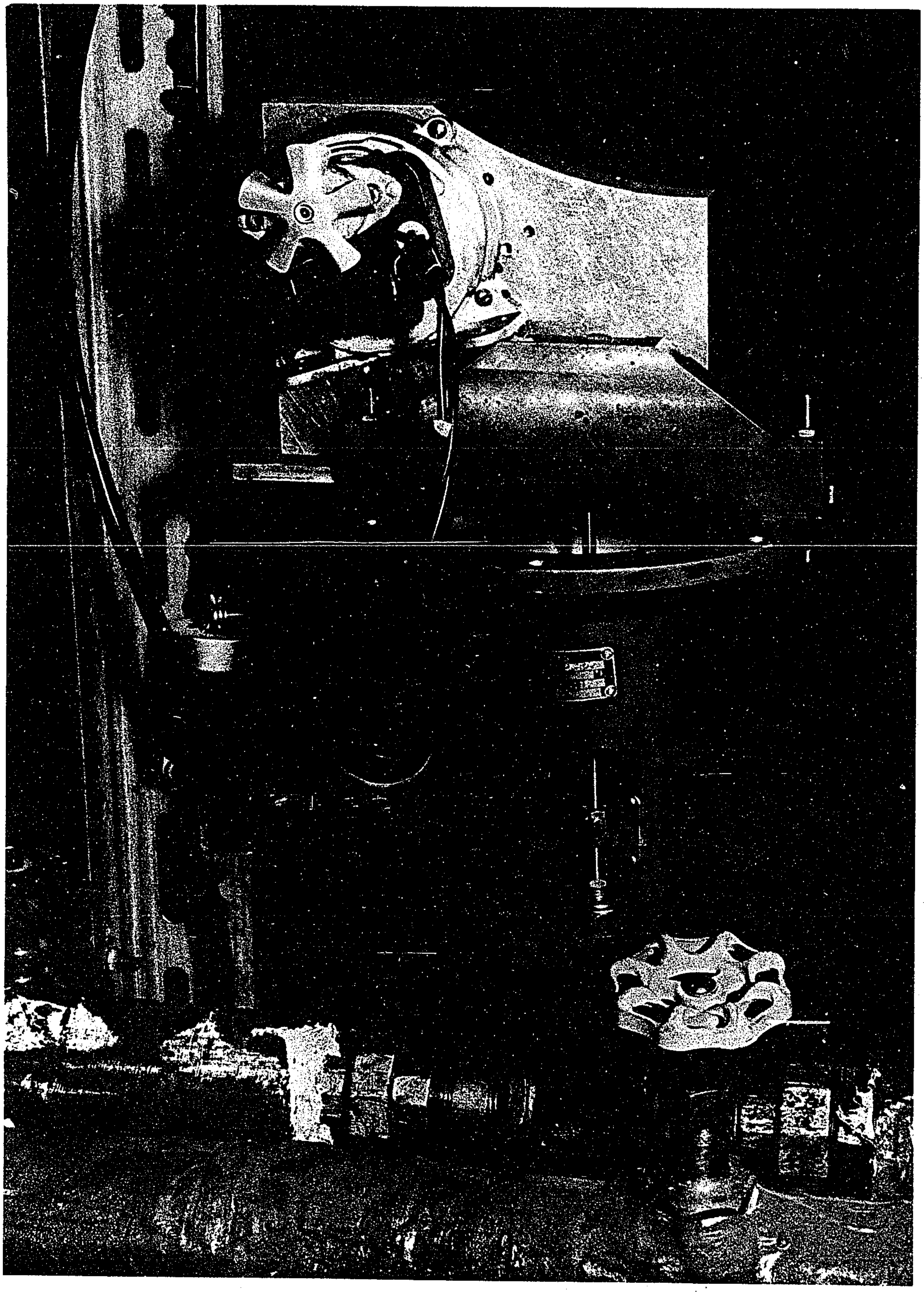

Figure 5. Rear View of Sine Wave Generator

The water was preheated in a feed tank and was pumped from the feed tank through the sine wave generator which imparted a sine wave to the flow rate. From the sine wave generator the hot water passed through the turbine flowmeter and into the reactor where heat was exchanged. From the reactor the cooled water flowed into the recycle accumulator and was then pumped back to the preheater.

The coolant (Freon-12) flow pattern was the same as for any simple refrigeration cycle. The jacket of the reactor served as the evaporator part of the refrigeration cycle. The coolant was boiled at a constant temperature. This temperature was maintained by a back pressure regulator in the vapor line.

The recorded variables for system No. 1 were the reactor inlet fluid flow rate and the reactor fluid temperature.

System No. 2. In system No. 2 the input forcing variable was the back pressure on the evaporator and the output forced variable was the reactor fluid temperature.

The water stream cycle was the same as in system No. 1 except that a constant flow rate was maintained and the flow rate was indicated by a rotameter.

The pressure of the coolant vapor was varied by means of an arrangement of solenoid valves and back pressure regulators. The arrangement is shown in Figure 6.

The recorded variables were the pressure on the volatile coolant and the reactor fluid temperature.

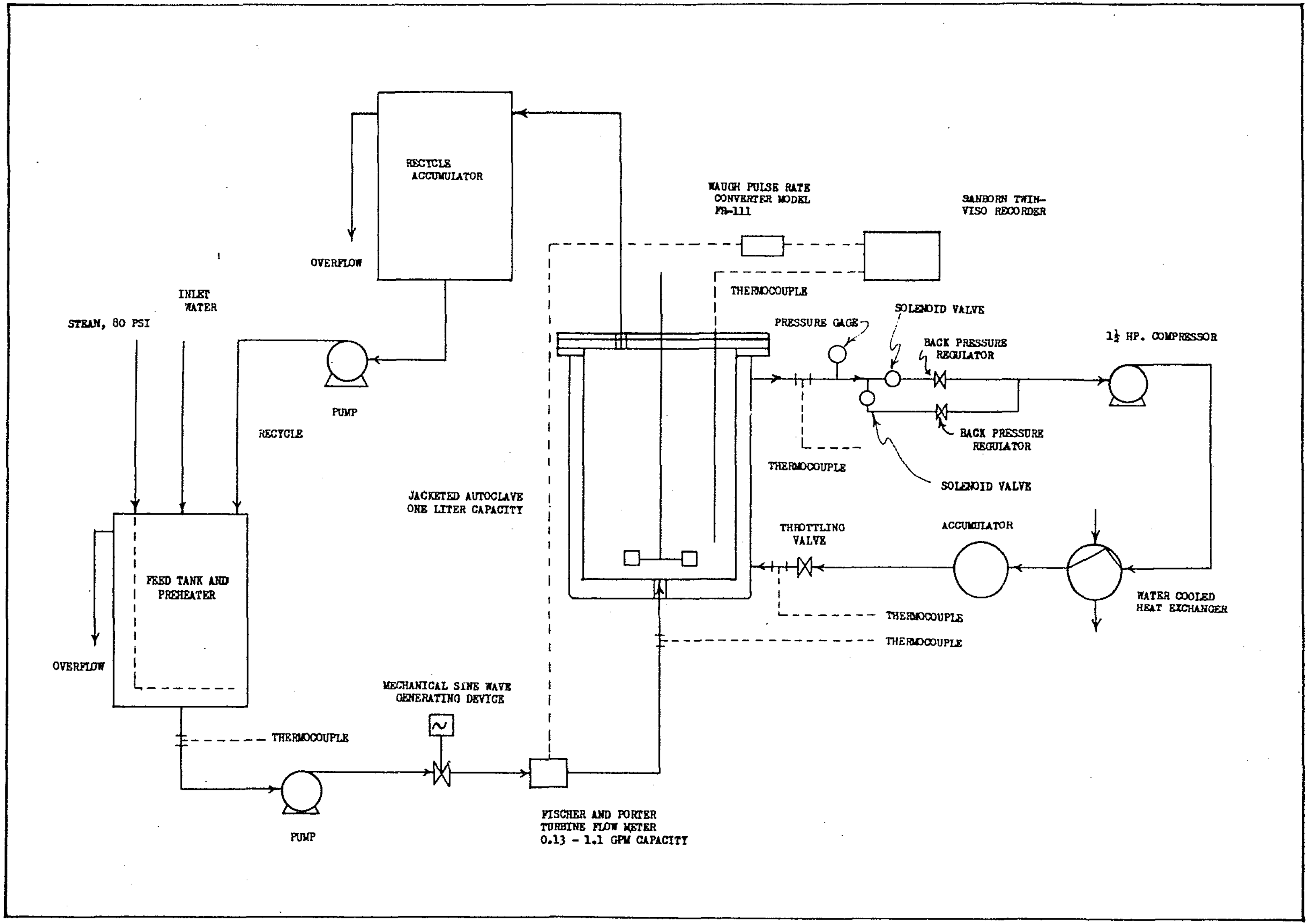

FIGURE 6. FLOW SHEET

CHAPTER IV

PROCEDURE

System No. 1

In the first system studied, the forcing variable was the inlet water flow rate and the forced variable was the temperature of the fluid in the vessel.

Experimental and analog simulation studies were conducted. The majority of the data taken was on the analog computer. The analog data were spot checked by data taken on the actual experimental system. Both frequency response and step response data were taken.

Frequency Response Studies

As a sine wave generator was available, the experimental apparatus was constructed for conducting frequency response. The frequency response data were taken while operating about one steady state value. This value was selected to give a maximum temperature variation, with amplitude of the input sinusodial flow rate, of about 10° Fahrenheit. Also as a precaution against a mishap, the coolant temperature was held slightly above the freezing point of water. The steady state value was selected by actual manipulation of the experimental apparatus. The operating conditions are given in Table 21, Appendix C.

Frequency response data were taken at twenty-three different frequencies, ranging from 0.05 cycles per minute to 20 cycles per minute, on the analog computer and at ten different frequencies ranging from 0.05 cycles per minute to five cycles per minute on the experimental apparatus. The various frequencies are listed in Tables 13 and 14 of Appendix B.

As the output of non linear systems can also depend on the amplitude of the input sine wave, frequency response data were taken for various amplitudes of the input sinusodial forcing function. Frequency response data were taken for five different amplitudes of the forcing function on the analog computer and for three different amplitudes on the experimental apparatus. The different amplitudes used on the analog computer were 0.475, 0.94, 1.42, 1.89, and 2.364 pounds per minute. The amplitudes used on the experimental apparatus were 0.94, 1.42, and 1.89 pounds per minute. The absolute values corresponding to the minimum and maximum flow rate for these amplitudes are given in Table 21 of Appendix C.

The amplitude ratio and phase angle information obtained from the frequency response data taken on the analog computer are summarized in Table 13, Appendix B. The same information obtained from the experimental data is given in Table 14, Appendix B. Amplitude ratio and phase angle values calculated from equation (78) are tabulated in Table 15, Appendix B.

A sample time record of the frequency response data obtained from the analog computer is shown in Figure 7. A sample time record of the frequency response data taken on the experimental apparatus is shown in Figure 8.

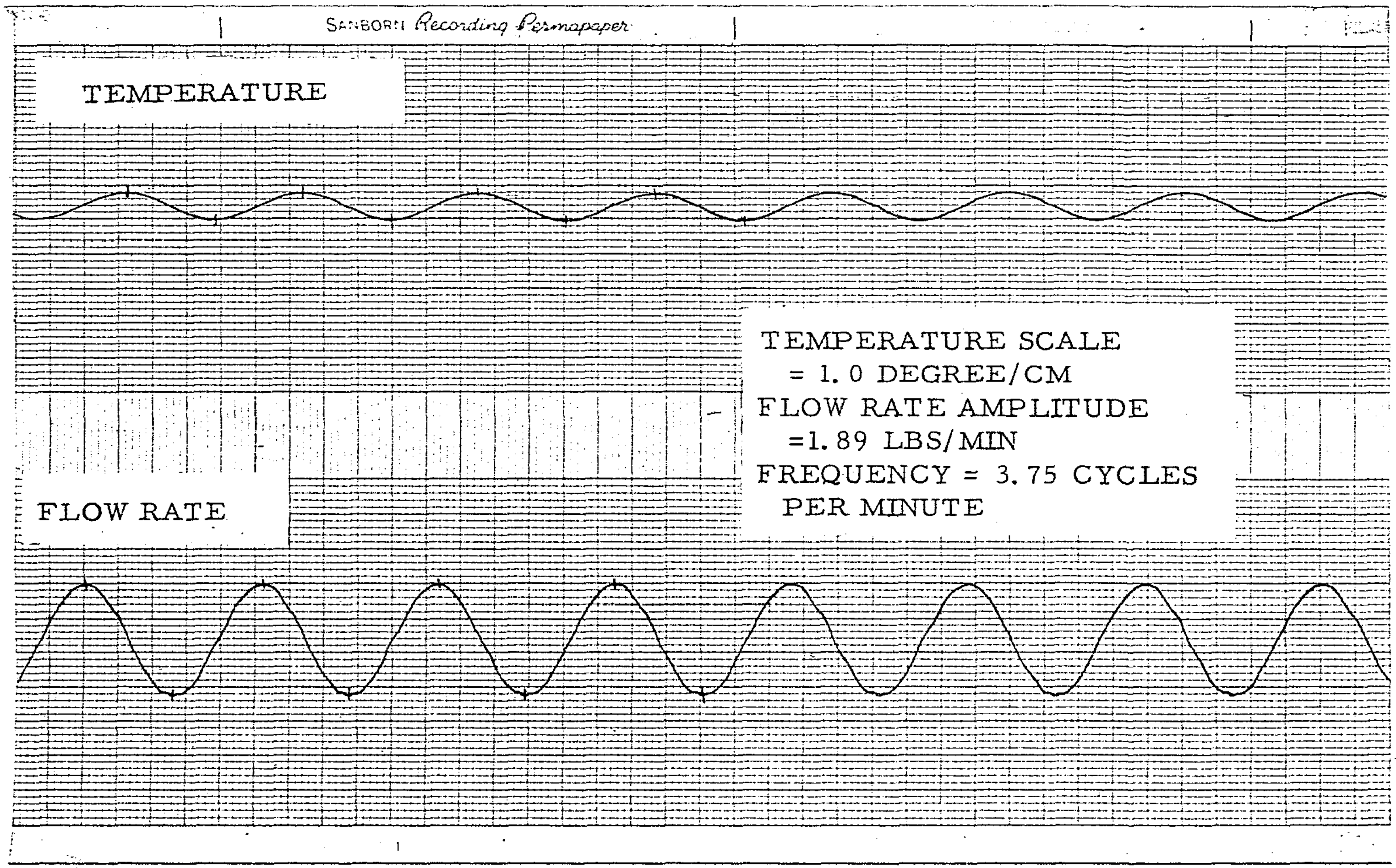

Figure 7. Sample of Frequency Response Data Taken on Analog Computer

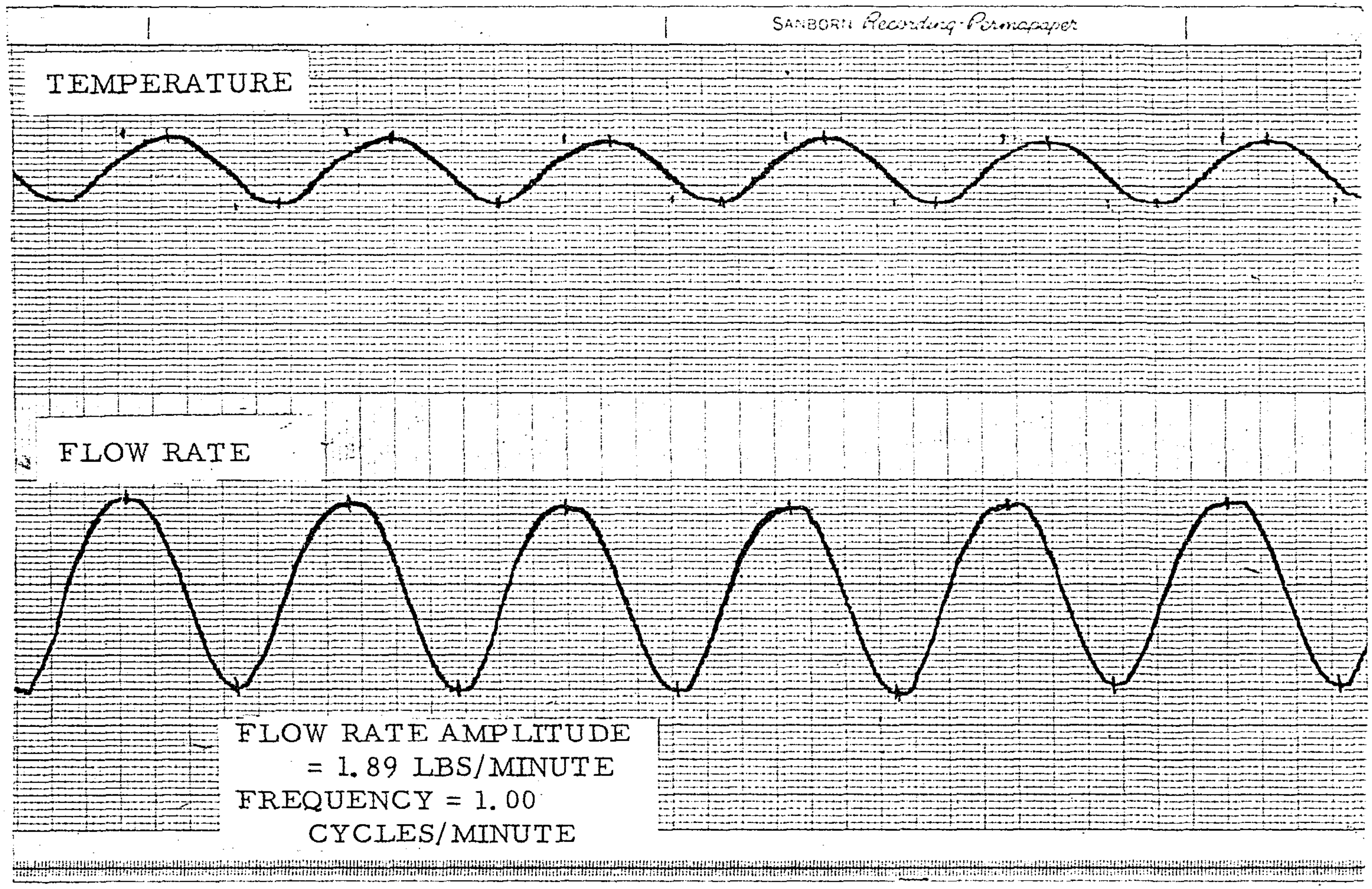

Figure 8. Sample of Experimental Frequency Response Data

Step Response Studies

As in non linear systems, the end results are very much dependent upon the type of input forcing function. It was therefore desirable to obtain data for some type of input forcing function other than a sinusodial forcing function primarily as a means of comparison. When the experimental apparatus was constructed, no provisions were included for taking step response data. However, attempts have been made to obtain step response data on the experimental apparatus by the manipulation of a globe valve. This procedure has not proved satisfactory. The step response information was therefore taken on the analog computer.

Step response data for various magnitudes of displacement were taken. A total of five positive displacements were used. The five positive displacements were 0.48, 0.94, 1.42, 1.89 and 2.36 pounds per minute and corresponded to the difference between the maximum flow rate and the steady state flow rate for each of the different amplitudes of the sinusodial forcing function used in the frequency response studies. Also a total of five negative displacements were used. These were -0.47, -0.94, -1.42, -1.89, and -2.36 pounds per minute. The negative displacements corresponded to the difference between the steady state flow rate and the minimum flow rate for each of the different amplitudes used in the frequency response studies. A sample time record of the step function response data taken on the analog computer is shown in Figure 9. The step function response data taken on the analog computer has been converted into real time and this information is given in Table 16, Appendix B.

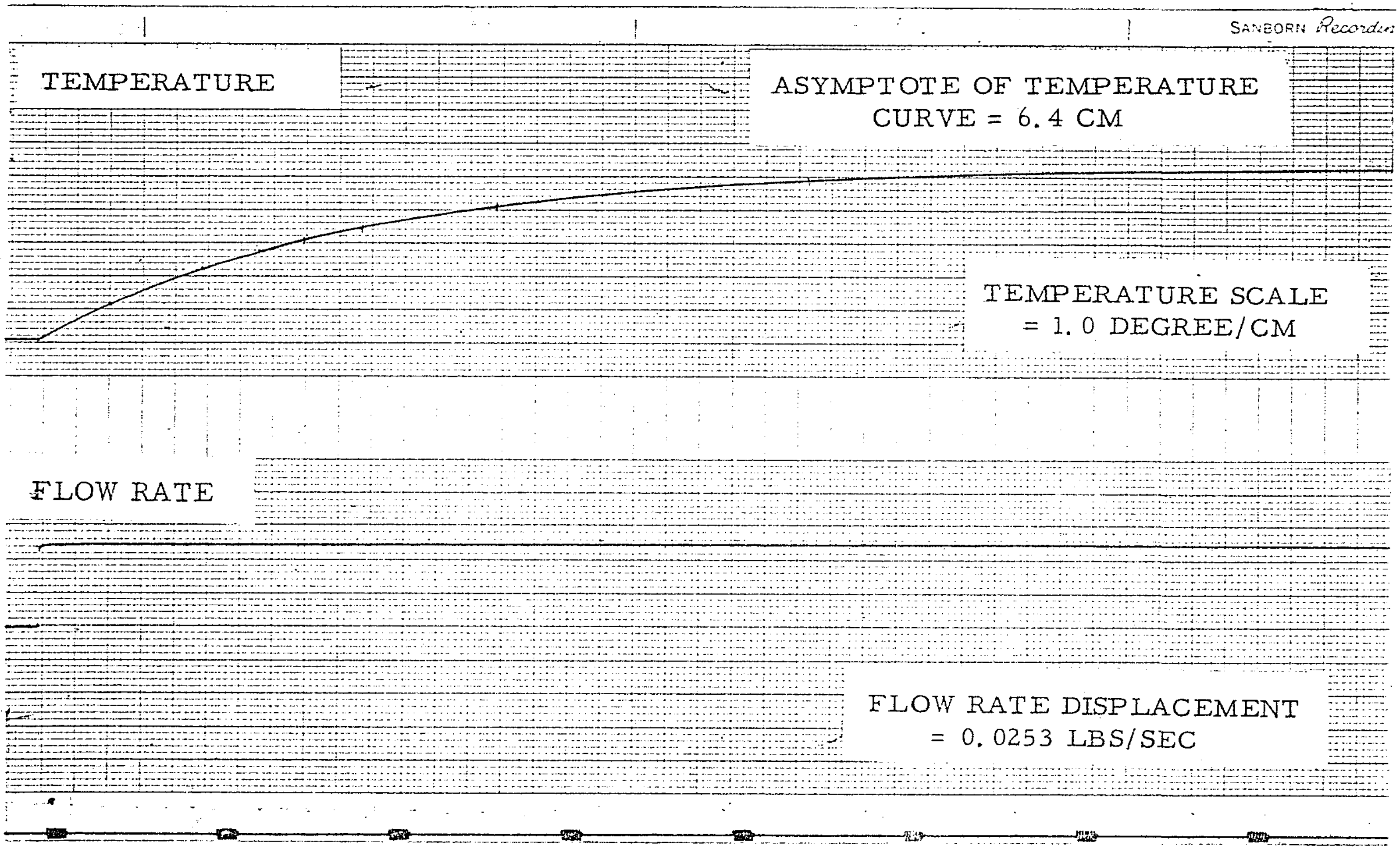

Figure 9. Sample of Step Response Data Taken on Analog Computer

System No. 2

In this system the coolant pressure, and hence the coolant temperature, was varied as the forcing variable. The output variable was again the temperature of the water in the vessel. During this study the water flow rate was held constant.

To obtain experimental frequency response data and experimental step response data was not considered practical in this case. The experimental method of testing used was the pulse response technique. The coolant pressure was allowed to vary between two different levels by means of an arrangement of solenoid valves. The coolant pressure and the exit water temperature were both recorded as a function of time. Figure 10 depicts a sample of the output data. The input signal was recorded by hand at two second intervals. These data are given in Tables 17 and 18, Appendix B.

The experimental pulse data were then converted to frequency response data by means of the Fourier integral. These calculations were made on an IBM 650 Computer.

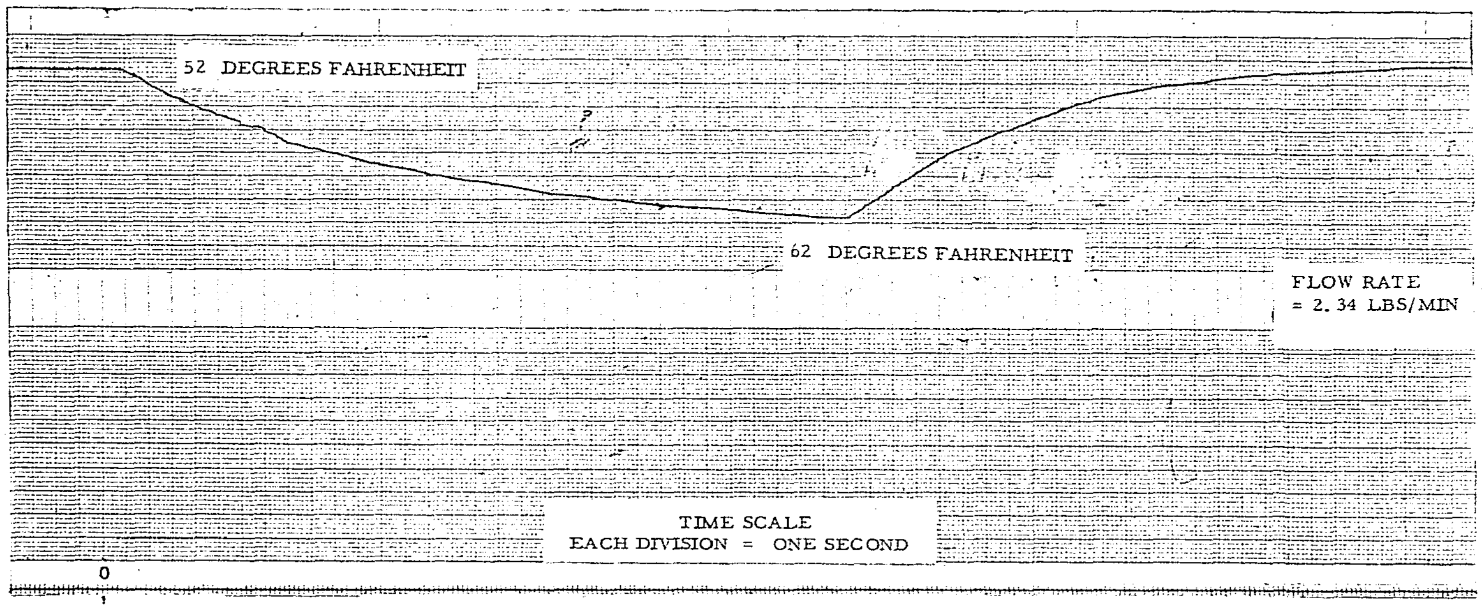

Figure 10. Sample of Output Experimental Pulse Response Data

CHAPTER V

THEORY

Derivation of Differential Equation Describing System No. 1

A schematic diagram of a jacketed, well-agitated continuous reactor is depicted in Figure 11.

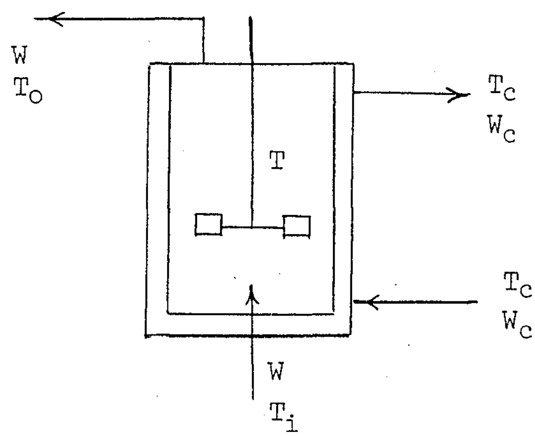

Figure 11. Schematic diagram of a jacketed, well-agitated continuous reactor.

In arrangement No. 1, the input forcing variable was the liquid flow rate W and the output forced variable was the reactor temperature T. Therefore for system No. 1 it is desired to obtain an equation relating W, T, and time. The desired expression is given by an energy balance on the liquid in the reactor.

$$\text{Input} - \text{Output} = \text{Accumulation}, \tag{1}$$

$$\text{Input} = WC_p(T_i - T_{ref})\,\Delta\theta \quad , \tag{2}$$

$$\text{Output} = WC_p(T_o - T_{ref})\,\Delta\theta + UA(T - T_c)\,\Delta\theta \quad , \tag{3}$$

$$\text{Accumulation} = \rho\, VC_p\,\Delta T \;. \tag{4}$$

Where:

A = Heat transfer area, sq. ft.

C_p = Heat capacity, BTU/lb-$^{\circ}$F

T = Temperature of fluid in reactor, $^{\circ}$F

T_i = Inlet temperature, $^{\circ}$F

T_c = Coolant temperature, $^{\circ}$F

T_o = Outlet temperature, $^{\circ}$F

T_{ref} = Reference temperature, $^{\circ}$F

U = Overall heat transfer coefficient, BTU/hr-sq. ft.-$^{\circ}$F

V = Reactor volume, cu. ft.

W = Flow rate, lbs./hr.

ρ = Density, lbs./cu. ft.

θ = Time, hours

Substituting equations (2), (3), and (4) into equation (1) gives:

$$WC_p(T_i - T_{ref})\,\Delta\theta - WC_p(T_o - T_{ref})\,\Delta\theta - UA(T - T_c)\,\Delta\theta = \rho\, VC_p\,\Delta T \;. \tag{5}$$

Collecting terms gives:

$$WC_p(T_i - T_o) - UA(T - T_c) = \rho\, VC_p \frac{\Delta T}{\Delta\theta} \;. \tag{6}$$

Assuming $T_o = T$, equation (6) reduces to:

$$WC_p(T_i - T) - UA(T - T_c) = \rho\, VC_p \frac{\Delta T}{\Delta\theta} \;. \tag{7}$$

In the limit equation (7) becomes:

$$\frac{dt}{d\theta} = \frac{W(T_i - T)}{\rho V} - \frac{UA(T - T_c)}{\rho\, VC_p} \;. \tag{8}$$

which is the desired expression.

In the derivation of equation (8), various assumptions were made.

1. The heat capacity ($C_p \approx C_v$) and the density of the liquid were taken as constants and were evaluated at the steady state temperature. This assumption should be justifiable as the temperature variations were less than 15 degrees Fahrenheit.

2. Transient effects occurring as a result of the transfer of heat across the two liquid films and the metal wall of the reactor were neglected; that is, it was assumed that an overall heat transfer coefficient could be used. The overall heat transfer coefficient was constant over the range of conditions studied, and it was determined experimentally at steady state conditions.

3. The outlet fluid temperature was taken to be equal to the temperature of the fluid in the reactor, that is perfect mixing was assumed.

4. It was assumed that equation (5) accounts for all of the energy of the system.

The above assumptions seem justifiable in view of the experimental data.

As the forcing variable is the flow rate, we have in addition to equation (8):

$$W = f(\theta) \; . \tag{9}$$

Substitution of equation (9) into equation (8) yields:

$$\frac{dT}{d\theta} + \frac{f(\theta)T}{\rho V} + \frac{UAT}{\rho V C_p} = \frac{f(\theta)T_i}{\rho V} + \frac{UAT_c}{\rho V C_p} \; , \tag{10}$$

or

$$dT + \left[\frac{f(\theta) + UA/C_p}{\rho V}\right] T d\theta = \left[\frac{f(\theta)T_i + UAT_c/C_p}{\rho V}\right] d\theta \; . \tag{11}$$

This equation is a first order linear differential equation which can be solved by means of an integrating factor. The integrating factor is:

$$e^{\int \left[\frac{f(\theta) + UA/C_p}{\rho V}\right] d\theta} \quad . \tag{12}$$

Multiplying equation (11) by the integrating factor and integrating gives:

$$Te^{\int \left[\frac{f(\theta) + UA/C_p}{\rho V}\right] d\theta} = \int \frac{T_i f(\theta)}{\rho V} e^{\int \left[\frac{f(\theta) + UA/C_p}{\rho V}\right] d\theta} d\theta$$

$$+ \int \frac{UAT_c}{\rho V C_p} e^{\int \left[\frac{f(\theta) + UA/C_p}{\rho V}\right] d\theta} d\theta \quad . \tag{13}$$

If the flow rate is known as a function of time, then the integration indicated by equation (13) can be carried out, at least in principle. For a sinusodial forcing function, equation (13) becomes unwieldy. The solution for a sinusodial input is readily obtained by means of complex convolution.

Linearity of a differential equation must not be confused with linearity of a control system. A control system is not necessarily linear just because the equations describing the system are linear equations. Equation (11) is non-linear insofar as control theory is concerned. The linearity of a control system is based upon the property of superposition. Superposition will be discussed later (see page 50).

The variables in equation (11) may be written as the sum of an unsteady state variation and a steady state component:

$$T = T^* + T_s \ , \tag{14}$$

and

$$W = W^* + W_s \ . \tag{15}$$

where the (*) quantities represent variations about the steady state value.

Substituting equations (14) and 15) into equation (10) yields:

$$\frac{dT^*}{d\theta} = \frac{(W^* + W_s)(T_i - T^* - T_s)}{\rho V} - \frac{UA(T^* + T_s - T_c)}{\rho V C_p} \,. \tag{16}$$

At steady state conditions:

$$0 = \frac{W_s(T_i - T_s)}{\rho V} - \frac{UA(T_s - T_c)}{\rho V C_p} \,. \tag{17}$$

Substracting equation (17) from equation (16) yields:

$$\frac{dT^*}{d\theta} = \frac{W^*(T_i - T^* - T_s)}{\rho V} - \frac{W_s T^*}{\rho V} - \frac{UAT^*}{\rho V C_p} \,. \tag{18}$$

Equation (18) can be rearranged to give:

$$\frac{dT^*}{d\theta} + \frac{W^* T^*}{\rho V} + \left(\frac{W_s + UA/C_p}{\rho V}\right)T^* = \left(\frac{T_i - T_s}{\rho V}\right)W^* \,, \tag{19}$$

or

$$\frac{dT^*}{d\theta} + k_3 W^* T^* + k_1 T^* - k_2 W^* = 0 \,; \tag{20}$$

where

$$k_3 = \frac{1}{\rho V} \,, \tag{21}$$

$$k_1 = \left(\frac{W_s - UA/C_p}{\rho V}\right) \,, \tag{22}$$

$$k_2 = (T_i - T_s)/\rho V \,. \tag{23}$$

Equation (20) is to be solved under the conditions:

$$W^* = \beta \sin \omega\theta \,, \tag{24}$$

$$T^*(\theta) = T^*(0) = 0 \,, \tag{25}$$

and

$$W^*(\theta) = W^*(0) = 0 \,. \tag{26}$$

Taking the Laplace Transform of equation (20) gives:

$$sT^*(s) + k_1T(s) + k_3\ \mathcal{L}(WT) - k_2W(s) \quad = \quad 0\ . \tag{27}$$

Equation (24) can be written as:

$$W^* \quad = \quad \beta\ \sin\omega\theta \quad = \frac{\beta}{2j}(e^{j\omega\theta} \quad - e^{-j\omega\theta}\ )\ . \tag{28}$$

Taking the Laplace Transform of equation (28) yields:

$$W^*(s) \quad = \quad \frac{\beta}{2j}\ (\frac{1}{s\ -\ j\omega} - \frac{1}{s\ +\ j\omega}) \quad . \tag{29}$$

The Laplace Transform of the product term in equation (27) may be treated by means of complex convolution (26, 58, 61). If $f_1(\theta)$ and $f_2(\theta)$ have the Laplace Transforms $F_1(s)$ and $F_2(s)$, respectively, then

$$\mathcal{L}\left[f_1(\theta)f_2(\theta)\right] \quad = \frac{1}{2\Pi j}\int_{\gamma - j\infty}^{\gamma + j\infty} F_1(s-\underline{\omega})F_2(\underline{\omega})d\underline{\omega}\ , \tag{30}$$

$$\max\ (\sigma_{a_1},\ \sigma_{a_1} + \sigma_{a_2}) \ < \ \sigma\ , \qquad \sigma_{a_2} < \gamma < \sigma - \sigma_{a_1}\ .$$

In which γ is a real constant, $\sigma = R(s)$, and σ_{a_1} and σ_{a_2} are the abscissas of absolute convergence of the function $f_1(\theta)$ and $f_2(\theta)$, respectively.

The output function will be assumed to be of the form:

$$T^*(\theta) \quad = \quad \sum_{n=0}^{\infty} B_n e^{s_n\theta} \quad . \tag{31}$$

Taking the Laplace Transform of equation (31) gives:

$$T^*(s) \quad = \quad \sum_{n=0}^{\infty} \frac{B_n}{s\ -\ s_n}\ . \tag{32}$$

Letting $f_1(\theta) \ = \ W^*(\theta)$, and $f_2(\theta) \ = \ T^*(\theta)$, then

$$W^*(s\ -\ \underline{\omega}) \quad = \quad \frac{\beta}{2j}\ (\frac{1}{s\ -\ \underline{\omega}\ -\ j\omega} \quad - \quad \frac{1}{s\ +\ j\omega\ -\ \underline{\omega}})\ , \tag{33}$$

$$T^*(\underline{\omega}) = \sum_{n=0}^{\infty} \frac{B_n}{\underline{\omega} - s_n} \, . \qquad (34)$$

Substituting equations (33) and (34) into equation (30) yields:

$$\mathcal{L}(W^*T^*) = \frac{1}{2\Pi j} \int_{\gamma - j\infty}^{\gamma + j\infty} \frac{\beta}{2j} \left[\frac{1}{(s-\underline{\omega}-j\omega)} - \frac{1}{(s-\underline{\omega}+j\omega)} \right] \sum_{n=0}^{\infty} \frac{B_n}{\underline{\omega}-s_n} \, d\underline{\omega} \, . \qquad (35)$$

$$\max \sigma_n < \gamma < \sigma - j\omega$$

Equation (35) can be rewritten as:

$$\mathcal{L}(W^*T^*) = \frac{1}{2\Pi j} \int_{\gamma - j\infty}^{\gamma + j\infty} \frac{}{2j} \sum_{n=0}^{\infty} \frac{B_n}{(s-\underline{\omega}-j\omega)(\underline{\omega}-s_n)} \, d\underline{\omega}$$

$$- \frac{1}{2\Pi j} \int_{\gamma - j\infty}^{\gamma + j\infty} \frac{\beta}{2j} \sum_{n=0}^{\infty} \frac{B_n}{(s-\underline{\omega}+j\omega)(\underline{\omega}-s_n)} \, d\underline{\omega} \, . \qquad (36)$$

Expanding the right hand side of equation (36) by partial fractions gives:

$$\mathcal{L}(W^*T^*) = \frac{1}{2\Pi j} \int_{\gamma - j\infty}^{\gamma + j\infty} \frac{\beta}{2j} \sum_{n=0}^{\infty} \frac{B_n}{(s-s_n-j\omega)(\underline{\omega}-s_n)} \, d\underline{\omega}$$

$$+ \frac{1}{2\Pi j} \int_{\gamma - j\infty}^{\gamma + j\infty} \frac{\beta}{2j} \left(\frac{1}{s-\underline{\omega}-j\omega} \right) \sum_{n=0}^{\infty} \frac{B_n}{(s-j\omega) - s_n} \, d\underline{\omega}$$

$$- \frac{1}{2\Pi j} \int_{\gamma - j\infty}^{\gamma + j\infty} \frac{\beta}{2j} \sum_{n=0}^{\infty} \frac{B_n}{(s-s_n+j\omega)(\underline{\omega}-s_n)} \, d\underline{\omega}$$

$$-\frac{1}{2\Pi j}\int_{\gamma-j\infty}^{\gamma+j\infty}\frac{\beta}{2j}\left(\frac{1}{s-\underline{\omega}+j\omega}\right)\sum_{n=0}^{\infty}\frac{B_n}{(s+j\omega)-s_n}\,d\underline{\omega}\ . \tag{37}$$

Rearranging equation (37):

$$\mathcal{L}(W^*T^*) = \frac{1}{2\Pi j}\left(\frac{\beta}{2j}\right)\int_{\gamma-j\infty}^{\gamma+j\infty}\left[\sum_{n=0}^{\infty}\frac{B_n}{(s-s_n-j\omega)(\underline{\omega}-s_n)}\right.$$

$$\left.-\sum_{n=0}^{\infty}\frac{B_n}{(s-s_n+j\omega)(\underline{\omega}-s_n)}\right]d\underline{\omega}$$

$$+\frac{1}{2\Pi j}\left(\frac{\beta}{2j}\right)\int_{\gamma-j\infty}^{\gamma+j\infty}\left[\sum_{n=0}^{\infty}\frac{1}{(s-\underline{\omega}-j\omega)}\left(\frac{B_n}{(s-j\omega)-s_n}\right)\right.$$

$$\left.-\sum_{n=0}^{\infty}\frac{1}{(s-\underline{\omega}+j\omega)}\left(\frac{B_n}{(s-j\omega)-s_n}\right)\right]d\underline{\omega}\ . \tag{38}$$

The poles of equation (38) are at $\underline{\omega} = s + j\omega$, $\underline{\omega} = s - j\omega$, and $\underline{\omega} = s_n$. Since the integration proceeds around a closed curve, the last integral in equation (38) is zero as the poles $s + j\omega$ and $s - j\omega$ lie outside the closed region. The first integral in equation (38) corresponding to the poles $\underline{\omega} = s_n$ can be evaluated by the residue theorem:

$$\int_c f(z)dz = 2\Pi j\,\Sigma\text{ Residues}\ . \tag{39}$$

The residues are, of course, the principle parts of the Laurent series expansions and, therefore, the first integral in equation (38) reduces to:

$$\frac{\beta}{2j} \sum_{n=0}^{\infty} \left[\frac{B_n}{(s-s_n-j\omega\ )} - \frac{B_n}{(s-s_n+j\omega\ )} \right] . \tag{40}$$

Thus equation (35) becomes:

$$\mathcal{L}(W^*T^*) = \frac{\beta}{2j} \sum_{n=0}^{\infty} \left[\frac{B_n}{s - (s_n+j\omega\ )} - \frac{B_n}{s - (s_n-j\omega\ )} \right] . \tag{41}$$

Substituting equation (41) into equation (27) gives:

$$(s + k_1)T^*(s) + \frac{k_3\beta}{2j} \sum_{n=0}^{\infty} \left[\frac{B_n}{s - (s_n+j\omega\ )} - \frac{B_n}{s - (s_n-j\omega\ )} \right]$$

$$-k_2W^*(s) = 0 . \tag{42}$$

The coefficients B_n must now be evaluated. Substituting equations (29) and (31) into equation (42):

$$(s + k_1) \sum_{n=0}^{\infty} \frac{B_n}{s-s_n} + \frac{k_3\beta}{2j} \sum_{n=0}^{\infty} \left[\frac{B_n}{s - (s_n+j\omega\ )} - \frac{B_n}{s - (s_n-j\omega\ )} \right]$$

$$- \frac{k_2\beta}{2j} \left[\frac{1}{s - j\omega} - \frac{1}{s + j\omega} \right] = 0 . \tag{43}$$

Dividing equation (43) by $s + k_1$ yields:

$$\sum_{n=0}^{\infty} \frac{B_n}{s-s_n} + \frac{k_3\beta}{2j(s+k_1)} \sum_{n=0}^{\infty} \left[\frac{B_n}{s - (s_n+j\omega\ )} - \frac{B_n}{s - (s_n-j\omega\ )} \right]$$

$$- \frac{k_2\beta}{2j(s+k_1)} \left[\frac{1}{s - j\omega} - \frac{1}{s + j\omega} \right] = 0 . \tag{44}$$

Expanding equation (44) by partial fractions:

$$\sum_{n=0}^{\infty} \frac{B_n}{s-s_n} + \frac{k_3\beta}{2j(s+k_1)} \sum_{n=0}^{\infty} \left[\frac{B_n}{-k_1 - (s_n+j\omega\ )} - \frac{B_n}{-k_1 - (s_n-j\omega\ )} \right]$$

$$+ \frac{k_3\beta}{2j} \sum_{n=0}^{\infty} \left[\left(\frac{1}{(s_n+j\omega) + k_1} \right) \left(\frac{B_n}{s - (s_n+j\omega)} \right) \right.$$

$$\left. - \left(\frac{1}{(s_n - j\omega) + k_1} \right) \left(\frac{B_n}{s - (s_n-j\omega)} \right) \right]$$

$$- \frac{k_2\beta}{2j(s+k_1)} \left[\frac{1}{(-k_1-j\omega)} - \frac{1}{(-k_1+j\omega)} \right] - \frac{k_2\beta}{2j(j\omega+k_1)} \left(\frac{1}{s-j\omega} \right)$$

$$+ \frac{k_2\beta}{2j(-j\omega+k_1)} \left(\frac{1}{s+j\omega} \right) = 0 . \tag{45}$$

Letting $s_o = -k_1$:

$$\frac{B_o}{s+k_1} + \sum_{n=1}^{\infty} \frac{B_n}{(s-s_n)} + \frac{k_3\beta}{2j(s+k_1)} \sum_{n=0}^{\infty} \left[\frac{B_n}{-k_1 - (s_n+j\omega)} - \frac{B_n}{-k_1 - (s_n-j\omega)} \right]$$

$$+ \frac{k_3\beta}{2j} \sum_{n=0}^{\infty} \left[\left(\frac{1}{s_n + j\omega + k_1} \right) \left(\frac{B_n}{s - (s_n+j\omega)} \right) \right.$$

$$\left. - \left(\frac{1}{(s_n-j\omega) + k_1} \right) \left(\frac{B_n}{s - (s_n-j\omega)} \right) \right]$$

$$- \frac{k_2\beta}{2j(s+k_1)} \left[\frac{1}{(-k_1-j\omega)} - \frac{1}{(-k_1+j\omega)} \right] - \frac{k_2\beta}{2j(j\omega+k_1)} \left(\frac{1}{s-j\omega} \right)$$

$$+ \frac{k_2\beta}{2j(-j\omega+k_1)} \left(\frac{1}{s+j\omega} \right) = 0 . \tag{46}$$

Collecting all of the terms involving $(s + k_1)$ gives:

$$\frac{1}{s+k_1} \left[B_o + \frac{k_3\beta}{2j} \sum_{n=0}^{\infty} \left(\frac{B_n}{-k_1 - (s_n+j\omega)} - \frac{B_n}{-k_1 - (s_n-j\omega)} \right) \right.$$

$$- \frac{k_2\beta}{2j}\left(\frac{1}{-k_1-j\omega} - \frac{1}{-k_1+j\omega}\right)\Bigg] \quad . \tag{47}$$

Requiring that the coefficient of $(\frac{1}{s + k_1})$ must vanish, yields:

$$B_o + \frac{k_3\beta}{2j}\sum_{n=0}^{\infty}\left(\frac{B_n}{-k_1 - (s_n+j\omega)} - \frac{B_n}{-k_1 - (s_n-j\omega)}\right)$$

$$- \frac{k_2\beta}{2j}\left(\frac{1}{-k_1-j\omega} - \frac{1}{-k_1+j\omega}\right) = 0 \ . \tag{48}$$

This leaves:

$$\sum_{n=1}^{\infty}\frac{B_n}{s-s_n} + \frac{k_3\beta}{2j}\sum_{n=0}^{\infty}\Bigg[\frac{1}{(s_n+j\omega)+k_1}\left(\frac{B_n}{s - (s_n+j\omega)}\right)$$

$$- \frac{1}{(s_n-j\omega)+k_1}\left(\frac{B_n}{s - (s_n-j\omega)}\right)\Bigg] - \frac{k_2\beta}{2j(j\omega+k_1)}\left(\frac{1}{s-j\omega}\right)$$

$$+ \frac{k_2\beta}{2j(-j\omega+k_1)}\left(\frac{1}{s+j\omega}\right) = 0 \ . \tag{49}$$

Upon repeating the procedure and letting:

$$s_1 = 0$$

$$s_2 = -j\omega$$

$$s_3 = j\omega$$

$$s_4 = -k_1 - j\omega$$

$$s_5 = -k_1 + j\omega$$

$$s_6 = -2j\omega$$

$$s_7 = 2j\omega$$

.

.

.

$$s_2 + 4n = -j(n+1)\omega$$

$$s_3 + 4n = j(n+1)\omega$$

$$s_4 + 4n = -k_1 - j(n+1)\omega$$

$$s_5 + 4n = -k_1 + j(n+1)\omega \quad , \tag{50}$$

the remaining coefficients are determined. The coefficients can be grouped into sets. Table 1 gives the sets of coefficients.

TABLE 1

SETS OF COEFFICIENTS

B_o	B_2	B_3
B_4, B_5	B_1	B_1
B_8, B_9	B_6	B_7
.	B_{10}	B_{11}
.	.	.

The B_o coefficient is also a function of the B_2 and B_3 coefficients. The B_o coefficient is associated with the transient solution of the problem. Therefore, the B_o, B_4, B_5, etc. coefficients no longer need to be considered.

The coefficients B_2 and B_3, B_6 and B_7, B_{10} and B_{11}, etc. are complex conjugates. Therefore it is only necessary to calculate one set of coefficients.

The relations between the coefficients are:

$$B_1 = \frac{-k_3\beta}{k_1} \operatorname{Im} B_2 \ , \tag{51}$$

$$B_2 + \frac{k_2 \beta}{2j(-j\omega + k_1)} - \frac{k_3 \beta B_1}{2j(-j\omega + k_1)} + \frac{k_3 \beta B_6}{2j(-j\omega + k_1)} = 0 , \tag{52}$$

$$B_6 - \frac{k_3 \beta B_2}{2j(-2j\omega + k_1)} + \frac{k_3 \beta B_{10}}{2j(-2j\omega + k_1)} = 0 , \tag{53}$$

and in general:

$$B_{2+4(n+1)} - \frac{k_3 \beta B_{2+4n}}{2j\left[-(n+2)j\omega + k_1\right]} + \frac{k_3 \beta B_{2+4(n+2)}}{2j\left[-(n+2)j\omega + k_1\right]} = 0 . \tag{54}$$

Equation (51) arises from terms involving $1/s$. These terms are obviously of the nature of a step function and give rise to a constant term.

The B_2 coefficient cannot be obtained in closed form, but it can be calculated to any accuracy desired. Upon substituting equation (53) into equation (52):

$$B_2 \left[1 + \left(\frac{k_3 \beta}{2j} \right)^2 \left(\frac{1}{(-j\omega + k_1)(-2j\omega + k_1)} \right) \right] + \frac{k_2 \beta}{2j(-j\omega + k_1)}$$
$$- \frac{k_3 \beta \, \mathrm{Im} B_2}{2j(-j\omega + k_1)} - \left(\frac{k_3 \beta'}{2j} \right)^2 \frac{B_{10}}{(-2j\omega + k_1)} = 0 . \tag{52a}$$

Upon repeating the procedure with the relations obtained from equation (54), the B_{10} coefficient in equation (52a) can ultimately be replaced by the coefficient $B_{2+4(n+2)}$ which for large n can be discarded. The additional relationships:

$$R(\text{equation } 52a) = 0 ,$$
$$\mathrm{Im}(\text{equation } 52a) = 0 , \tag{55}$$

allows the calculation of the B_2 coefficient from which all of the other coefficients may be obtained.

Finally, the solution of equation (20) is:

$$T(\theta) = \sum_{n=0}^{\infty} B_n e^{s_n \theta} = \frac{-k_3\beta}{k_1} \operatorname{Im} B_2 + \sum_{n=0}^{\infty} B_{2+4n} e^{s_{2+4n}\theta}$$

$$+ \sum_{n=0}^{\infty} B_{3+4n} e^{s_{3+4n}\theta} \quad . \tag{56}$$

Equation (8) is readily studied by means of an analog computer. The equation may be simulated in various ways. Figures 12 and 13 depict the analog simulations which were used. The analog simulations were excited both by means of sinusodial and step input functions.

The simulation shown in Figure 12 was used for frequency response studies. In this simulation the steady state component was not subtracted out. As only a single speed sine wave generator (one cycle per second) was available for this study, frequency variations were obtained by varying the capacitance of the capacitor b_1, shown in Figure 12. Table 22 of Appendix C gives the values of b_1 corresponding to various frequencies.

The scaling of equation (8) for analog simulation was performed by means of the following transformation of variables:

$$T = aT_n = 100T_n, \tag{57}$$

$$W = cW_n = 0.1W_n, \tag{58}$$

$$= b_1 b_2 \theta_n = 20.82 b_1 \theta_n \ . \tag{59}$$

This transformation of variables gives:

$$T_n = b_1 \int (W_n - 0.896 W_n T_n - 0.1805 T_n + 0.0687) d\theta_n \ , \tag{60}$$

which was the equation simulated on the analog computer. The full scale voltage of 25 volts was determined from the multiplier characteristics. The simulation shown in Figure 13 was used for the step response studies.

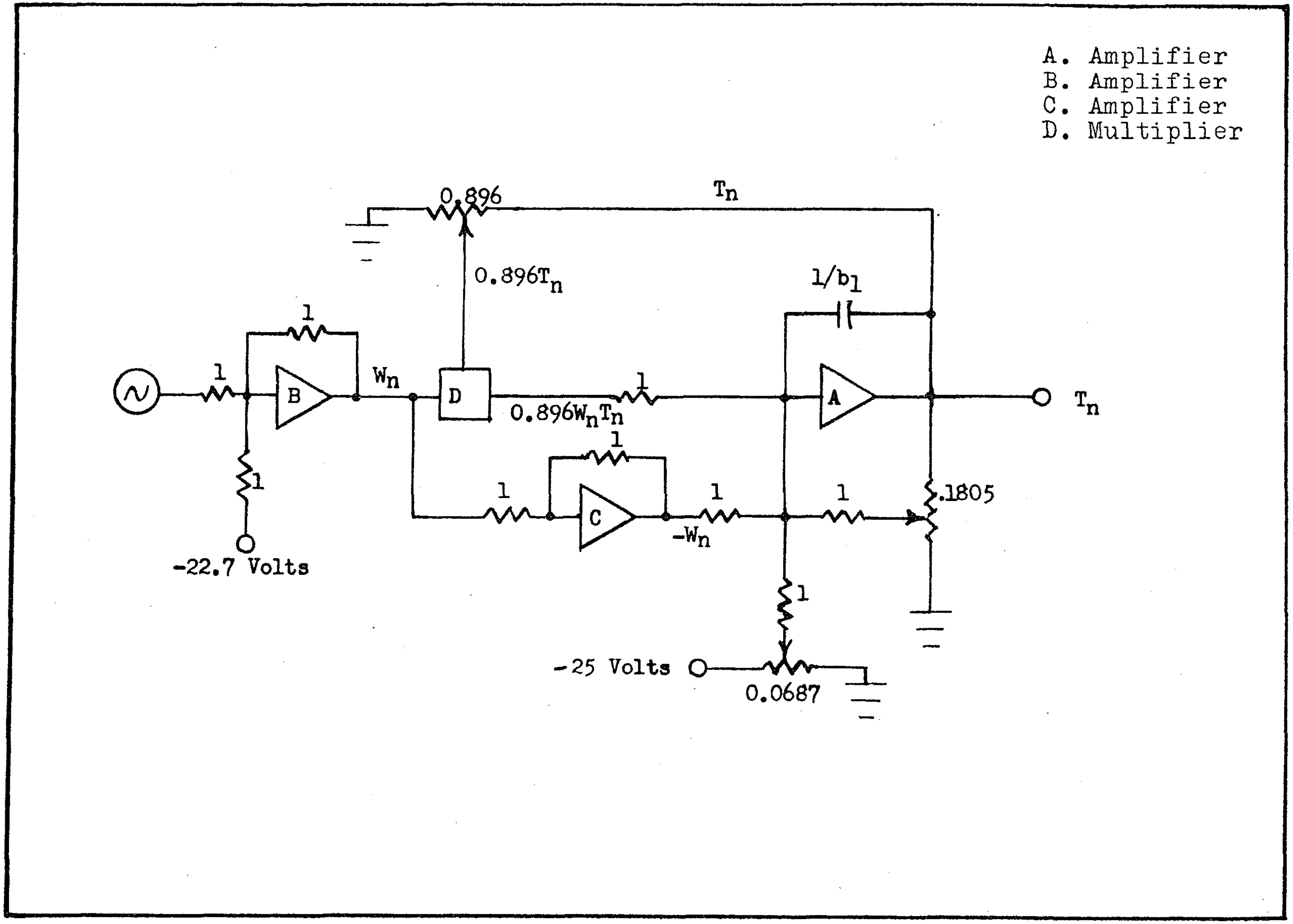

Figure 12. Analog Simulation for Frequency Response Studies

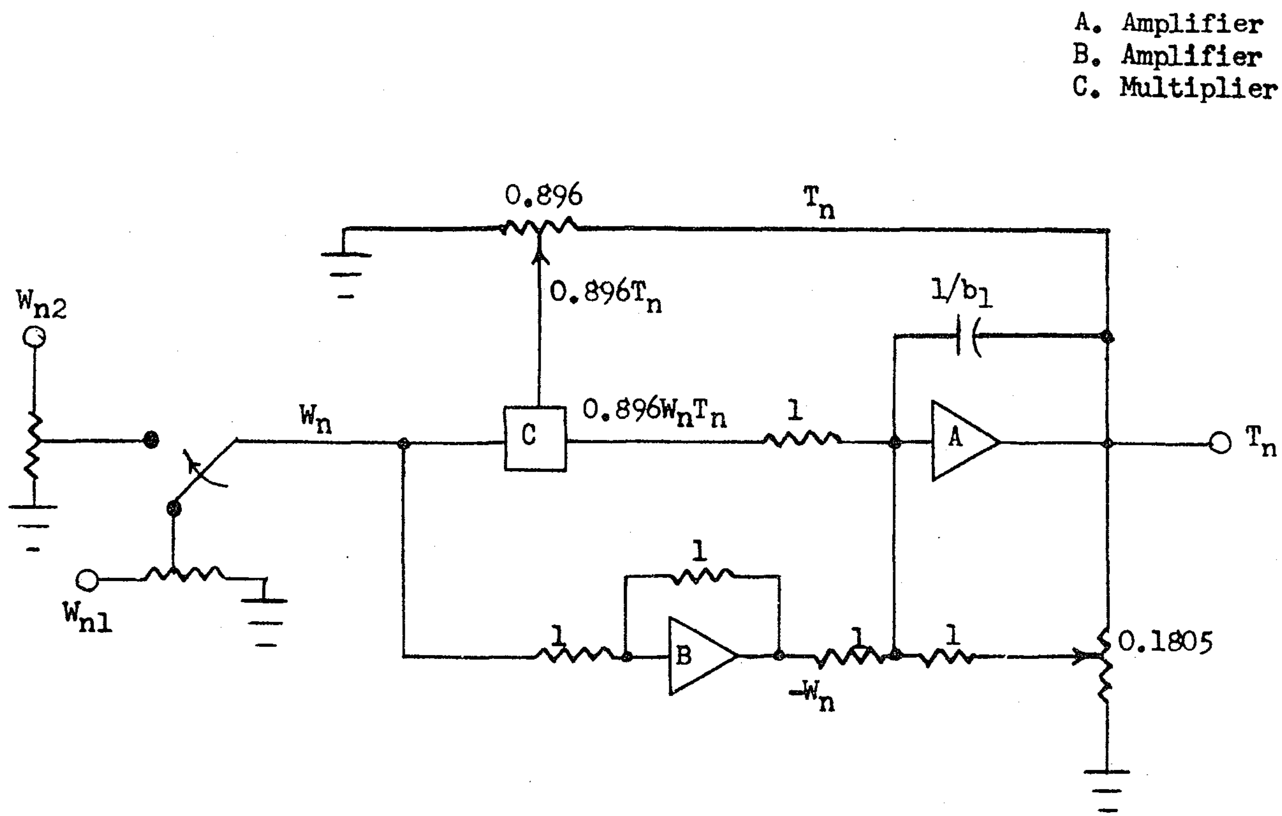

Figure 13. Analog Simulation for Step Response Studies

In this simulation the steady state component was subtracted out, and was scaled using the same values given in equations (57), (58), and (59). The time scale for the step response was $b_1 b_2 = 10$, i. e., one second of analog time was the equivalent of ten seconds of real time.

In process dynamics the quantities of interest are input-output relationships. In this sense equation (8) is non linear because it does not allow superposition. A system is said to be linear if for every pair of inputs $X_1(\theta)$, $X_2(\theta)$ and corresponding outputs $Y_1(\theta)$, $Y_2(\theta)$, the input $X_1(\theta) + X_2(\theta)$ produces an output $Y_1(\theta) + Y_2(\theta)$. The non-linearity in equation (8) results from the product of variables; that is, the term involving WT. This condition may be demonstrated as follows, using L to represent the action of the system on an input to give the corresponding output:

$$L(\text{Input}) = \text{Output}, \tag{61}$$

$$L[X_1(\theta)] = Y_1(\theta), \tag{62}$$

$$L[X_2(\theta)] = Y_2(\theta). \tag{63}$$

The following must hold for a linear system:

$$L[X_1(\theta) + X_2(\theta)] = Y_1(\theta) + Y_2(\theta). \tag{64}$$

Referring now to equation (8) which can be written in the form

$$\frac{dY}{d\theta} + XY + Y = X\,, \tag{65}$$

gives

$$\frac{dY_1}{d\theta} + X_1Y_1 + Y_1 = X_1\,, \tag{66}$$

and

$$\frac{dY_2}{d\theta} + X_2Y_2 + Y_2 = X_2\,. \tag{67}$$

From equation (64)

$$\frac{d(Y_1 + Y_2)}{d\,\theta} + (X_1 + X_2)(Y_1 + Y_2) + (Y_1 + Y_2) = X_1 + X_2 \,. \qquad (68)$$

Adding equations (66) and (67) gives:

$$\frac{dY_1}{d\theta} + \frac{dY_2}{d\theta} + X_1Y_1 + X_2Y_2 + Y_1 + Y_2 = X_1 + X_2 \,. \qquad (69)$$

For linearity, equation (68) and (69) must be equal. This condition is true only if

$$(X_1 + X_2)(Y_1 + Y_2) = X_1Y_1 + X_2Y_2 \,, \qquad (70)$$

which is not the case, and the system is therefore non linear.

In process dynamics, as linear systems can be readily treated, non linear systems are usually treated as linear systems with the hope that the result will adequately describe the non linear case. Equation (8) can be linearized by various assumptions and approximations. One method for linearizing the equation is by means of a power series expansion in which only the linear terms are retained (2, 8, 9). Hence

$$f\,[\,(x_o+h),(y_o+k)] = f(x_o,y_o) + h\left(\frac{\partial f}{\partial x}\right)_{x_o,y_o} + k\left(\frac{\partial f}{\partial y}\right)_{x_o,y_o} + \cdots \,. \qquad (71)$$

Again, the variables can be written as the sum of an unsteady state variation and steady state components:

$$T = T^* + T_s \,, \qquad (14)$$

and

$$W = W^* + W_s \,. \qquad (15)$$

Then

$$f\,[\,(X_o + h),(Y_o + k)\,] = \frac{dT^*}{d\theta} \,, \qquad (72)$$

$$f(X_o, Y_o) = \left(\frac{dT^*}{d\theta}\right)_s = 0 , \tag{73}$$

$$h\left(\frac{\partial f}{\partial x}\right)_{x_o, y_o} = -\left(\frac{W_s + UA/C_p}{\rho V}\right) T^* , \tag{74}$$

and

$$k\left(\frac{\partial f}{\partial y}\right)_{x_o, y_o} = -\left(\frac{T_s - T_i}{\rho V}\right) W^* . \tag{75}$$

Substituting equations (72), (73), (74), and (75) into equation (71) yields:

$$\frac{dT^*}{d\theta} + \left(\frac{W_s + UA/C_p}{\rho V} \right) T^* = -\left(\frac{T_s - T_i}{\rho V} \right) W^* . \tag{76}$$

The partial derivatives in equations (74) and (75) were evaluated under steady state conditions. Taking the Laplace Transform of equation (76) gives:

$$sT^*(s) + k_1 T^*(s) = k_2 W^*(s) , \tag{77}$$

or

$$\frac{T^*}{W^*}(s) = \frac{k_2}{s + k_1} , \tag{78}$$

where $k_2 = \left(\frac{T_i - T_s}{\rho V}\right)$ and $k_1 = \left(\frac{W_s + UA/C_p}{\rho V}\right)$. Here k_1 is the reciprocal of the time constant.

To point out more clearly the result of linearizing equation (8) by means of the power series, the problem will be attacked in a different manner. Substitution of equations (14) and (15) into equation (8) gives:

$$\frac{dT^*}{d\theta} = \frac{(W^* + W_s)(T_i - T^* - T_s)}{\rho V} - \frac{UA(T^* + T_s - T_c)}{\rho V C_p} . \tag{79}$$

At steady state conditions:

$$0 = \frac{W_s(T_i - T_s)}{\rho V} - \frac{UA(T_s - T_c)}{\rho VC_p} . \qquad (80)$$

Subtracting equation (80) from equation (79) yields:

$$\frac{dT^*}{d\theta} = \frac{W^*(T_i - T^* - T_s)}{\rho V} - \frac{W_s T^*}{\rho V} - \frac{UAT^*}{\rho VC_p} . \qquad (81)$$

This equation can be rearranged to give:

$$\frac{dT^*}{d\theta} + \frac{W^*T^*}{\rho V} + \left(\frac{W_s + UA/C_p}{\rho V}\right) T^* = \left(\frac{T_i - T_s}{\rho V}\right) W^* . \qquad (82)$$

When

$$\frac{W^*T^*}{\rho V} = 0 , \qquad (83)$$

equation (82) reduces to equation (76). Hence, linearization by means of a power series expansion in which only the linear terms are retained assumed that $\frac{W^*T^*}{\rho V} = 0$

Derivation of Equation Describing System No. 2

Equation (8) is again applicable:

$$\frac{dT}{d\theta} = \frac{W(T_i - T)}{\rho V} - \frac{UA(T - T_c)}{\rho VC_p} , \qquad (8)$$

or

$$\frac{dT}{d\theta} + \left(\frac{W + UA/C_p}{\rho V}\right) T = \frac{UAT_c}{\rho VC_p} + \frac{WT_i}{\rho V} . \qquad (84)$$

In system No. 2 the desired input forcing function is T_c and the output variable is T. However, T_c cannot be varied directly. T_c is indirectly varied by varying the coolant pressure P_c. Hence, T_c must be expressed in terms of P_c. A linear relationship will be assumed, i. e.:

$$T_c = mP_c + n . \qquad (85)$$

Substitution of equation (85) into equation (84) gives:

$$\frac{dT}{d\theta} + \left(\frac{W + UA/C_p}{\rho V} \right) T = \frac{mUAP_c}{\rho VC_p} + \frac{nUA}{\rho VC_p} + \frac{WT_i C_p}{\rho VC_p} \; . \tag{86}$$

Equation (86) does not allow superposition. This may be demonstrated as before.

$$L(\text{Input}) = \text{Output} \; , \tag{61}$$

$$L[X_1(\theta)] = Y_1(\theta) \; , \tag{62}$$

$$L[X_2(\theta)] = Y_2(\theta) \; , \tag{63}$$

and for a linear system:

$$L[X_1(\theta) + X_2(\theta)] = Y_1(\theta) + Y_2(\theta) \; . \tag{64}$$

Equation (86) may be put into the form:

$$\frac{dY}{d\theta} + k_1 Y = KP_c + K_1 \; . \tag{87}$$

Applying equations (62), (63), and (64) gives:

$$\frac{dY_1}{d\theta} + k_1 Y_1 = KP_{c_1} + K_1 \; , \tag{88}$$

$$\frac{dY_2}{d\theta} + k_1 Y_2 = KP_{c_2} + K_1 \; , \tag{89}$$

and

$$\frac{d(Y_1 + Y_2)}{d\theta} + k_1(Y_1 + Y_2) = K(P_{c_1} + P_{c_2}) + K_1 \; . \tag{90}$$

Equation (86) allows superposition only is the sum of equations (88) and (89) equals equation (90) which is not the case.

If the variables are again expressed as the sum of an unsteady state variation and a steady state component:

$$T = T^* + T_s \; , \tag{14}$$

and

$$P_c = P^*_c + P_{cs} \; , \tag{91}$$

and upon substituting equations (14) and (91) into equation (86) gives:

$$\frac{dT^*}{d\theta} + k_1 T^* + k_1 T_s = KP^*_c + KP_{cs} + K_1 . \tag{92}$$

At steady state:

$$k_1 T_s = KP_{cs} + K_1 . \tag{93}$$

Subtracting equation (93) from equation (92) gives:

$$\frac{dT^*}{d\theta} + k_1 T^* = KP^*_c . \tag{94}$$

Taking the Laplace Transform of equation (94) yields:

$$\frac{T^*}{P^*_c}(s) = \frac{K}{s + k_1} , \tag{95}$$

where $k_1 = \dfrac{(W + UA/C_p)}{\rho V}$ and $K = \dfrac{mUA}{\rho V C_p}$. Equation (95) is the desired input and output relationship for system No. 2.

If P_c is known as a function of time, then equation (86) could be solved by the integrating factor method. The pulses used in the experimental work are not known analytically; therefore, no attempt was made to obtain an analytic solution of equation (86).

CHAPTER VI

RESULTS

Results of Analytic Solution Describing System No. 1

The analytic solution of the equation describing system No. 1 is:

$$T^*(\theta) = \frac{-k_3\beta}{k_1} \mathrm{Im}B_2 + \sum_{n=0}^{\infty} B_{2+4n} e^{s_{2+4n}\theta}$$

$$+ \sum_{n=0}^{\infty} B_{3+4n} e^{s_{3+4n}\theta} \quad . \tag{56}$$

Equation (56) can be written as

$$T^*(\theta) = \frac{-k_3\beta}{k_1} \mathrm{Im}B_2 + B_2 e^{-j\omega\theta} + B_3 e^{j\omega\theta}$$

$$+ \sum_{n=1}^{\infty} B_{2+4n} e^{s_{2+4n}\theta} + \sum_{n=1}^{\infty} B_{3+4n} e^{s_{3+4n}\theta} \quad . \tag{96}$$

The coefficients B_2 and B_3 are complex conjugates and can be written:

$$B_2 = \left| B_2 \right| e^{-j\,\phi_2} \ , \tag{97}$$

$$B_3 = \left| B_3 \right| e^{-j\,\phi_3} \ , \tag{98}$$

and

$$\left| B_2 \right| = \left| B_3 \right| \quad . \tag{99}$$

Hence:

$$B_2e^{-j\omega\theta} + B_3e^{j\omega\theta} = \left|B_2\right| \left[e^{-j(\omega\theta + \phi_2)} + e^{j(\omega\theta - \phi_3)}\right] . \tag{100}$$

But

$$\phi_2 = 2\Pi - \phi_3 . \tag{101}$$

Substituting equation (101) into equation (100) gives:

$$\begin{aligned} &\left|B_2\right| \left[e^{j(\omega\theta - \phi_3)} + e^{-j(\omega\theta + \phi_2)}\right] \\ &= \left|B_2\right| \left[e^{-j(\omega\theta + 2\Pi - \phi_3)} + e^{j(\omega\theta - \phi_3)}\right] \\ &= \left|B_2\right| \left[e^{-j(\omega\theta - \phi_3)} e^{-2\Pi j} + e^{j(\omega\theta - \phi_3)}\right] . \end{aligned} \tag{102}$$

But

$$e^{-2\Pi j} = 1, \tag{103}$$

so that equation (102) reduces to:

$$\left|B_2\right| \left[e^{j(\omega\theta - \phi_3)} + e^{-j(\omega\theta - \phi_3)}\right] = 2\left|B_2\right| \cos(\omega\theta - \phi_3) , \tag{104}$$

or

$$\left|B_2\right| \left[e^{j(\omega\theta - \phi_3)} + e^{-j(\omega\theta - \phi_3)}\right] = 2\left|B_2\right| \sin\left(\omega\theta + \frac{\Pi}{2} - \phi_3\right) . \tag{105}$$

Substituting equation (105) into equation (96) gives:

$$\begin{aligned} T^*(\theta) = &\frac{-k_3\beta}{k_1} \mathrm{Im}B_2 + 2\left|B_2\right| \sin\left(\omega\theta + \frac{\Pi}{2} - \phi_3\right) \\ &+ \sum_{n=1}^{\infty} B_{2+4n}e^{s_{2+4n}\theta} + \sum_{n=1}^{\infty} B_{3+4n}e^{s_{3+4n}\theta} . \end{aligned} \tag{106}$$

Repeating the procedure for the coefficients B_6 and B_7 gives:

$$T^*(\theta) = \frac{-k_3\beta}{k_1} \mathrm{Im}B_2 + 2\left|B_2\right| \sin\left(\omega\theta + \frac{\Pi}{2} - \phi_3\right)$$

$$+ 2\left|B_6\right| \sin\left(2\omega\theta + \frac{\Pi}{2} - \phi_7\right) + \sum_{n=2}^{\infty} B_{2+4n} e^{s_{2+4n}\theta}$$

$$+ \sum_{n=2}^{\infty} B_{3+4n} e^{s_{3+4n}\theta} \quad , \tag{107}$$

and in general:

$$T^*(\theta) = \frac{-k_3\beta}{k_1} \operatorname{Im}B_2 + 2\left|B_2\right| \sin\left(\omega\theta + \frac{\Pi}{2} - \phi_3\right)$$

$$+ 2\left|B_6\right| \sin\left(2\omega\theta + \frac{\Pi}{2} - \phi_7\right) + \ldots + 2\left|B_{2+4n}\right| \sin\left(n\omega\theta + \frac{\Pi}{2} - \phi_{3+4n}\right). \tag{108}$$

The absolute values of the first several coefficients at various frequencies have been calculated and are listed in Table 2.

In Table 3 are tabulated the values of the imaginary part of the B_2 coefficient and values of the constant term.

From Table 2 it is apparent that only the first and second harmonics need be considered. At frequencies greater than 6.28 rad/min., the second harmonic can be dropped at least when the values of k_1, k_2, k_3, and β are approximately those listed at the bottom of Table 2. Table 3 also shows that the constant term can be neglected at frequencies greater than 6.28 rad/min. For the range of values of k_1, k_2, k_3, and β considered, equation (108) reduces to:

$$T^*(\theta) = \frac{-k_3\beta}{k_1} \operatorname{Im}B_2 + 2\left|B_2\right| \sin\left(\omega\theta + \frac{\Pi}{2} - \phi_3\right)$$

$$+ 2\left|B_6\right| \sin\left(2\omega\theta + \frac{\Pi}{2} - \phi_7\right) . \tag{109}$$

For values of k_1, k_2, k_3, and β sufficiently different from those considered, it would be necessary to re-calculate Tables 2 and 3. It may be

TABLE 2

ABSOLUTE VALUES OF THE B_n COEFFICIENTS AT VARIOUS FREQUENCIES

Frequency Rad/min ω	Coefficients					
	B_2	B_6	B_{10}	B_{14}	B_{18}	B_{22}
0.314	1.936	0.2687	0.036	0.004	0.0005	0.00007
0.628	1.902	0.248	0.029	0.003	0.0002	-
1.884	1.630	0.139	0.009	-	-	-
3.140	1.312	0.077	0.003	-	-	-
6.280	0.808	0.026	-	-	-	-
18.84	0.292	0.003	-	-	-	-
31.40	0.177	0.001	-	-	-	-
62.80	0.088	-	-	-	-	-
125.60	0.044	-	-	-	-	-

$k_1 = 2.86$ $k_2 = 5.90$ $k_3 = 0.43$ $\beta = 1.89$

TABLE 3

VALUES OF CONSTANT TERM AT VARIOUS FREQUENCIES

Frequency Rad/min ω	$-\text{Im } B_2$	Constant Term
0.314	1.861	0.528
0.628	1.36	0.388
1.884	0.884	0.251
3.14	0.335	0.095
6.28	0.044	-
18.84	0.016	-
31.40	0.004	-
62.80	-	-
125.60	-	-

$k_1 = 2.86$ $k_2 = 5.90$ $k_3 = 0.43$ $\beta = 1.89$

necessary in certain cases to retain more than the first and second harmonics.

Analysis and Results of the Experimental and Analog Computer Data

Frequency Response Data

The frequency response data were analyzed primarily for magnitude ratio and phase angle information. The magnitude ratios and phase angles were then plotted versus frequency to give the familiar Bode plot. From the Bode plots the order of the system, the system time constant, and the frequency independent factor were ascertained. The equivalent transfer function for the system was also obtained from these plots.

Such non linear effects as appeared were analyzed. The non linear effects appear primarily as a shifting of the Bode plot curves with variations in the amplitude of the sinusodial input forcing function. This shifting of the Bode plot curves results in a variation of the system time constant and frequency independent factor. In non linear systems a pure sinusodial input forcing function will not necessarily give rise to a pure sinusodial output. The time record of the frequency response data was therefore examined for such effects.

Bode plots constructed from frequency response data taken on the analog computer are shown in Figures 24, 25, 26, 27, and 28 of Appendix D.

The experimental Bode plots are shown in Figures 29, 30, and 31 of Appendix D.

Order of the System

An examination of the Bode plots readily shows that the system can be very closely approximated by a first order transfer function. For a first order system the magnitude ratio must have a limiting slope of minus six decibels per octave and the phase angle must level off at minus 90 degrees. Both of these conditions are closely approximated as can be seen from the Bode plots in Appendix D. These conditions are also in agreement with the power series approximation which predicts (equation 78) a first order system.

Time Constants

The time constants were obtained from both the magnitude ratio and phase angle portions of the Bode plot. The time constant is the reciprocal of the break frequency. The time constants were obtained by asymptotic approximation from the magnitude ratio portion of the Bode plot. On the phase angle portion of the Bode plot, the time constant is, of course, the reciprocal of the frequency corresponding to minus 45 degrees.

In obtaining time constants by the asymptotic approximation method, the magnitude ratio portion of the Bode plot is frequently normalized. In this case the normalization would amount to plotting the ratio:

$$\frac{\left[\frac{T}{W}(s)\right]_{\omega}}{\left[\frac{T}{W}(s)\right]_{\omega=0}} \, . \qquad (110)$$

The normalization is desired because the absolute value of the frequency independent factor is sometimes not known with certainty. The frequency independent factor for the normalized plot is equal to unity. The normalization procedure is legitimate for linear systems, but caution must be used with non linear systems. In non linear systems the value of

$\left[\frac{T}{W}(s)\right]_{\omega=0}$ is not necessarily a constant. For this reason the Bode plots have not been normalized.

A comparison of the magnitude ratio portion of the Bode plots constructed from the experimental data, analog data, and the values calculated by the power series approximation are shown in Figure 14. The three curves almost coincide. A comparison of the other Bode plots in Appendix D shows that the analog data and the experimental data are in good agreement at least insofar as magnitude ratio is concerned. The magnitude ratio calculated from the power series approximation will, of course, not vary with changes in amplitude.

A comparison of the phase angle portion of the bode plots constructed from the experimental and analog data, and from values calculated from equation (78), is shown in Figure 15. A variation in these curves is noted.

Table 4 summarizes the time constants obtained from the Bode plots. The experimental time constant is about five seconds greater than the time constant obtained from the analog data, and about four seconds greater than the time constant calculated from equation (78). The time constants obtained from both the magnitude ratio and phase angle portions of the Bode plots are seen to decrease with amplitude.

Frequency Independent Factor

The frequency independent factor is the value of the transfer function at zero frequency, i. e.,

$$\left[\frac{T}{W}(s)\right]_{\omega=0} . \qquad (111)$$

The frequency independent factors were obtained from the magnitude ratio

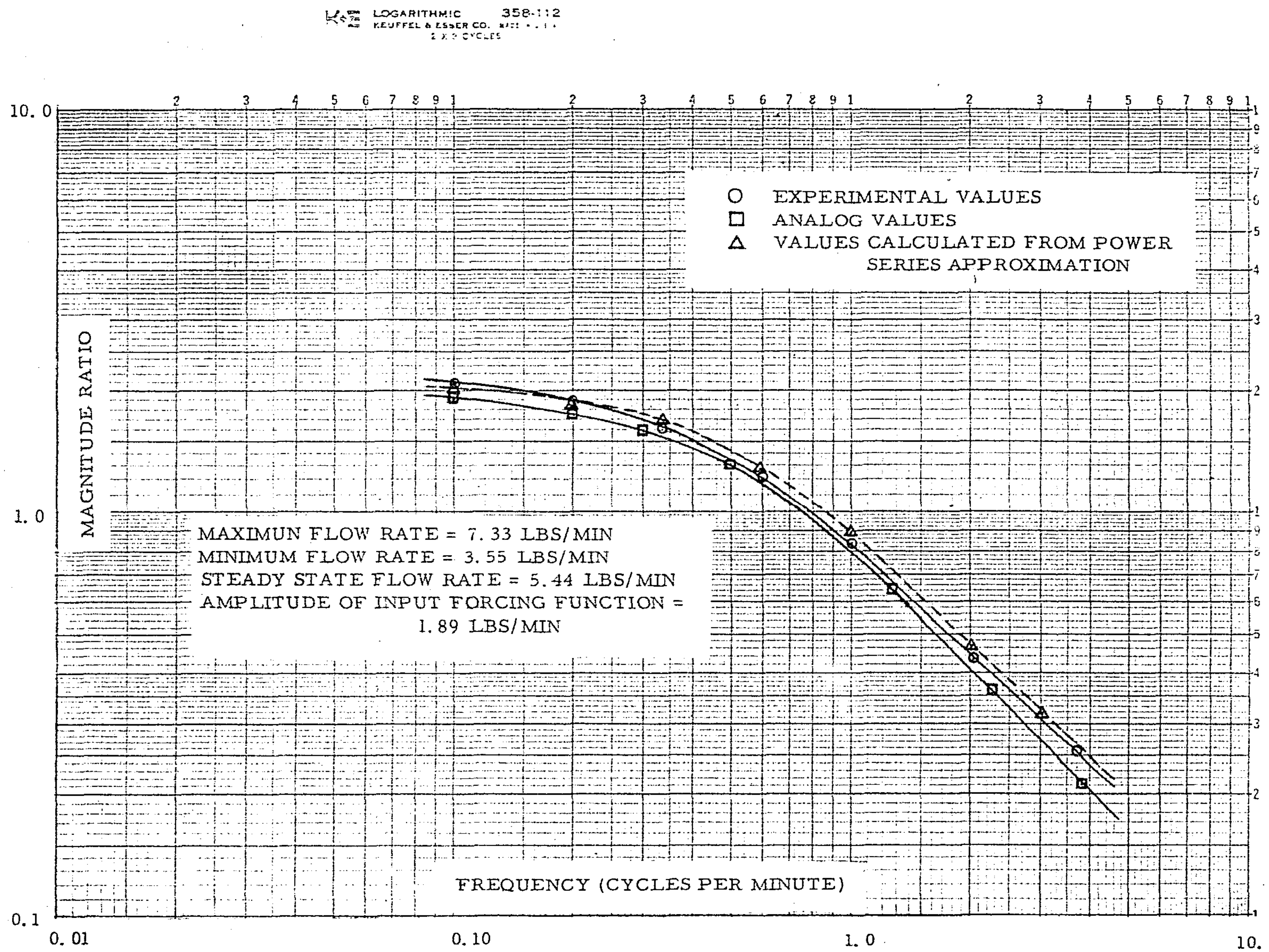

Figure 14. Comparison of Amplitude Ratios Obtained from Experimental and Analog Data, and from Power Series Approximation

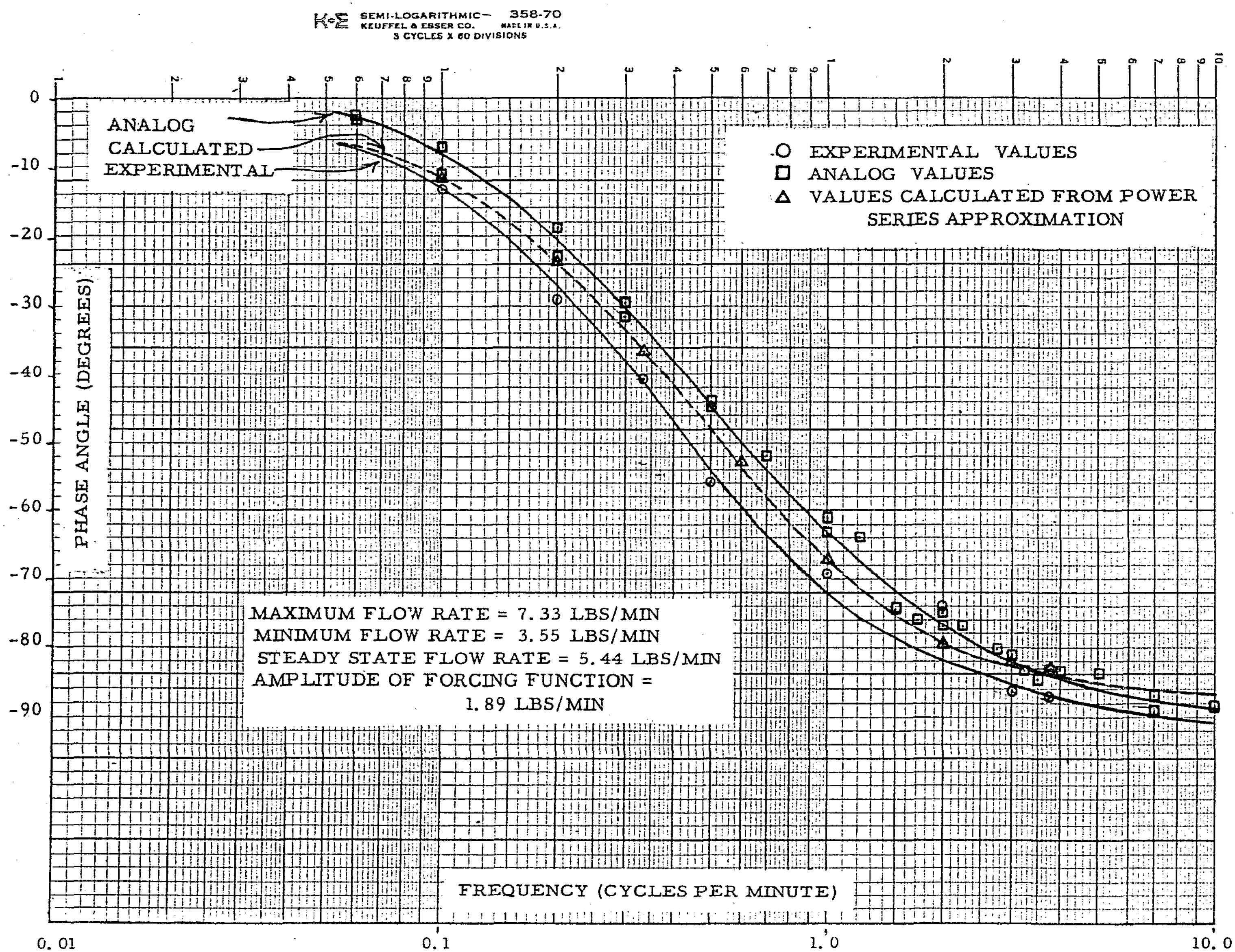

Figure 15. Comparison of Phase Angles Obtained from Experimental and Analog Data, and from Power Series Approximation

TABLE 4

TIME CONSTANTS OBTAINED FROM FREQUENCY RESPONSE DATA

Amplitude of Sinusodial Input (lbs/sec)	Frequency $\omega = 1/\tau$ (Cycles/min)	Time Constant τ (sec)
Time Constants Obtained from Magnitude Ratio Portion of Bode Plots for Analog Computer Data:		
0.0394	0.47	20.3
0.0315	0.46	20.7
0.0237	0.46	20.7
0.0157	0.45	21.2
0.0079	0.44	21.7
Time Constants Obtained from Phase Angle Portion of Bode Plots for Analog Computer Data:		
0.0394	0.52	18.40
0.0315	0.50	19.1
0.0237	0.48	19.9
0.0157	0.475	20.1
0.0079	0.470	20.3
Time Constants Obtained from Magnitude Ratio Portion of Bode Plots for Experimental Data:		
0.0315	0.38	25.1
0.0237	0.38	25.1
0.0157	0.40	23.9
Time Constants Obtained from Phase Angle Portion of Bode Plots for Experimental Data:		
0.0315	0.39	24.5
0.0237	0.40	23.9
0.0157	0.43	22.2

Calculated Time Constant

$$\tau = \frac{\rho V C_p}{W_s C_p + UA} = 21.0 \text{ sec}$$

portion of the Bode plots.

The trouble that can arise from normalizing a Bode plot is readily apparent when the frequency independent factor is considered.

$$\frac{\left[\frac{T}{W}(j\omega)\right]_{\omega}}{\left[\frac{T}{W}(j\omega)\right]_{\omega=0}} = \frac{\frac{k_2}{j\omega + k_1}}{\frac{k_2}{k_1}} = \frac{k_1}{j\omega + k_1} . \qquad (112)$$

Hence, the factor k_2 does not appear in the normalized Bode plot. A normalized Bode plot used to compare experimental data and theoretical calculations is only good in comparing time constants. A transfer function obtained from a normalized Bode plot can be greatly in error.

Table 5 summarizes the frequency independent factors obtained from the Bode plots. Also the frequency independent factor calculated from equation (78) is given in Table 5. Some variation in the frequency independent factor with amplitude is noted.

Non Linearities

The variations in time constants and frequency independent factors noted previously are non linear effects. One pronounced non linear effect appeared at low frequencies. At low frequencies a pure sinusodial input did not give rise to a pure sinusodial output. The output was rather a distorted sine wave. Figure 16 shows the effect on the analog computer. The wavy line superimposed on the output curve is 60 cycle pick up. For the experimental apparatus, a distortion was also noted in the output sine wave as shown in Figure 17. This effect is to be expected from consideration of the steady state relationship between W and T, i.e.:

$$T_s = \frac{W_s C_p T_i + UAT_c}{W_s C_p + UA} . \qquad (113)$$

TABLE 5

FREQUENCY INDEPENDENT FACTORS

Amplitude of Sinusodial Input (lbs/sec)	Frequency Independent Factor (degree-min/lb)
Frequency Independent Factor Obtained from Bode Plots for Analog Computer Data:	
0.0315	2.0
0.0237	1.8
0.0157	1.9
0.0079	2.1
Frequency Independent Factor Obtained from Bode Plots for Experimental Data:	
0.0315	2.15
0.0237	2.09
0.0157	2.14
Frequency Independent Factor Calculated from Power Series Approximation:	
	2.10

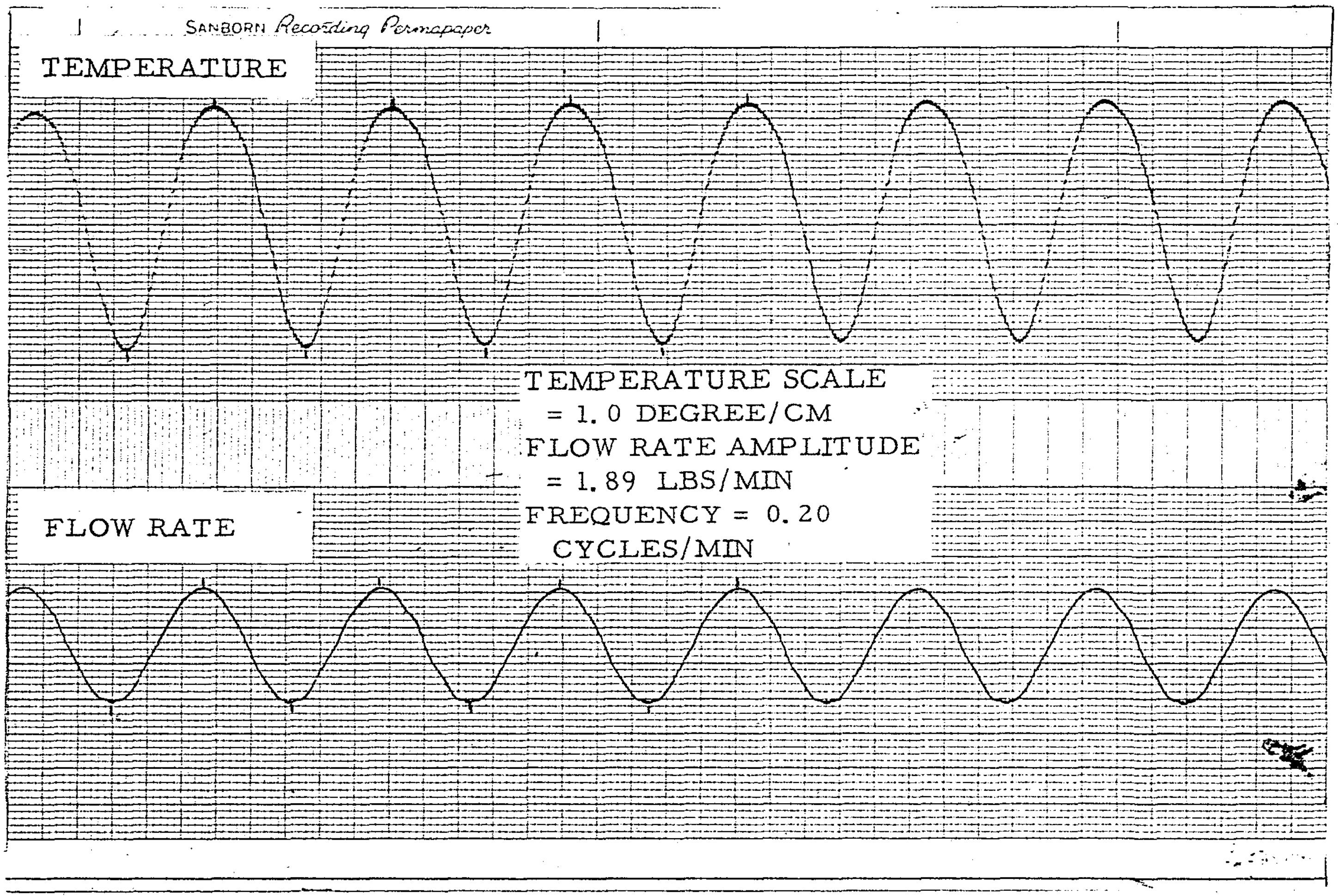

Figure 16. Sample of Analog Data for Low Frequency Sinusodial Input

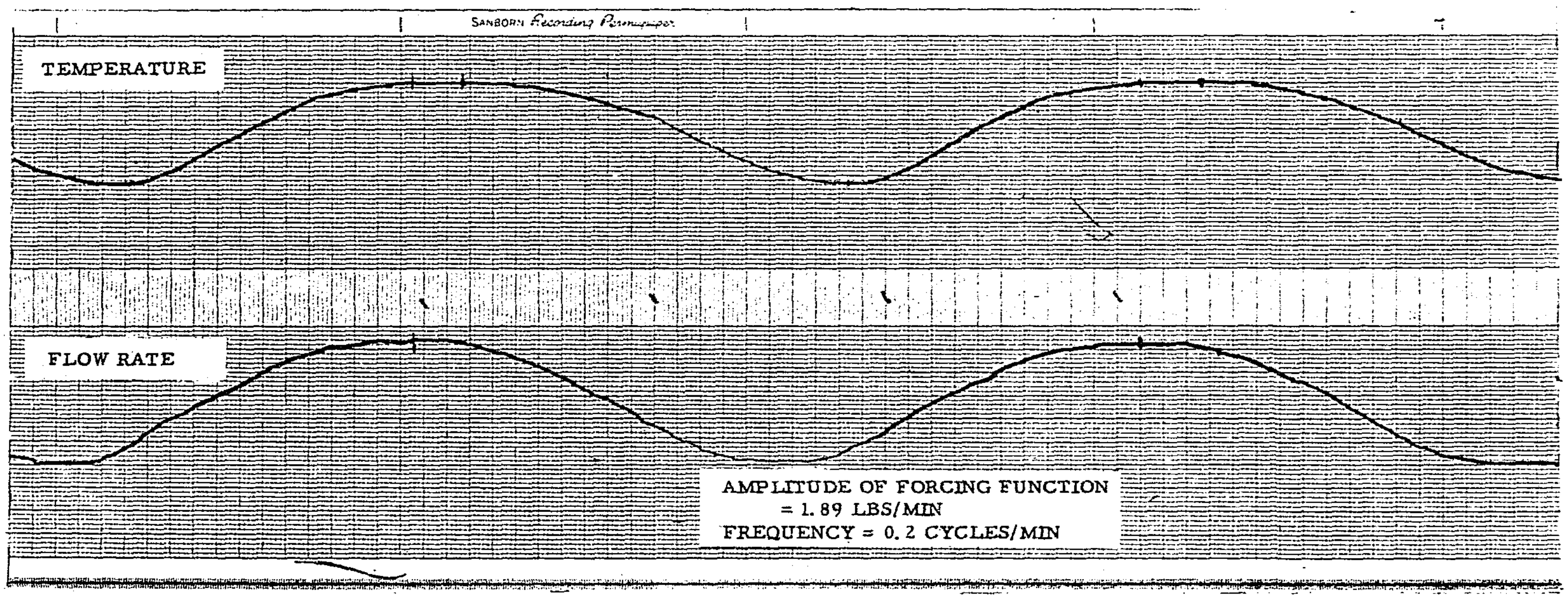

Figure 17. Sample of Experimental Data for Low Frequency Sinusodial Input

Equation (113) is non linear. At the low frequencies the temperature at any instant is closely approaching the steady state value corresponding to the flow rate at that instant. It is to be pointed out here that at low frequencies the temperature will average slightly higher than would be predicted from equation (113) if the average flow rate over the interval were used as the steady state value.

The distortion of the output is precisely calculated from equation (109). Figure 18 shows a comparison of the output calculated from equation (109) with that obtained on the analog computer. The values obtained on the analog computer are listed in Table 23.

Some variation with amplitude of the magnitude ratio curves were observed at low frequencies. This variation is shown in Figure 19.

In connection with variations in the magnitude ratio curves and the phase angle curves shown in Figures 14 and 15, equation (109) gives some very interesting information. It is obvious from Figures 16, 17, and 18 that both the amplitude ratio and the phase angle depend upon the location at which they were measured, i. e., whether measurements were taken from peak to peak or elsewhere. Table 6 lists the amplitude ratio taken at various locations, and for several frequencies, obtained from Phasor plots of equation (109). The calculated variation for the magnitude ratio is not very large. Table 7 compares the variations shown in Figure 14 with those calculated. The values shown in Figure 14 are average values obtained from various points of several cycles. It must be pointed out that the variations shown in Table 6 have nothing to do with experimental error. These variations will exist even if the ex-

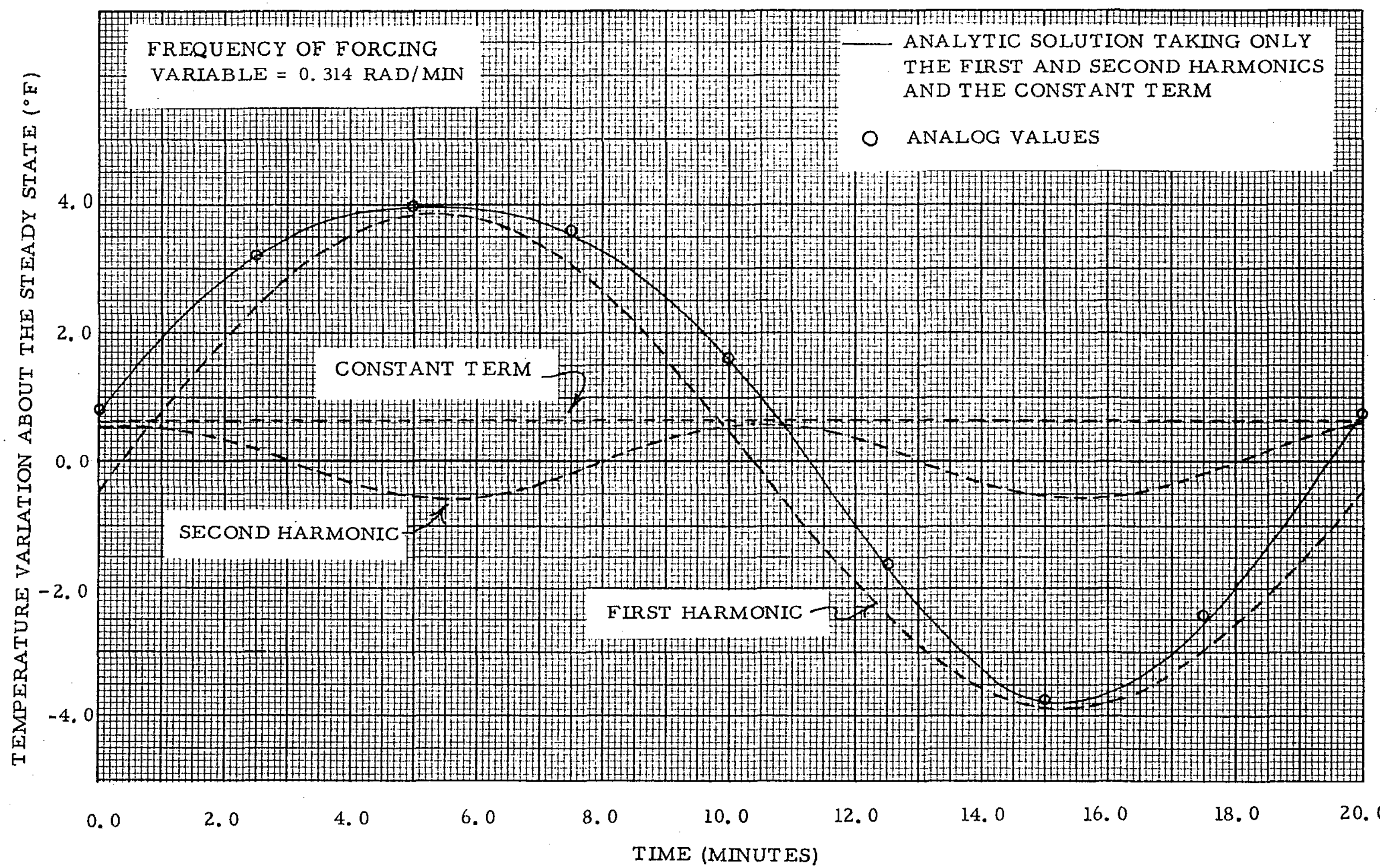

Figure 18. Comparison of Theoretically Calculated Output with Values Obtained from Analog Computer for Low Frequency Input

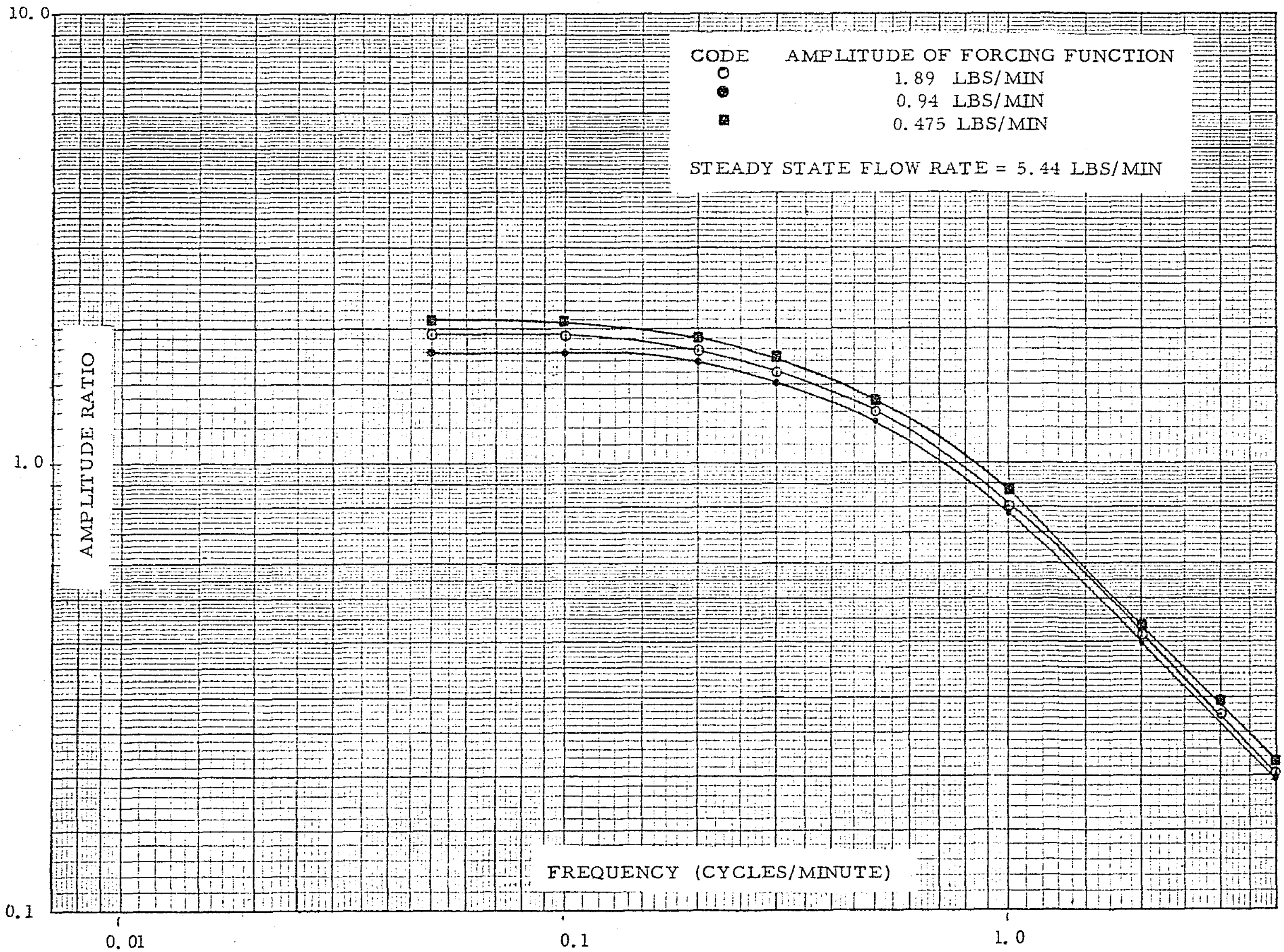

Figure 19. Variation of Magnitude Ratio with Variation of Amplitude of Forcing Function

TABLE 6

VARIATION IN AMPLITUDE RATIO WITH POSITION OF MEASUREMENT

Time (min)	Magnitude Ratio	Limits of Variation
Frequency = 0.314 rad/min		
0	2.16	1.99 - 2.16
2	2.17	
4	2.09	
6	2.06	
8	2.08	
10	2.10	
12	2.05	
14	1.99	
16	2.00	
18	2.07	
Frequency = 0.628 rad/min		
0	2.07	1.96 - 2.07
2	2.04	
4	2.04	
6	1.99	
8	1.96	
Frequency = 1.884 rad/min		
0	1.80	1.72 - 1.80
2	1.75	
4	1.73	
6	1.73	
8	1.72	

TABLE 7

COMPARISON OF VARIATIONS IN FIGURE 14 WITH THOSE CALCULATED FROM EQUATION (109)

Frequency rad/min	Variations in Figure (14)	Calculated Variations
0.314	1.99 → 2.16	2.01 –
0.628	1.96 → 2.07	1.88 → 2.05
1.884	1.72 → 1.80	1.78 → 1.84

perimental error is zero.

In Table 8 are listed the variations in phase angle calculated from equation (109). A surprisingly large variation is noticed. This large variation might explain the deviation noticed in Figure 15.

It is interesting to note that equation (109) might be used to place reliability limits to a Bode plot.

Transfer Function

In a non linear system it is not theoretically correct to speak of a transfer function. The amplitudes of the signal used to excite the system were, in this case, quite large. As long as only small disturbances are being considered, then a transfer function could be used to approximate the behavior of the system at least insofar as frequency response is concerned. The transfer function derived from the power series approximation seems to represent adequately the system if the disturbances are kept small. The transfer function obtained from the power series expansion is:

$$\frac{T^*}{W^*}(j\,\omega) = \frac{k_2}{j\omega + k_1} ; \tag{114}$$

where

$$k_2 = \frac{C_p(T_i - T_s)}{\rho\, VC_p} , \tag{115}$$

and

$$k_1 = \frac{W_s C_p + UA}{\rho\, VC_p} . \tag{116}$$

Step Response Data

Both time constants and frequency independent factors were taken from the step response data. In doing so the system was assumed to be of

TABLE 8

VARIATIONS IN PHASE ANGLE WITH TIME, CALCULATED FROM EQUATION (109)

Time (min)	Phase Angle (degrees)	Limits of Variation (degrees)
Frequency = 0.314 rad/min		
0	10	$-22.2 \rightarrow +10$
2	8.6	
4	1.0	
6	-9.3	
8	-18.4	
10	-22.2	
12	-20.5	
14	-14.2	
16	-3.5	
18	6.0	
Frequency = 0.628 rad/min		
0	8.8	$-20.7 \rightarrow 8.8$
2	0.8	
4	-17.5	
6	-20.7	
8	-3.2	

first order. For a first order system, the time constant for a step input is the time required for 63.2 per cent of the total change to occur. The frequency independent factor is simply the total change in the output variable divided by the total change in the input variable.

The time constants obtained from the step response data are given in Table 9. The frequency independent factors obtained from the step response data are summarized in Table 10. Variations in the time constants and the frequency independent factors with the magnitude of the displacement are seen. This variation is a non linear effect and is to be expected. The time constant and frequency independent factor obtained from the power series approximation, given in Tables 11 and 12, both contain a term for the steady state flow rate. The frequency independent factor also contains a term for the steady state temperature. In step response both the steady state flow rate and steady state temperature change.

Comparison of Frequency Response and Step Response Data

In non linear systems the same result will not necessarily be obtained with one type of input forcing function as will be obtained with some other type of input forcing function. Therefore, the two different types of responses were studied for the purpose of comparison.

Figure 20 shows a comparison of the time constants obtained from the step function response, calculated from $\tau = \dfrac{\rho V C_p}{W_s C_p + UA}$, the time constant for a linear system, and the time constants obtained by frequency response. The variation in the time constants shown by the step response data is to be expected by considering the time constant obtained

TABLE 9

TIME CONSTANTS OBTAINED FROM STEP RESPONSE DATA

Magnitude of Step Displacement (lbs/sec)	Time Constant (sec)
-0.0059	22.0
-0.0154	23.9
-0.0239	26.5
-0.0315	29.5
-0.0405	27.0
0.0078	21.25
0.0157	19.25
0.0253	18.75
0.0313	18.50
0.0393	16.75

TABLE 10

FREQUENCY INDEPENDENT FACTORS OBTAINED FROM STEP RESPONSE DATA

Displacement (lb/sec)	Frequency Independent Factor (degree-min/lb)
-0.0405	3.22
-0.0315	2.91
-0.0239	2.62
-0.0154	2.45
-0.0059	2.34
0.0078	1.88
0.0157	1.81
0.0253	1.69
0.0313	1.59
0.0393	1.52

TABLE 11

TIME CONSTANT CALCULATED FROM POWER SERIES APPROXIMATION

Magnitude of Step Displacement (lbs/sec)	Time Constant τ (sec)
-0.04	32.4
-0.03	28.7
-0.02	25.6
-0.01	23.0
0.01	19.20
0.02	17.80
0.03	16.50
0.04	15.40

TABLE 12

FREQUENCY INDEPENDENT FACTOR CALCULATED FROM POWER SERIES APPROXIMATION

Displacement (lb/sec)	Frequency Independent Factor (degree-min/lb)
-0.0405	4.97
-0.0315	4.03
-0.0239	3.32
-0.0154	2.80
-0.0059	2.39
0.0078	1.80
0.0157	1.58
0.0253	1.40
0.0313	1.25
0.0393	1.12

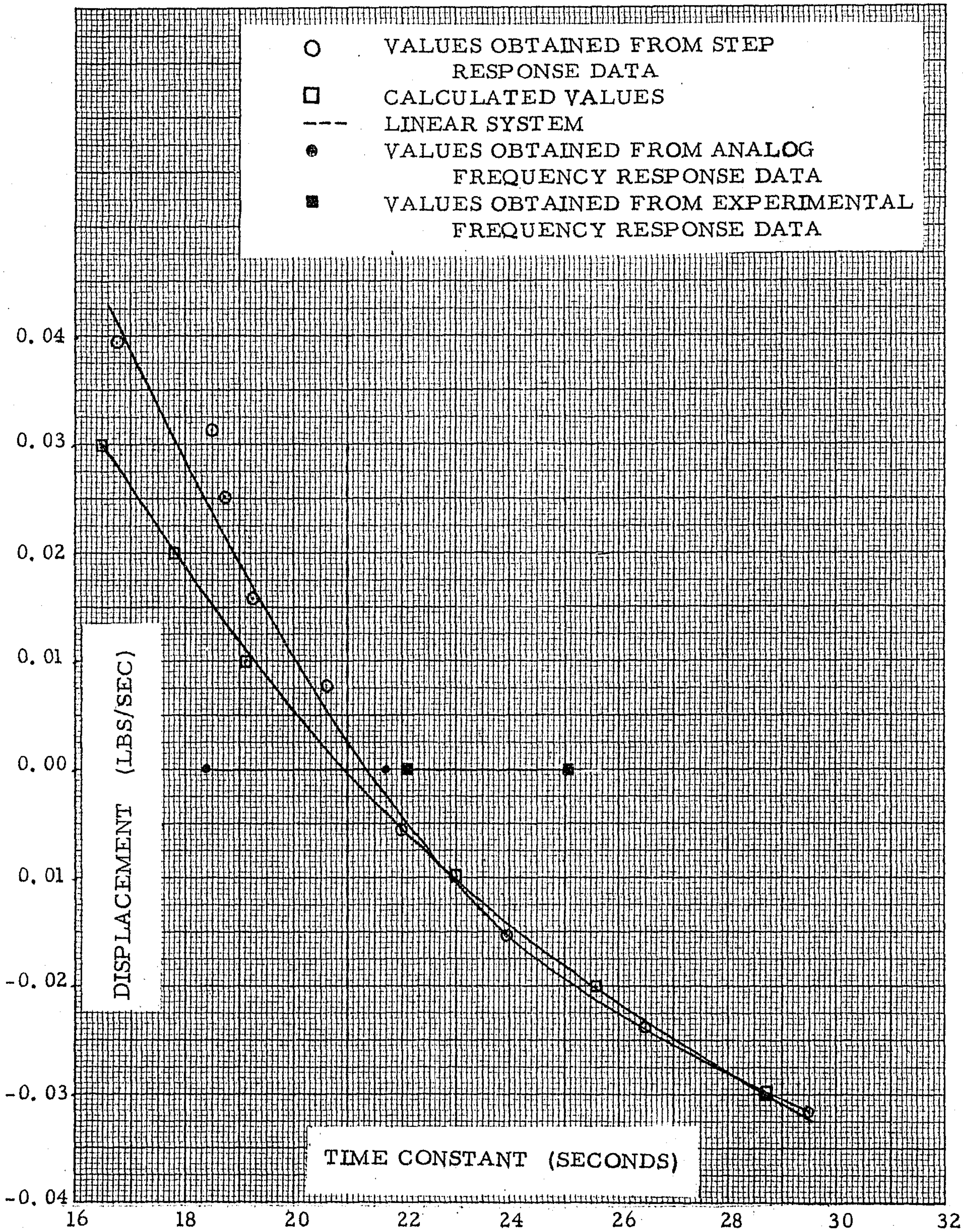

Figure 20. Time Constant Variation

by the power series approximation. This time constant contains the steady state flow rate term which, of course, changes with step response. The trend of the change in time constant for step response is predicted fairly well by the time constant obtained from the power series approximation. The time constant for a linear system must be, of course, a constant. The one shown was calculated for zero displacement and corresponds to the theoretical frequency response time constant. The time constants for the experimental and analog frequency response appear as a horizontal line because the average displacement is zero for all amplitudes with frequency response. The deviation from a linear system is quite noticeable at the larger displacements (both positive and negative). For small displacements the step function time constant, frequency response time constant and the time constant obtained for the linear case are all nearly the same. Therefore, for small upsets a linear approximation would be good, but for large upsets a linear approximation could give rise to difficulties.

Figure 21 shows the frequency independent factors obtained by step function response, experimental and analog data, and that calculated from the power series approximation. The frequency independent factor contains both the steady state temperature and the steady state flow rate. The frequency independent factors calculated from $\frac{C_p(T_i - T_s)}{W_s C_p + UA}$ for the frequency response corresponds to that observed. However, the frequency independent factors calculated from $\frac{C_p(T_i - T_s)}{W_s C_p + UA}$ for the step response predicts a greater change than actually occurred. In either case the deviation at larger displacements between the frequency independent factors

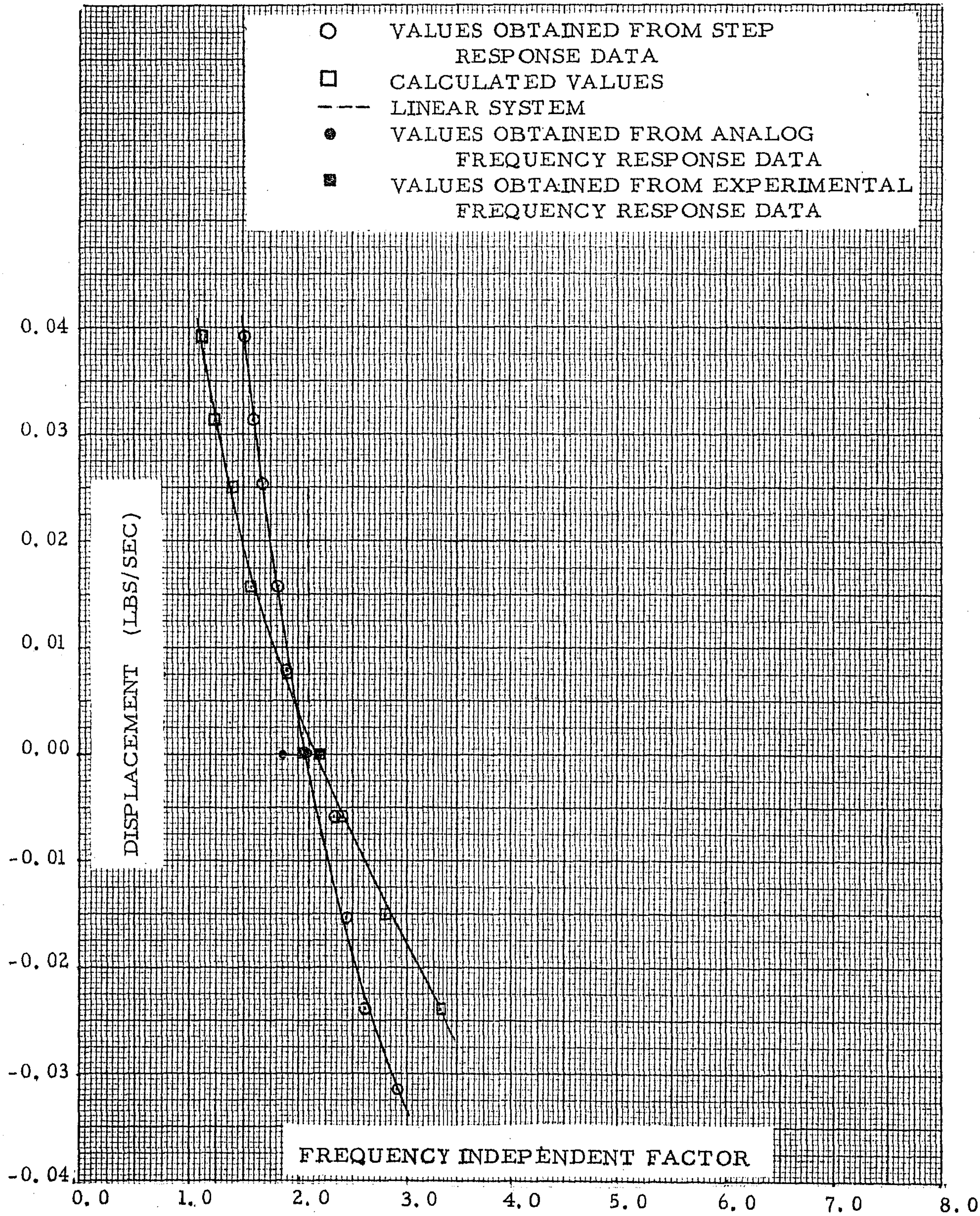

Figure 21. Frequency Independent Factor Variation

obtained by step response and those obtained by frequency response is noticeable. Again at small displacements the frequency independent factors obtained from step response, frequency response, and calculated from the power series approximation are in good agreement. Therefore, for small upsets the linear approximation holds fairly well, but for large upsets trouble may arise.

System No. 2

The pulse response data were converted to frequency response data by means of the Fourier integral. That is, a variable $F(\theta)$ which is a function of time can be converted into a function of frequency $F(j\omega)$ by:

$$F(j\omega) = \int_{-\infty}^{\infty} F(\theta)e^{-j\omega\theta}\, d\theta \approx \int_{-\theta}^{\theta} F(\theta)e^{-j\omega\theta}\, d\theta \; . \tag{117}$$

In terms of the variables under consideration we have:

Output variable

$$T(j\omega) = \int_{-\theta}^{\theta} T(\theta)e^{-j\omega\theta}\, d\theta \quad , \tag{118}$$

and

Input variable

$$P_c(j\omega) = \int_{-\theta}^{\theta} P_c(\theta)e^{-j\omega\theta}\, d\theta \quad . \tag{119}$$

The transfer function is then given by:

$$\frac{T}{P_c}(j\omega) = \frac{\int_{-\theta}^{\theta} T(\theta)e^{-j\omega\theta}\, d\theta}{\int_{-\theta}^{\theta} P_c(\theta)e^{-j\omega\theta}\, d\theta} \quad . \tag{120}$$

A program for making these computations was available for use on an IBM 650 computer. The experimental pulse response data are tabulated in Table 17 and 18 of Appendix B. The values of the variables at $\theta = 0$ were subtracted from the data and the resulting numbers were fed into the computer. The computed results are tabulated in Table 19 of Appendix B.

Figures 22 and 23 are Bode plots for system No. 2. In Figures 22 and 23 the transformed frequency response data are compared with frequency response values calculated from equation (95). Pertinent data regarding the theoretical calculations are given in Table 21 of Appendix C. The magnitude ratios are in fair agreement. A considerable deviation is seen in the phase angle plots. The deviation indicates the presence of dead time. In the pulse data listed in Tables 17 and 18 of Appendix B, the presence of six seconds of dead time is observed. Dead time affects only the phase angle portion of the Bode plot. Figures 22 and 23 show calculated frequency response curves including dead time. The dead time calculations bring the experimental and the theoretical curves into better agreement.

Some deviations between the theoretical and the experimental curves in Figures 22 and 23 are still noted; but in view of the uncertainties involved in the Fourier transformation, the results are considered to be good. Thus, for small disturbances system No. 2 can be represented by a first order system with dead time; that is,

$$\frac{T^*}{P_c^*}(j\omega) = \frac{Ke^{-j\omega t}}{j\omega + k_1} \; ; \qquad (121)$$

where

$$k_1 = \frac{W + UA/C_p}{\rho V} , \qquad (122)$$

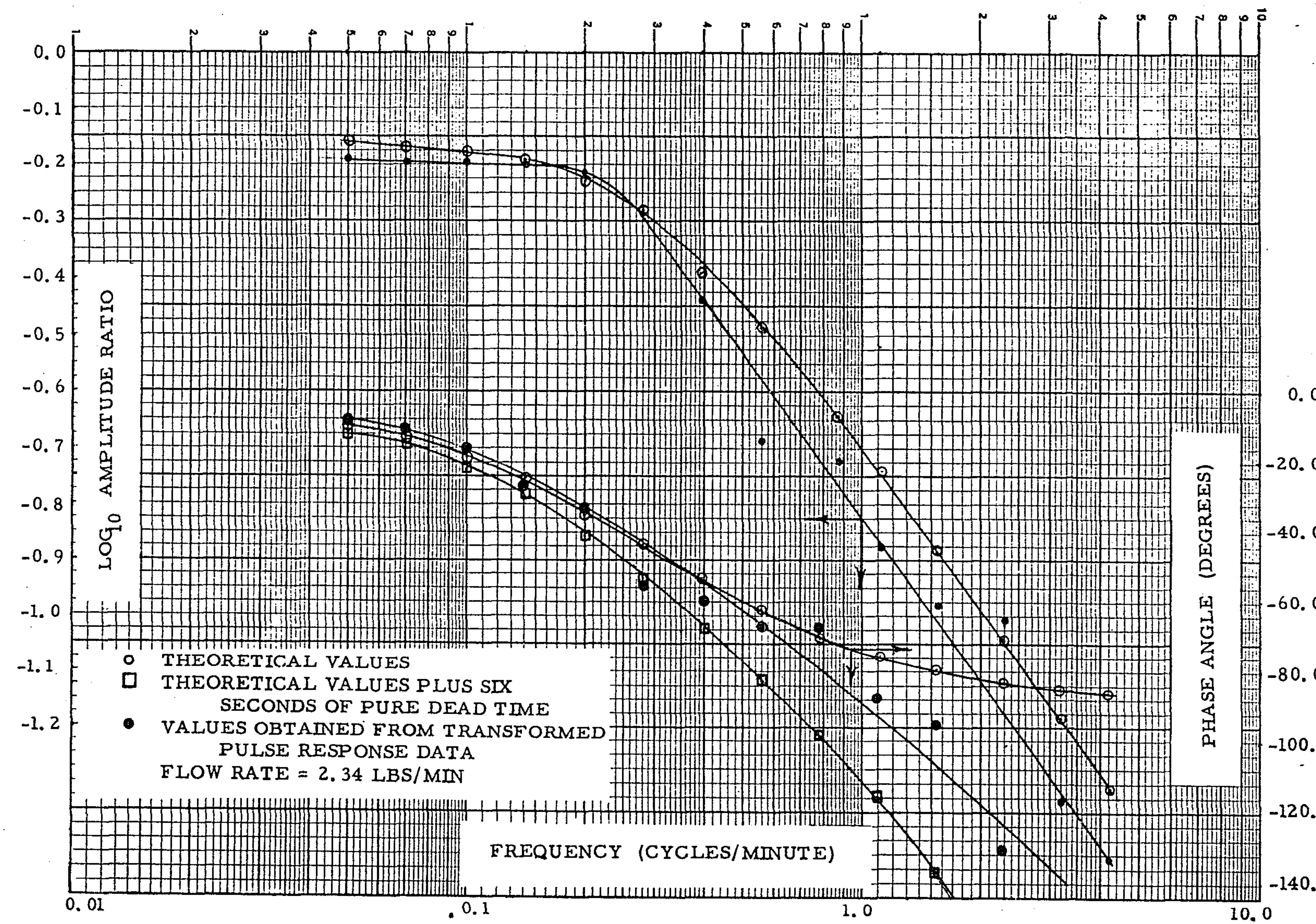

Figure 22. Comparison of Theoretically Calculated Frequency Response Values with Frequency Response Values Obtained from Transformed Pulse Response Data

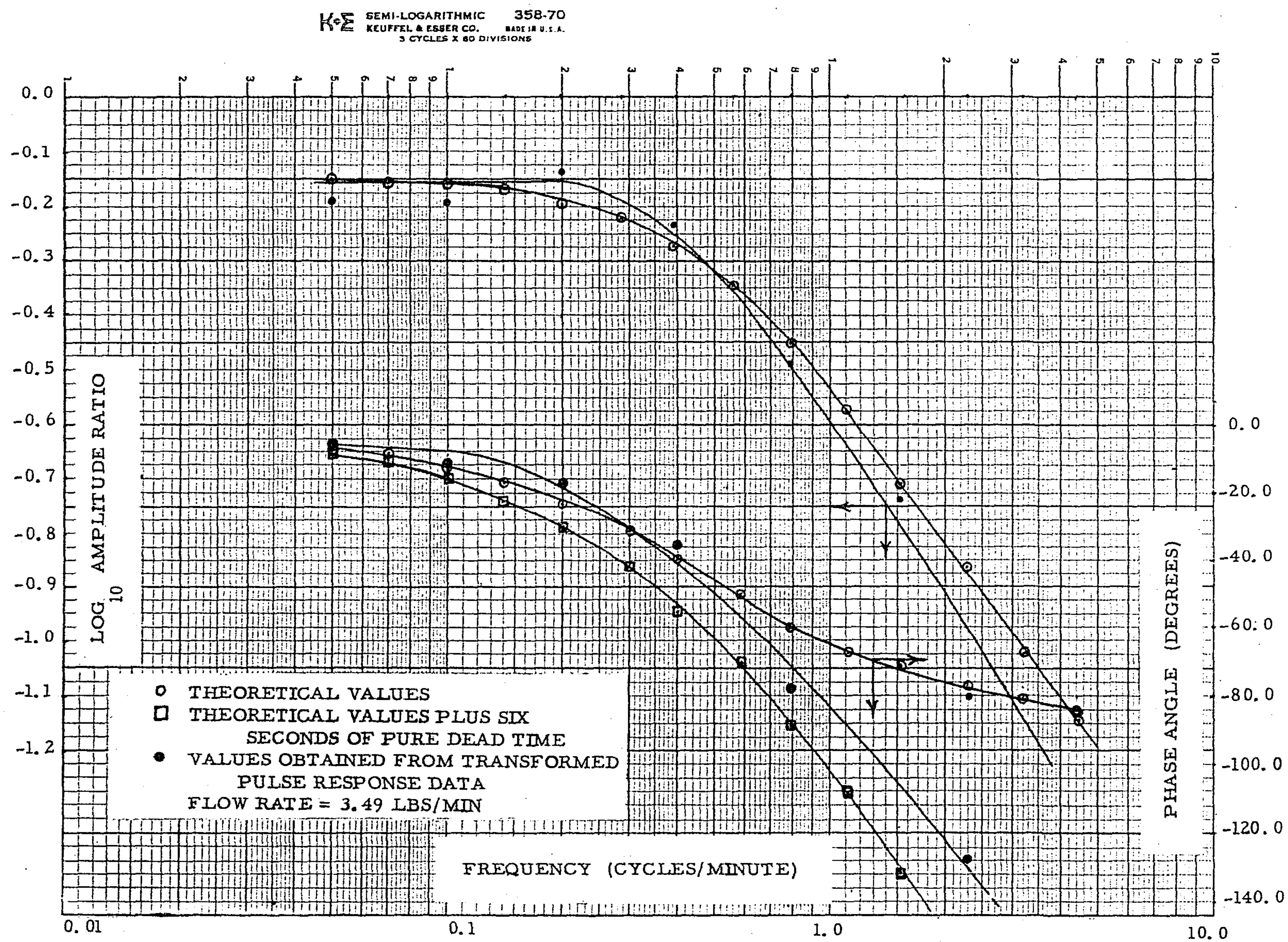

Figure 23. Comparison of Theoretically Calculated Frequency Response Values with Frequency Response Values Obtained from Transformed Pulse Response Data

$$K = \frac{mUA}{\rho VC_p} , \qquad (123)$$

and where t is the dead time. The dead time would have to be determined for each apparatus. It is seen that system No. 2 has the same time constant as system No. 1. The experimental and the theoretical frequency independent factors are in good agreement. The assumption of a linear relation between the coolant pressure and the coolant temperature is supported by these results as this assumption affects only the frequency independent factor.

In the design of a control loop for system No. 2, the time required for the pressure wave to travel from the control valve to the vessel must be taken into account.

Both of the systems studied are inherently stable.

CHAPTER VII

CONCLUSIONS

The following conclusions can be drawn from the results of the investigation of system No. 1.

1. In the derivation of equation (8), certain assumptions were made. The assumptions were (a) the only two variables were the flow rate W and the fluid temperature T, and (b) perfect mixing. The results show that these assumptions are valid under the conditions studied.

2. The analytic solution to equation (8) for a sinusodial input is:

$$T^*(\theta) = \frac{-k_3\beta}{k_1}\,\mathrm{Im}B_2 + \sum_{n=0}^{\infty} B_{2+4n}e^{s_{2+4n}\theta}$$

$$+ \sum_{n=0}^{\infty} B_{3+4n}e^{s_{3+4n}\theta} \quad . \tag{56}$$

3. The analytic solution consists of a constant term and all harmonics. For the problem studied only the constant term and the first and second harmonics need be considered. Thus, for the conditions studied the analytic solution reduces to:

$$T^*(\theta) = \frac{-k_3\beta}{k_1}\,\mathrm{Im}B_2 + 2\left|B_2\right|\sin\left(\omega\theta + \frac{\Pi}{2} - \phi_3\right)$$

$$+ 2 \left| B_6 \right| \sin \left(2 \omega\theta + \frac{\Pi}{2} - \phi_7\right) . \tag{109}$$

For conditions other than those studied, higher ordered terms may have to be considered.

4. Magnitude ratios and phase angles are dependent upon the position of measurement. Equation (109) can be employed to calculate the variation and to establish reliability limits to the Bode plots of frequency response data for system No. 1.

5. The constant term and the second harmonic, whose presence has not been discussed in the literature, can be neglected at frequencies above 6.28 radians per minute. At frequencies below 6.28 radians per minute the constant term and the second harmonic should be considered if the disturbances are large.

6. For large disturbances variations in the frequency independent factor and the system time constant are observed. These variations are to be expected.

In the case of a sinusodial disturbance, the output is distorted at low frequencies. This distortion is caused by the system closely approaching the steady state value for the flow rate at any given time. The distortion is predicted from equation (109) by the second harmonic. The distortion can be precisely calculated from equation (109).

7. For small disturbances the power series approximation holds and the system can be represented by a first order transfer function. Namely,

$$\frac{T^*}{W^*} (j \omega) = \frac{k_2}{j\omega + k_1} ; \tag{114}$$

where

$$k_2 = \frac{C_p(T_i - T_s)}{\rho VC_p} , \tag{115}$$

and

$$k_1 = \frac{W_s C_p + UA}{\rho VC_p} . \tag{116}$$

The system time constant is the reciprocal of k_1. The power series approximation neglects the term W^*T^* in equation (20) and is the equivalent of considering only the first harmonic in equation (109). Both k_1 and k_2 contain the steady state values W_s and T_s. Therefore, the value of k_1 and k_2 will change with any disturbance that caused a change in the steady state values W_s and T_s.

With large vessels, the WT term in equation (20) can be neglected because the coefficient $(\frac{1}{\rho V})$ of the WT term is small in comparison with the remaining terms in equation (20).

The following conclusions can be drawn from the results of the investigation of system No. 2.

1. Equation (8) is applicable for system No. 2. Equation (8) applied to system No. 2 involves the following assumptions: (a) the only variables are the coolant temperature T_c and the fluid temperature T, and (b) perfect mixing. In addition, the assumption of a linear relationship between coolant temperature and coolant pressure was made. That is:

$$T_c = mP_c + n . \tag{85}$$

The results indicate that these assumptions are valid under the conditions studied.

2. System No. 2 can be represented by a first order transfer function with a pure time delay. That is,

$$\frac{T^*}{P^*_c}(j\omega) = \frac{Ke^{-j\omega t}}{j\omega + k_1} ; \qquad (121)$$

where

$$k_1 = \left(\frac{W_s + UA/C_p}{\rho V}\right) , \qquad (122)$$

and

$$K = \frac{mUA}{\rho V C_p} . \qquad (123)$$

The time constant, the reciprocal of k_1, is the same for system No. 1 and system No. 2. However, in system No. 2 the time constant does not contain the steady state value of a variable.

SUMMARY

A study was made of the dynamic heat removal from a jacketed, agitated vessel. Heat was removed from the vessel by means of utilizing the heat of vaporization of a liquid boiling in the jacket surrounding the vessel.

From the standpoint of input and output relationships, two different systems were considered. In the first system, the input or forcing variable was the flow rate of the liquid entering the vessel and the output variable was the temperature of the fluid inside the vessel. Both analog computer and experimental studies were made. Frequency response and step response techniques were used. The differential equation describing the system was solved mathematically for a sinusodial input. The mathematical solution shows the presence of a constant term and two harmonics in the output. The presence of the constant term and the two harmonics was observed experimentally at low frequencies. At frequencies above 6.28 radians per minute, the constant term and the second harmonic can be neglected. For small disturbances the analog and experimental results showed that the system can be represented by a first order transfer function.

In the second system studied, the input variable was the coolant pressure and the output variable was the temperature of the fluid in the

vessel. The pulse response technique was employed in the study of this system. The results showed that the system could be represented by a first order transfer function with pure dead time.

BIBLIOGRAPHY

1. Acton, F. S., and Lapidus, L., Ind. Eng. Chem., Vol. 47 (1955), pp. 706-710.

2. Aris, R. and Amundson, N. R., Chem. Eng. Prog., Vol. 53 (May, 1957), pp. 227-230.

3. Aris, R., and Amundson, N. R., Chem. Eng. Sci., Vol. 7, No. 3 (1958), pp. 121-154.

4. Aris, R., and Amundson, N. R., Chem. Eng. Sci., Vol. 9 (1959), pp. 250-262.

5. Aronson, M. H., Instr. and Automation, Vol. 30 (1957), pp. 237-239.

6. Bathe, T. L., Franks, R. G., and James, E. W., "Analog Computer Simulation of a Chemical Reactor," ISA Journal, Vol. 4 (January, 1957), pp. 14-18.

7. Beutler, J. A., and Roberts, J. B., "Electronic Analog in Reactor Design," Chem. Eng. Prog., Vol. 52, No. 2 (1956), pp. 69F-74F.

8. Bilous, O., and Amundson, N. R., AIChE Journal, Vol. 1, No. 4 (1955), pp. 513-521.

9. Bilous, O., and Amundson, N. R., AIChE Journal, Vol. 2, No. 1 (1956), pp. 117-126.

10. Bilous, O., Block, H. D., and Piret, E. L., AIChE Journal, (1957), pp. 248-261.

11. Brown, G. S., and Campbell, D. P., Principles of Servomechanisms, New York: John Wiley and Sons, 1948.

12. Campbell, D. P., Process Dynamics, New York: John Wiley and Sons, 1958.

13. Cannon, K. J., and Denbigh, K. G., "Studies on Gas-Solid Reactions; Causes of Thermal Instability," Chem. Eng. Sci., Vol. 6 (1957), pp. 155-159.

14. Carslaw, H. S., and Jaeger, J. C., Conduction of Heat in Solids, London: Oxford University Press, 1947.

15. "Computers, Mathematics, Statistics, and Automation," Ind. Eng. Chem., Vol. 49, No. 3 (1957), pp. 554-564.

16. Danckwerts, P. V., Chem. Eng. Sci., Vol. 2 (1953), p. 1.

17. Danckwerts, P. V., Jenkins, J. W., and Place, G., Chem. Eng. Sci., Vol. 3 (1954), p. 26.

18. Deisler, P. F., Jr., and Wilheim, R. H., Ind. Eng. Chem., Vol. 45 (1953), p. 1219.

19. Dreifke, G. E., Hougen, J. O., and Williams, T. J., Chem. Eng. News, Vol. 35 (July 15, 1957), p. 38.

20. Eckman, D. P., Automatic Process Control, New York: John Wiley and Sons, 1958.

21. Eckman, D. P., and Lefkowitz, I., "Automatic Control of a Chemical Process," Control Engineering, Vol. 4 (September, 1957), pp. 197-204.

22. Ehrenfeld, J. R., "The Dynamics and Control of Chemical Processes," MIT Thesis, Cambridge, Massachusetts, (1957).

23. Ellingsen, W. R., and Ceaglske, N. H., "Control-System Design for a Chemical Process by the Root-Locus Method," AIChE Journal, Vol. 5, No. 1 (1959), pp. 30-36.

24. Fanning, R. J., "The Dynamic Heat Transfer Characteristics of a Continuous Agitated Tank Reactor," Ph. D. Thesis, University of Oklahoma, Norman, Oklahoma, (1958).

25. Fanning, R. J., and Sliepcevich, C. M., "The Dynamics of Heat Removal from a Continuous Agitated Tank Reactor," AIChE Journal, (June, 1959), pp. 240-248.

26. Gardner, M. F., and Barnes, J. L., Transients in Linear Systems, New York: John Wiley and Sons, 1942.

27. Ham, A., and Coe, H. S., Chem. and Met. Eng., Vol. 19 (1918), p. 663.

28. Head, F. E., "Determination of the Performance Function of Mixing in a Model of a Tubular Reactor," M. S. Thesis, St. Louis University, St. Louis, Missouri, (1959).

29. Higgins, T. J., Trans. Am. Soc. Mech. Eng., Vol. 79 (1957), pp. 445-453.

30. Hirniak, J., Z. for Physik Chemi., Vol. 75 (1908), pp. 675-680.

31. Hoelscher, H. E., "Temperature Stability of Fixed-bed Catalytic Reactors," Chem. Eng. Sci., Vol. 6 (1957), pp. 183-189.

32. Johnson, J. D., and Edwards, L. J., Trans. Faraday Soc., Vol. 45 (1949), p. 286.

33. Kandiner, H. J., Chem. Eng. Prog., Vol. 44 (1948), p. 383.

34. Kramers, H. and Alberda, G., Chem. Eng. Sci., Vol. 2 (1953), p. 173.

35. Lewis, L. G., Instr. and Automation, Vol. 31, No. 4 (1958), pp. 644-647.

36. Lotka, A. J., J. Phys. Chem., Vol. 14 (1910), p. 271 ff.

37. Lotka, A. J., Z. fur Physik Chemi., Vol. 72 (1910), pp. 508-511.

38. MacMullin, R. B., and Weber, M., Jr., Trans. Am. Inst. Chem. Engrs., Vol. 31 (1935), p. 409.

39. Marr, G. R., Jr., and Johnson, E. F., "The Dynamics of Stirred-Tank Reactors," Symposium on Process Dynamics, Part II, Fifty-Second Meeting of the American Institute of Chemical Engineers, (1959).

40. Mason, D. R., and Piret, E. L., Ind. Eng. Chem., Vol. 42 (1950), pp. 817-825.

41. Mason, D. R., and Piret, E. L., Ind. Eng. Chem., Vol. 43 (1951), pp. 1210-1219.

42. Oncutt, J. C., and Lamb, D. E., "Stability of a Fixed-bed Catalytic Reactor System with Feed-Effluent Heat Exchange," Paper submitted at 41st National Meeting of the AIChE at St. Paul, Minn., (1959).

43. Prausnitz, J. M., and Wilhelm, R. H., Ind. Eng. Chem., Vol. 49 (1957), p. 978.

44. "Process Control," Ind. Eng. Chem., Vol. 50, No. 3 (1958), pp. 520-524; Vol. 51, No. 3 (1959), pp. 432-436.

45. "Process Control Round Table Discussion," Chem. Eng. Prog., Vol. 53, (May, 1957), p. 209-.

46. Roberts, J. B., Johnson, E. J., and others, Chem. Eng. Prog., Vol. 54, No. 9 (1958), pp. 37-57.

47. Roberts, S. M., and Laspe, C. G., "Development of on-line Computer Control Equations for a Thermal Cracking Reaction," Paper submitted at the 41st National Meeting of the AIChE at St. Paul, Minn.,(1959).

48. Romano, R. C., Ph. D. Thesis, University of Delaware, (June, 1958).

49. Savant, C. J., Basic Feedback Control System Design, New York: McGraw-Hill Book Company, Inc., 1958.

50. Shinskey, F. G., "Temperature Control in Gas Phase Reactors," Paper submitted at 41st National Meeting of the AIChE at St. Paul, Minn., (1959).

51. Smith, O. J. M., "Closer Control of Loops with Dead Time," Chem. Eng. Prog., Vol. 53 (May, 1959), pp. 217-219.

52. Stout, T. M., Trans. Am. Soc. Mech. Eng., Vol. 79 (1957), pp. 497-508.

53. Thaler, G. J., and Brown, R. G., Servomechanism Analysis, New York: McGraw-Hill Book Company, Inc., 1953.

54. Tierney, John W., Homan, C. J., Nemanic, D. J., and Amundson, N. R., "The Digital Computer as a Process Controller," Control Engineering, Vol. 4 (1957), pp. 166-175.

55. Tolin, E. D., and Fleugel, D. A., "An Analog Computer for on-line Control of a Chemical Reactor," Paper submitted at the 41st National Meeting of the AIChE at St. Paul, Minn., (1959).

56. Truxal, J. G., Control System Synthesis, New York: McGraw-Hill Book Company, Inc., 1955.

57. von Heerden, C., "The Character of the Stationary State of Exothermic Processes," Chem. Eng. Sci., Vol. 8 (1958), pp. 133-143.

58. Weber, E., "Complex Convolution Applied to Nonlinear Problems," Proceedings of the Symposium on Nonlinear Circuit Analysis, Brooklyn Polytechnic Institute, Vol. 6 (1956).

59. Williams, T. J., Blake, J. H., and others, Education on Process Control, New York: AIChE publication, 1958.

60. Woods, F. A., Ind. Eng. Chem., Vol. 50 (1958), pp. 1631-1635.

61. Young, D., University of Oklahoma, private communication.

APPENDIX A

Nomenclature

NOMENCLATURE

A = Heat transfer area, square feet

B_n = Coefficients of exponential expansion

C_p = Heat capacity, BTU/lb-^{o}F

F = Functional notation

Im = Imaginary part of a complex number

K = $\frac{mUA}{\rho VC_p}$

K_1 = $\frac{nUA + WT_i}{\rho VC_p}$

L = Linear operator notation

P_c = Coolant pressure, psia

P_c^* = Unsteady state variation in coolant pressure, psia

P_{cs} = Steady state coolant pressure, psia

T = Temperature of fluid in agitated vessel, ^{o}F

T_c = Coolant temperature, ^{o}F

T_i = Inlet fluid temperature, ^{o}F

T_n = Fluid temperature converted to analog scale, volts

T_o = Outlet fluid temperature, ^{o}F

T_{ref} = Reference temperature, ^{o}F

T_s = Steady state temperature, ^{o}F

T^* = Unsteady state variation of fluid temperature, ^oF

U = Overall heat transfer coefficient, BTU/min-sq.ft.-^oF

V = Volume of agitated vessel, ft^3

W = Flow rate, lbs/min

W_n = Flow rate, converted to analog scale, volts

W_s = Steady state flow rate, lbs/min

W^* = Unsteady state variation of flow rate, lbs/min

X = Variable notation

Y = Variable notation

a = Scale factor for analog computer

b_1 = Scale factor for analog computer

b_2 = Scale factor for analog computer

c = Scale factor for analog computer

f = Functional notation

h = Constant in power series expansion

j = $\sqrt{-1}$

k = Constant in power series expansion

k_1 = $(W_s C_p + UA)/\rho V C_p$

k_2 = $(T_i - T_s)/\rho V C_p$

k_3 = $1/\rho V C_p$

m = Slope of vapor pressure-temperature curve for linear approximation

n = Constant in linear equation relating vapor pressure and temperature

s = Complex domain

t = Dead time, min.

x = Variable in power series expansion

y	=	Variable in power series expansion
z	=	Complex variable
β	=	Amplitude of sinusodial input
γ	=	Constant in the integration limits of the complex convolution integral
θ	=	Time, min.
θ_n	=	Analog time, sec.
ρ	=	Density, lbs/ft^3
σ	=	Real part of s
σ_a	=	Abscissas of absolute convergence
τ	=	Time constant, min.
ϕ	=	Phase angle of harmonics
ω	=	Frequency (rad/min)
$\underline{\omega}$	=	Dummy variable in complex convolution

APPENDIX B

Response Data

TABLE 13

FREQUENCY RESPONSE DATA TAKEN ON THE ANALOG COMPUTER

Amplitude of Input Sinusodial Flow Rate = 0.475 lb/min

Frequency (Cycles/minute)	Amplitude Ratio (degree-min/lb)	Phase Angle (degrees)
0.05	2.07	-5.04
0.10	2.06	-8.64
0.20	1.88	-22.60
0.30	1.73	-30.60
0.50	1.39	-42.59
0.70	1.01	-54.40
1.00	0.87	-64.20
1.25	0.68	-66.12
1.50	0.60	-70.18
1.75	0.53	-72.21
2.00	0.46	-77.44
2.25	0.39	-75.56
2.50	0.34	-75.3
2.75	0.34	-76.54
3.00	0.305	-77.15
3.25	0.305	-82.01
3.50	0.260	-80.41
3.75	0.237	-80.40
4.00	0.230	-79.33
5.00	0.179	-79.95
7.00	0.105	-86.47

TABLE 13--Continued

Amplitude of Input Sinusodial Flow Rate = 0.94 lb/min

Frequency (Cycles/minute)	Amplitude Ratio (degree-min/lb)	Phase Angle (degrees)
0.05	1.90	-3.87
0.10	1.85	-10.76
0.20	1.77	-21.93
0.30	1.61	-34.08
0.50	1.30	-46.12
0.70	0.96	-54.35
1.00	0.81	-62.77
1.25	0.65	-68.24
1.50	0.56	-70.59
1.75	0.45	-71.68
2.00	0.44	-73.59
2.25	0.37	-79.76
2.50	0.32	-80.01
2.75	0.29	-78.41
3.00	0.27	-82.94
3.25	0.21	-77.76
3.50	0.21	-82.31
3.75	0.21	-81.18
4.00	0.21	-86.39
5.00	0.16	-85.23
7.00	0.11	-84.12
10.00	0.04	-86.82

TABLE 13--Continued

Amplitude of Input Sinusodial Flow Rate = 1.42 lb/min

Frequency (Cycles/minute)	Amplitude Ratio (degree-min/lb)	Phase Angle (degrees)
0.05	1.8	-3.65
0.10	1.8	-11.8
0.20	1.73	-20.0
0.30	1.55	-31.8
0.50	1.25	-45.8
0.70	0.92	-62.5
1.00	0.78	-65.5
1.25	0.62	-70.1
1.50	0.55	-71.6
1.75	0.46	-73.0
2.00	0.39	-78.4
2.25	0.36	-77.9
2.50	0.32	-81.7
2.75	0.30	-80.0
3.00	0.28	-80.5
3.25	0.23	-79.3
3.50	0.21	-80.8
3.75	0.20	-85.4
4.00	0.20	-84.0
5.00	0.14	-86.9
7.00	0.106	-88.8
10.00	0.071	-86.3

TABLE 13--Continued

Amplitude of Input Sinusodial Flow Rate = 1.89 lb/min

Frequency (Cycles/minute)	Amplitude Ratio (degree-min/lb)	Phase Angle (degrees)
0.05	2.01	-3.43
	1.93	-3.49
0.10	1.88	-10.39
	1.88	-7.01
0.20	1.77	-18.98
	1.79	-23.52
0.30	1.59	-30.96
	1.59	-29.90
0.50	1.27	-45.0
	1.30	-44.56
0.70	0.93	-53.9
1.00	0.80	-61.44
	0.79	-62.71
1.25	0.63	-66.19
1.50	0.57	-75.15
1.75	0.48	-74.71
2.00	0.53	-77.64
	0.41	-75.59
2.25	0.36	-77.14
2.50	0.34	-75.59
2.75	0.32	-80.56
3.00	0.29	-80.83
	0.278	-79.51
3.25	0.246	-83.9
3.50	0.238	-85.4
3.75	0.22	-83.9
4.00	0.20	-83.67
	0.22	-84.11
5.00	0.16	-83.80
	0.12	-83.45
7.00	0.10	-87.12
	0.106	-90.14
10.00	0.079	-78.75
	0.079	-89.90
20.00	0.040	-91.00
	0.038	-91.89

TABLE 13--Continued

Amplitude of Input Sinusodial Flow Rate = 2.364 lb/min

Frequency (Cycles/minute)	Amplitude Ratio (degree-min/lb)	Phase Angle (degrees)
0.05	1.86	-3.53
0.10	1.81	-7.94
0.20	1.60	-23.31
0.30	1.54	-26.47
0.50	1.43	-43.47
0.70	0.855	-58.53
1.00	0.752	-61.56
1.25	0.614	-67.06
1.50	0.530	-69.71
1.75	0.445	-76.59
2.00	0.403	-76.58
2.25	0.340	-78.07
2.50	0.318	-81.35
2.75	0.286	-78.61
3.00	0.244	-77.90
3.25	0.233	-79.54
3.50	0.212	-81.34
3.75	0.192	-82.97
4.00	0.202	-78.09
5.00	0.160	-81.90
7.00	0.102	-87.80
10.00	0.066	-87.60
20.00	0.042	-91.76

TABLE 14

EXPERIMENTAL FREQUENCY RESPONSE DATA

Amplitude of Input Sinusodial Flow Rate = 0.94 lb/min

Frequency (Cycles/minute)	Amplitude Ratio (degree-min/lb)	Phase Angle (degrees)
0.05	2.15	-6.5
0.10	2.10	-12.2
0.20	1.93	-26.4
0.333	1.58	-42.0
0.600	1.33	-55.0
1.000	0.90	-67.2
2.000	0.44	-80.4
3.000	0.28	-81.4
3.650	0.21	-79.0
5.000	0.19	-83.0

TABLE 14--Continued

Amplitude of Input Sinusodial Flow Rate = 1.41 lb/min

Frequency (Cycles/minute)	Amplitude Ratio (degree-min/lb)	Phase Angle (degrees)
0.05	2.0	-6.0
0.10	1.9	-13.0
0.20	1.81	-23.5
0.333	1.65	-40.0
0.600	1.27	-56.0
1.000	0.80	-67.0
2.000	0.37	-79.0
3.000	0.27	-82.5
3.650	0.237	-88.0
5.000	0.15	-87.0

TABLE 14--Continued

Amplitude of Input Sinusodial Flow Rate = 1.89 lb/min

Frequency (Cycles/minute)	Amplitude Ratio (degree-min/lb)	Phase Angle (degrees)
0.1	2.05	-13.6
0.2	1.84	-27.4
0.333	1.58	-40.32
0.6	1.196	-56.04
1.000	0.812	-69.51
2.000	0.429	-74.44
3.000	0.341	-84.20
3.650	0.256	-87.34

TABLE 15

CALCULATED FREQUENCY RESPONSE DATA

Amplitude of Sinusodial Forcing Function = 1.89 lb/min

Frequency (Cycles/minute)	Amplitude Ratio (degree-min/lb)	Phase Angle (degrees)
0.1	2.02	-11.5
0.2	1.89	-23.7
0.333	1.67	-36.2
0.6	1.25	-52.8
1.000	0.855	-65.5
2.000	0.46	-77.15
3.000	0.31	-81.35
3.650	0.257	-82.89

TABLE 16

STEP RESPONSE DATA TAKEN ON THE ANALOG COMPUTER

Initial Flow Rate (lb/min)	Final Flow Rate (lb/min)	Displacement (lb/min)	Response Time (sec)	Response Temperature Scale
5.44	3.08	-2.36	0.00	8.20
			7.10	6.94
			16.00	5.05
			21.20	4.23
			27.00	3.47
			40.10	2.53
			86.50	1.90
5.44	3.55	-1.89	0.00	8.20
			6.30	7.29
			15.00	6.38
			16.00	5.93
			29.50	5.33
			39.60	4.79
			65.00	4.10
			100.00	3.70
5.44	4.02	-1.42	0.00	8.20
			5.80	7.64
			13.50	7.08
			17.70	6.80
			26.50	6.44
			32.40	6.10
			59.80	5.68
			91.50	5.59
5.44	4.50	-0.94	0.00	8.20
			4.00	8.02
			10.60	7.84
			17.30	7.75
			23.90	7.63
			31.40	7.52
			53.40	7.39
			74.60	7.30

TABLE 16--Continued

Initial Flow Rate (lb/min)	Final Flow Rate (lb/min)	Displacement (lb/min)	Response Time (sec)	Response Temperature Scale
5.44	4.97	-0.47	0.00	8.39
			5.40	8.17
			10.20	7.95
			12.50	7.84
			22.00	7.70
			25.20	7.56
			35.20	7.40
			51.50	7.29
5.44	5.92	0.48	0.00	1.10
			5.60	1.56
			12.50	2.02
			16.50	2.25
			21.25	2.50
			34.20	2.83
			57.30	3.17
			84.60	3.30
5.44	6.38	0.94	0.00	1.00
			4.10	1.80
			11.50	2.60
			13.40	3.00
			19.25	3.53
			26.40	4.00
			45.20	4.60
			100.00	5.00
5.44	6.86	1.42	0.00	1.10
			4.10	2.16
			9.60	3.22
			13.10	3.75
			18.75	4.44
			25.10	5.08
			45.20	5.87
			112.00	6.40

TABLE 16--Continued

Initial Flow Rate (lb/min)	Final Flow Rate (lb/min)	Displacement (lb/min)	Response Time (sec)	Response Temperature Scale
5.44	7.33	1.89	0.00	1.10
			3.80	2.32
			8.80	3.54
			12.30	4.15
			18.50	4.94
			25.60	5.68
			42.40	6.59
			87.60	7.20
5.44	7.80	2.36	0.00	1.10
			3.80	2.54
			8.70	3.98
			11.50	4.70
			16.75	5.64
			23.40	6.50
			38.80	7.58
			96.00	8.30

TABLE 17

PULSE DATA

Time (sec)	Temperature °F	Pressure (psig)
0	52.0	15
1	52.0	17.35
2	52.0	18.95
3	52.0	19.66
4	52.0	20.35
5	52.0	20.90
6	52.2	21.35
7	52.5	21.70
8	52.6	21.85
9	52.7	22.05
10	53.0	22.20
11	53.3	22.35
12	53.5	22.55
13	53.6	22.70
14	53.8	22.80
15	53.9	22.95
16	54.0	23.15
17	54.1	23.25
18	54.3	23.40
19	54.4	23.50
20	54.5	23.65
21	54.7	23.75
22	54.8	23.80
23	54.9	24.05
24	55.0	24.15
25	55.1	24.25
26	55.2	24.40
27	55.3	24.50
28	55.4	24.60
29	55.5	24.70
30	55.7	24.8
31	55.7	25.0
32	55.9	25.15
33	56.0	25.25
34	56.2	25.35
35	56.3	25.50
36	56.4	25.60
37	56.6	25.70
38	56.7	25.75
39	56.9	25.85
40	57.0	26.00
41	57.0	26.15

TABLE 17--Continued

Time (sec)	Temperature °F	Pressure (psig)
42	57.1	26.20
43	57.2	26.35
44	57.2	26.40
45	57.3	26.50
46	57.4	26.60
47	57.5	26.70
48	57.6	26.75
49	57.7	26.80
50	57.8	27.00
51	57.9	27.10
52	57.9	27.20
53	58.0	27.25
54	58.1	27.30
55	58.2	27.45
56	58.3	27.55
57	58.3	27.60
58	58.4	27.65
59	58.5	27.70
60	58.5	27.80
61	58.6	27.85
62	58.6	27.90
63	58.6	27.95
64	58.7	27.96
65	58.8	27.98
66	58.9	27.99
67	58.9	28.00
68	59.0	28.00
69	59.1	28.00
70	59.2	28.00
71	59.2	28.00
72	59.3	28.00
73	59.4	28.00
74	59.4	28.00
75	59.4	28.00
76	59.5	28.00
77	59.5	28.00
78	59.6	28.00
79	59.6	28.00
80	59.6	28.00
81	59.7	28.00
82	59.8	28.00
83	59.8	28.00
84	59.8	28.00
85	59.9	28.00

TABLE 17--Continued

Time (sec)	Temperature °F	Pressure (psig)
86	59.9	28.00
87	60.0	28.00
88	60.1	28.00
89	60.1	28.00
90	60.2	28.00
91	60.3	28.00
92	60.3	28.00
93	60.3	28.00
94	60.4	28.00
95	60.4	28.00
96	60.4	28.00
97	60.4	28.00
98	60.4	28.00
99	60.4	28.00
100	60.5	28.00
101	60.6	28.00
102	60.6	28.00
103	60.7	28.00
104	60.7	28.00
105	60.7	28.00
106	60.7	28.00
107	60.8	28.00
108	60.8	28.00
109	60.9	28.00
110	61.0	28.00
111	61.0	28.00
112	61.0	28.00
113	61.0	28.00
114	61.0	28.00
115	61.1	28.00
116	61.1	28.00
117	61.1	28.00
118	61.1	28.00
119	61.2	28.00
120	61.2	28.00
121	61.2	28.00
122	61.3	28.00
123	61.3	28.00
124	61.3	28.00
125	61.3	28.00
126	61.3	28.00
127	61.3	28.00
128	61.3	28.00
129	61.3	28.00

TABLE 17--Continued

Time (sec)	Temperature °F	Pressure (psig)
130	61.4	28.00
131	61.4	28.00
132	61.5	28.00
133	61.5	28.00
134	61.6	28.00
135	61.6	28.00
136	61.6	28.00
137	61.6	28.00
138	61.6	28.00
139	61.7	28.00
140	61.7	28.00
141	61.7	28.00
142	61.7	28.00
143	61.8	28.00
144	61.8	28.00
145	61.8	28.00
146	61.8	28.00
147	61.9	28.00
148	61.9	28.00
149	61.9	28.00
150	61.98	28.00
151	61.98	26.00
152	61.98	24.5
153	62.0	23.5
154	62.0	22.7
155	62.0	22.1
156	61.7	21.5
157	61.5	21.05
158	61.2	20.70
159	61.0	20.45
160	60.8	20.35
161	60.7	20.30
162	60.5	20.00
163	60.2	19.75
164	60.1	19.65
165	59.8	19.55
166	59.6	19.40
167	59.4	19.35
168	59.2	19.25
169	59.0	19.20
170	58.8	19.10
171	58.6	18.95
172	58.5	18.85
173	58.2	18.80

TABLE 17--Continued

Time (sec)	Temperature °F	Pressure (psig)
174	58.0	18.75
175	57.8	18.70
176	57.6	18.65
177	57.5	18.63
178	57.3	18.60
179	57.1	18.50
180	57.0	18.45
181	56.9	18.40
182	56.8	18.35
183	56.6	18.27
184	56.5	18.20
185	56.3	18.15
186	56.2	18.08
187	56.1	18.00
188	56.0	17.95
189	55.9	17.80
190	55.7	17.75
191	55.6	17.70
192	55.5	17.65
193	55.4	17.63
194	55.3	17.60
195	55.2	17.55
196	55.1	17.53
197	54.9	17.52
198	54.8	17.51
199	54.6	17.50
200	54.4	17.49
201	54.4	17.47
202	54.3	17.46
203	54.2	17.45
204	54.1	17.42
205	54.1	17.40
206	54.0	17.36
207	53.8	17.33
208	53.8	17.30
209	53.7	17.28
210	53.6	17.25
211	53.5	17.23
212	53.5	17.20
213	53.4	17.18
214	53.4	17.15
215	53.3	17.10
216	53.3	17.05
217	53.2	17.00

TABLE 17--Continued

Time (sec)	Temperature °F	Pressure (psig)
218	53.2	16.95
219	53.1	16.90
220	53.1	16.85
221	53.0	16.80
222	52.9	16.75
223	52.9	16.75
224	52.9	16.75
225	52.9	16.70
226	52.8	16.65
227	52.8	16.60
228	52.8	16.55
229	52.7	16.50
230	52.6	16.45
231	52.6	16.40
232	52.6	16.35
233	52.5	16.30
234	52.5	16.25
235	52.5	16.20
236	52.4	16.15
237	52.4	16.10
238	52.3	16.05
239	52.2	16.00
240	52.2	15.90
241	52.2	15.80
242	52.2	15.70
243	52.2	15.60
244	52.2	15.50
245	52.2	15.60
246	52.2	15.50
247	52.1	15.40
248	52.1	15.30
249	52.1	15.20
250	52.1	15.10
251	52.05	15.05
252	52.03	15.00
253	52.02	15.00
254	52.02	15.00
255	52.0	15.00
256	52.0	15.00
257	52.0	15.00
258	52.0	15.00
259	52.0	15.00
260	52.0	15.00
261	52.0	15.00

TABLE 17--Continued

Time (sec)	Temperature °F	Pressure (psig)
262	52.0	15.00
263	52.0	15.00
264	52.0	15.00
265	52.0	15.00
266	52.0	15.00
267	52.0	15.00
268	52.0	15.00
269	52.0	15.00
270	52.0	15.00
271	52.0	15.00
272	52.0	15.00
273	52.0	15.00
274	52.0	15.00
275	52.0	15.00
276	52.0	15.00
277	52.0	15.00
278	52.0	15.00
279	52.0	15.00
280	52.0	15.00
281	52.0	15.00

Inlet water flow rate = 2.338 lbs/min

Inlet water temperature = 80°F

$T_c = mP_c + n$

$m = 1.46$

TABLE 18

PULSE DATA

Time (sec)	Temperature °F	Pressure (psig)
0	51.5	14.5
1	51.5	16.3
2	51.5	17.7
3	51.5	18.6
4	51.5	19.4
5	51.5	20.0
6	51.51	20.4
7	51.58	20.6
8	51.78	20.7
9	51.98	20.85
10	52.16	21.0
11	52.28	21.15
12	52.36	21.20
13	52.54	21.30
14	52.65	21.45
15	52.88	21.55
16	52.95	21.65
17	53.02	21.70
18	53.09	21.85
19	53.16	22.00
20	53.19	22.20
21	53.31	22.25
22	53.44	22.30
23	53.58	22.45
24	53.72	22.60
25	53.85	22.70
26	53.99	22.80
27	54.10	22.90
28	54.20	23.05
29	54.34	23.15
30	54.43	23.30
31	54.55	23.35
32	54.62	23.49
33	54.68	23.60
34	54.75	23.70
35	54.82	23.85
36	54.89	23.95
37	54.90	24.10
38	55.11	24.20
39	55.24	24.33
40	55.38	24.45
41	55.52	24.52

TABLE 18--Continued

Time (sec)	Temperature °F	Pressure (psig)
42	55.57	24.60
43	55.61	24.70
44	55.65	24.85
45	55.75	25.00
46	55.93	25.10
47	56.00	25.25
48	56.08	25.35
49	56.17	25.48
50	56.21	25.55
51	56.25	25.65
52	56.35	25.74
53	56.41	25.85
54	56.41	25.90
55	56.54	25.95
56	56.62	26.05
57	56.66	26.10
58	56.72	26.15
59	56.76	26.25
60	56.79	26.30
61	56.91	26.40
62	57.00	26.45
63	57.11	26.50
64	57.18	26.60
65	57.32	26.65
66	57.38	26.70
67	57.45	26.75
68	57.51	26.80
69	57.55	26.85
70	57.60	26.88
71	57.61	26.90
72	57.68	26.95
73	57.73	27.00
74	57.84	27.05
75	57.87	27.10
76	57.90	27.15
77	58.01	27.20
78	58.06	27.25
79	58.12	27.30
80	58.16	27.35
81	58.17	27.40
82	58.22	27.45
83	58.26	27.50
84	58.28	27.55
85	58.37	27.60

TABLE 18--Continued

Time (sec)	Temperature °F	Pressure (psig)
86	58.42	27.70
87	58.48	27.75
88	58.52	27.80
89	58.56	27.85
90	58.59	27.90
91	58.63	27.92
92	58.66	27.95
93	58.70	27.97
94	58.73	27.99
95	58.84	28.0
96	58.90	28.0
97	58.95	28.0
98	58.98	28.0
99	59.00	28.0
100	59.05	28.0
101	59.12	28.0
102	59.14	28.0
103	59.17	28.0
104	59.20	28.0
105	59.23	28.0
106	59.33	28.0
107	59.39	28.0
108	59.41	28.0
109	59.48	28.0
110	59.50	28.0
111	59.53	28.0
112	59.56	28.0
113	59.57	28.0
114	59.59	28.0
115	59.60	28.0
116	59.63	28.0
117	59.67	28.0
118	59.70	28.0
119	59.72	28.0
120	59.74	28.0
121	59.77	28.0
122	59.81	28.0
123	59.86	28.0
124	59.92	28.0
125	60.0	28.0
126	60.03	28.0
127	60.04	28.0
128	60.06	28.0
129	60.07	28.0

TABLE 18--Continued

Time (sec)	Temperature °F	Pressure (psig)
130	60.08	28.0
131	60.10	28.0
132	60.17	28.0
133	60.22	28.0
134	60.33	28.0
135	60.36	28.0
136	60.38	28.0
137	60.39	28.0
138	60.42	28.0
139	60.44	28.0
140	60.50	28.0
141	60.57	28.0
142	60.58	28.0
143	60.60	28.0
144	60.61	28.0
145	60.64	28.0
146	60.65	28.0
147	60.67	28.0
148	60.68	28.0
149	60.69	28.0
150	60.71	28.0
151	60.72	28.0
152	60.75	28.0
153	60.78	28.0
154	60.85	28.0
155	60.93	28.0
156	60.94	28.0
157	60.96	28.0
158	60.96	28.0
159	60.97	28.0
160	60.98	28.0
161	61.00	27.20
162	61.00	26.25
163	61.0	25.40
164	61.0	24.50
165	61.0	23.70
166	61.0	23.00
167	60.92	22.35
168	60.78	21.70
169	60.39	21.20
170	60.36	20.55
171	60.22	20.20
172	59.95	19.75
173	59.81	19.40

TABLE 18--Continued

Time (sec)	Temperature °F	Pressure (psig)
174	59.60	19.20
175	59.42	19.00
176	59.22	18.80
177	59.12	18.65
178	58.95	18.49
179	58.78	18.40
180	58.63	18.25
181	58.52	17.99
182	58.35	17.80
183	58.17	17.70
184	58.01	17.60
185	57.90	17.55
186	57.84	17.50
187	57.73	17.48
188	57.56	17.45
189	57.39	17.40
190	57.32	17.30
191	57.14	17.25
192	56.98	17.20
193	56.90	17.15
194	56.76	17.12
195	56.62	17.10
196	56.48	17.05
197	56.35	17.00
198	56.21	16.95
199	56.07	16.90
200	56.04	16.87
201	55.86	16.85
202	55.72	16.80
203	55.65	16.75
204	55.52	16.70
205	55.38	16.65
206	55.27	16.60
207	55.13	16.50
208	55.07	16.40
209	54.99	16.35
210	54.96	16.30
211	54.89	16.25
212	54.68	16.20
213	54.60	16.15
214	54.55	16.10
215	54.49	16.08
216	54.35	16.06
217	54.27	16.02

TABLE 18--Continued

Time (sec)	Temperature °F	Pressure (psig)
218	54.16	16.00
219	54.06	15.98
220	53.99	15.94
221	53.94	15.90
222	53.83	15.86
223	53.77	15.84
224	53.72	15.80
225	53.65	15.76
226	53.58	15.72
227	53.51	15.68
228	53.47	15.64
229	53.44	15.60
230	53.30	15.56
231	53.22	15.52
232	53.19	15.48
233	53.16	15.44
234	53.09	15.40
235	53.02	15.38
236	52.98	15.36
237	52.94	15.33
238	52.88	15.30
239	52.82	15.27
240	52.75	15.24
241	52.64	15.20
242	52.62	15.18
243	52.61	15.15
244	52.58	15.13
245	52.47	15.10
246	52.40	15.08
247	52.39	15.06
248	52.36	15.03
249	52.34	15.00
250	52.33	14.96
251	52.30	14.92
252	52.26	14.90
253	52.22	14.86
254	52.19	14.83
255	52.12	14.80
256	52.11	14.75
257	52.10	14.72
258	52.08	14.70
259	52.07	14.68
260	52.05	14.65
261	51.98	14.62

TABLE 18--Continued

Time (sec)	Temperature °F	Pressure (psig)
262	51.93	14.60
263	51.87	14.58
264	51.85	14.57
265	51.80	14.56
266	51.78	14.54
267	51.75	14.52
268	51.74	14.51
269	51.72	14.50
270	51.64	14.50
271	51.58	14.50
272	51.56	14.50
273	51.53	14.50
274	51.51	14.50
275	51.50	14.50
276	51.50	14.50
277	51.50	14.50
278	51.50	14.50
279	51.50	14.50
280	51.50	14.50
281	51.50	14.50

Inlet water flow rate = 3.49 lbs/min

Inlet water temperature = 83°F

$T_c = mP_c + n$

$m = 1.46$

TABLE 19

FREQUENCY RESPONSE VALUES OBTAINED FROM TRANSFORMED PULSE RESPONSE DATA

Inlet water flow rate = 2.338 lbs/min
Inlet water temperature = 80°F

Frequency (rad/min)	Amplitude Ratio	Phase Angle (degrees)
0.312	0.647	-8.3
0.441	0.643	-11.4
0.624	0.640	-16.3
0.883	0.631	-23.5
1.248	0.612	-34.6
1.765	0.514	-54.1
2.496	0.363	-60.0
3.530	0.246	-66.8
4.992	0.190	-67.8
7.062	0.132	-87.5
9.984	0.105	-95.9
14.12	0.0895	-131.0

Inlet water flow rate = 3.49 lbs/min
Inlet water temperature = 83°F

Frequency (rad/min)	Amplitude Ratio	Phase Angle (degrees)
0.312	0.66	-5.7
0.624	0.67	-11.8
1.248	0.71	-17.6
2.496	0.56	-35.5
4.992	0.32	-77.8
19.97	0.078	-120.6

TABLE 20

THEORETICAL FREQUENCY RESPONSE VALUES

Inlet water flow rate = 2.338 lbs/min
Inlet water temperature = 80°F
m = 1.46

Frequency (rad/min)	Amplitude Ratio	Phase Angle (degrees)	Phase Angle + 6 sec. of dead time (degrees)
0.312	0.690	-9.4	-11.1
0.441	0.668	-13.2	-13.7
0.624	0.665	-18.4	-22.0
0.883	0.633	-24.6	-29.7
1.248	0.584	-33.5	-40.7
1.765	0.518	-43.2	-53.3
2.496	0.423	-53.2	-67.5
3.530	0.330	-62.0	-82.2
4.992	0.243	-69.4	-98.0
7.062	0.180	-75.1	-115.6
9.984	0.130	-79.3	-136.5
14.12	0.093	-82.4	-162.3
19.97	0.065	-84.5	-199.0
28.24	0.046	-86.2	-248.1

TABLE 20--Continued

Inlet water flow rate = 3.49 lbs/min
Inlet water temperature = 83°F
m = 1.46

Frequency (rad/min)	Amplitude Ratio	Phase Angle (degrees)	Phase Angle + 6 sec. of dead time (degrees)
0.312	0.708	-6.2	-7.9
0.441	0.703	-8.6	-9.1
0.624	0.693	-12.2	-15.8
0.883	0.679	-17.0	-22.1
1.248	0.622	-23.3	-30.5
1.765	0.605	-31.4	-41.5
2.496	0.535	-40.9	-55.2
3.530	0.447	-50.3	-70.5
4.992	0.350	-60.0	-88.6
7.062	0.271	-67.8	-108.3
9.982	0.193	-73.9	-131.1
14.12	0.140	-78.4	-159.3
19.97	0.099	-81.1	-195.6
28.24	0.071	-84.2	-246.1

APPENDIX C

Miscellaneous Data

TABLE 21

OPERATING CONDITIONS

Inlet Temperature T_i	Coolant Temperature T_c	Maximum Variation in Fluid Temperature T_{max}	Steady State Fluid Temperature T_s	Steady State Flow Rate W_s (lbs/min)	Minimum Flow Rate W_{min} (lbs/min)	Maximum Flow Rate W_{max} (lbs/min)	Amplitude of Varying Flow Rate (lbs/min)
113.5°F	38.0°F	2.0°F	99.8°F	5.44	4.97	5.92	0.475
113.5	38.0	3.96	99.8	5.44	4.50	6.38	0.94
113.5	38.0	5.4	99.8	5.44	4.026	6.86	1.42
113.5	38.0	8.1	99.8	5.44	3.55	7.33	1.89
113.5	38.0	11.2	99.8	5.44	3.078	7.806	2.364

MISCELLANEOUS DATA

C_p of water = 1.0 BTU/lb-°F

ρ = 62.4 lb/ft^3

V = 0.03724 ft^3

UA(BTU/min-°F) varies and was calculated from steady state operating conditions.

TABLE 22

FREQUENCIES CORRESPONDING TO CAPACITANCE VALUES FOR THE ANALOG SIMULATION USED IN THE FREQUENCY RESPONSE STUDIES

Frequencies Cycles/minute	b_1	Capacitance $1/b_1$ Microfarads
0.05	1200	0.01735
0.10	600	0.0347
0.20	300	0.0694
0.30	200	0.1041
0.50	120	0.1730
0.70	85	0.2780
1.00	60	0.3470
1.25	48	0.434
1.50	40	0.522
1.75	34.3	0.608
2.00	30.0	0.695
2.25	25.6	0.814
2.50	24.0	0.869
2.75	21.8	0.956
3.00	20.0	1.041
3.25	18.45	1.130
3.50	17.15	1.215
2.75	16.0	1.302
4.00	15.0	1.388
5.00	12.0	1.73
7.00	8.5	2.78
10.00	6.0	3.47
20.00	3.0	6.94

TABLE 23

OUTPUT ANALOG COMPUTER VALUES
SHOWN IN FIGURE 18

Time (minutes)	Temperature Scale (CM.)	Temperature Variation from Steady State (°F)
0.0	5.2	0.8
2.5	7.6	3.2
5.0	8.37	3.97
7.5	8.0	3.60
10.0	6.0	1.60
12.5	2.8	-1.60
15.0	0.7	-3.70
17.5	2.0	-2.40
20.0	5.2	0.80

1 CM on temperature scale = 1 degree Fahrenheit

0 °F variation = 4.4 CM

APPENDIX D

Bode Plots

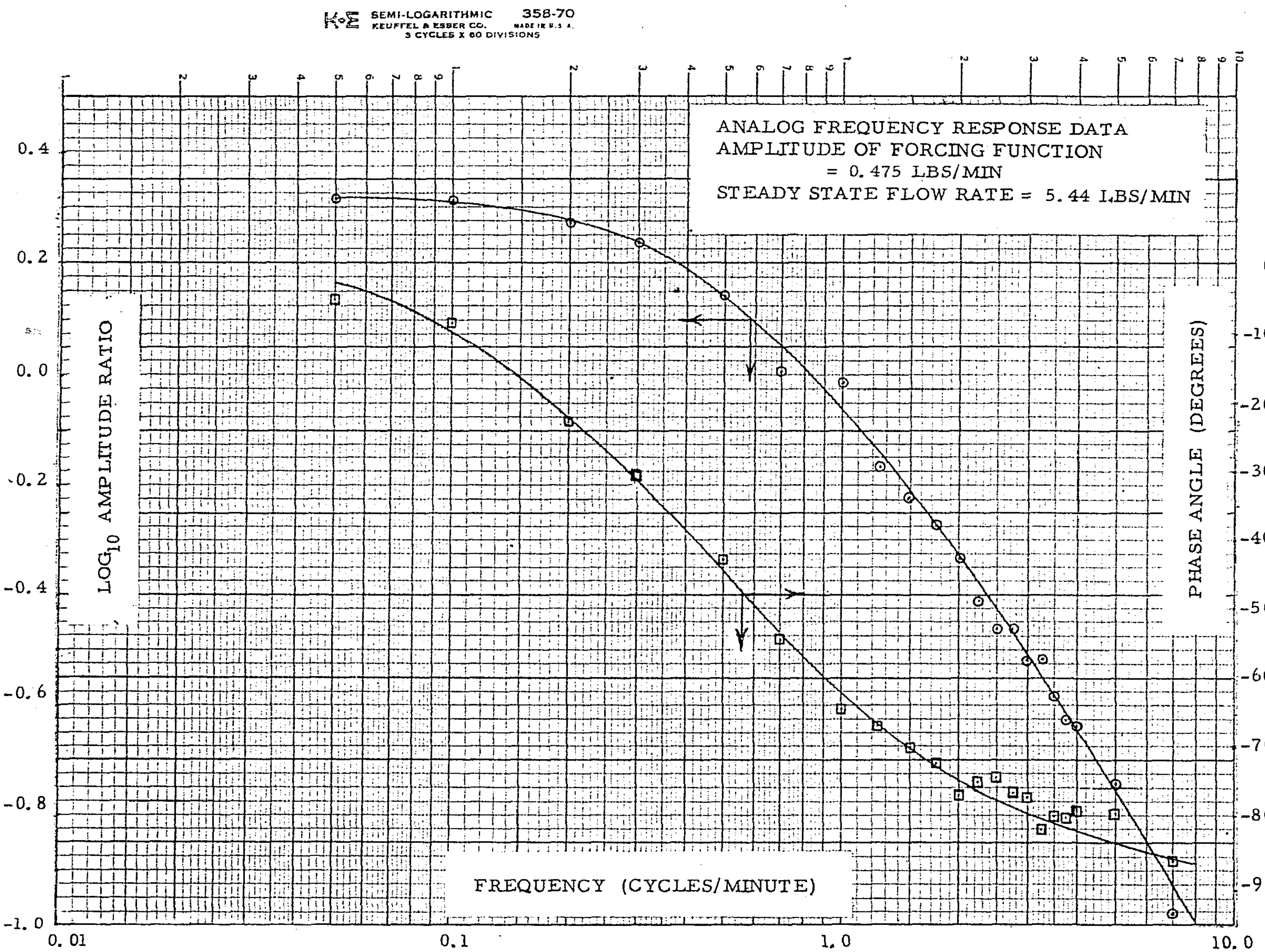

Figure 24. Bode Plot of Analog Frequency Response Data

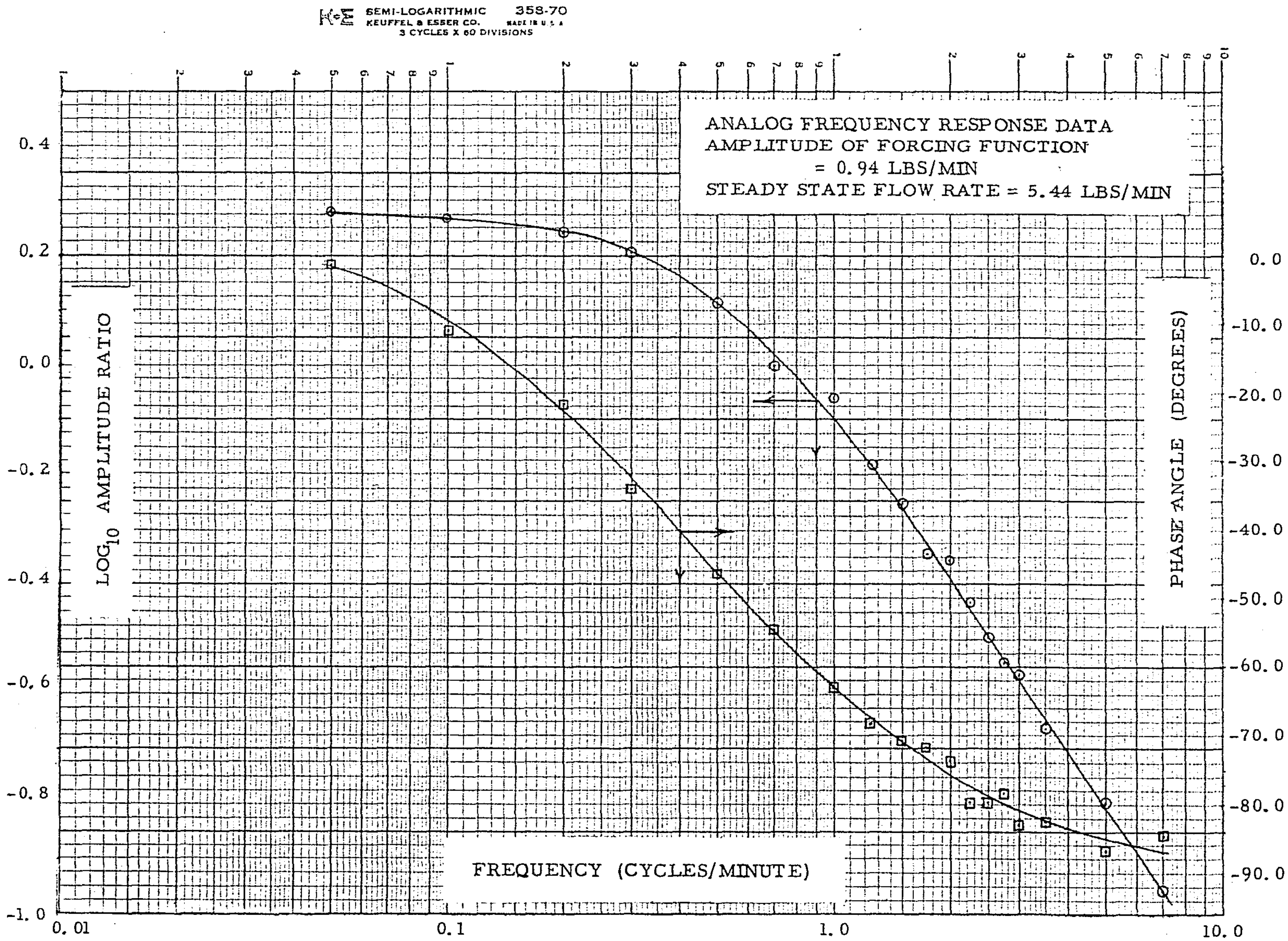

Figure 25. Bode Plot of Analog Frequency Response Data

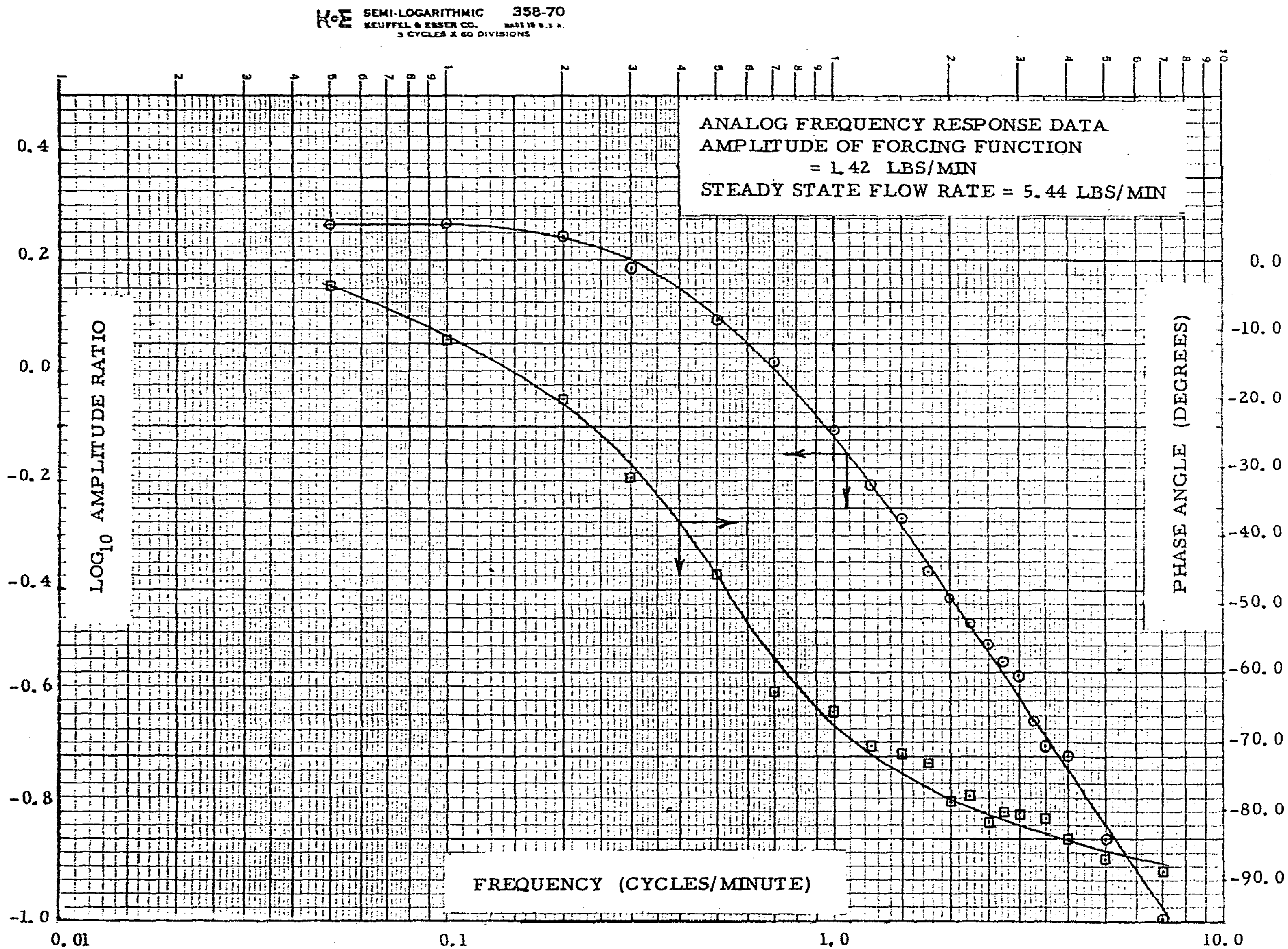

Figure 26. Bode Plot of Analog Frequency Response Data

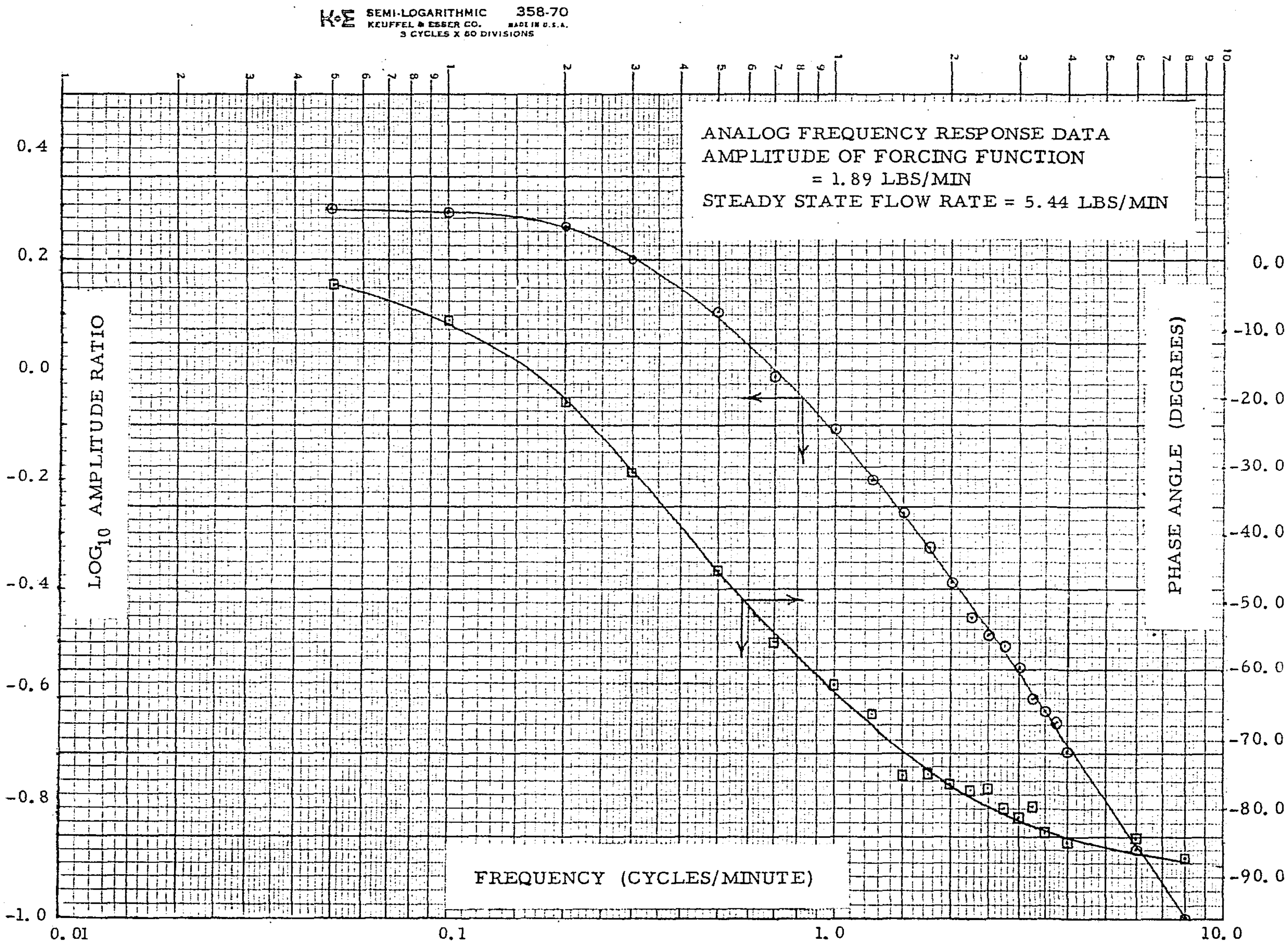

Figure 27. Bode Plot of Analog Frequency Response Data

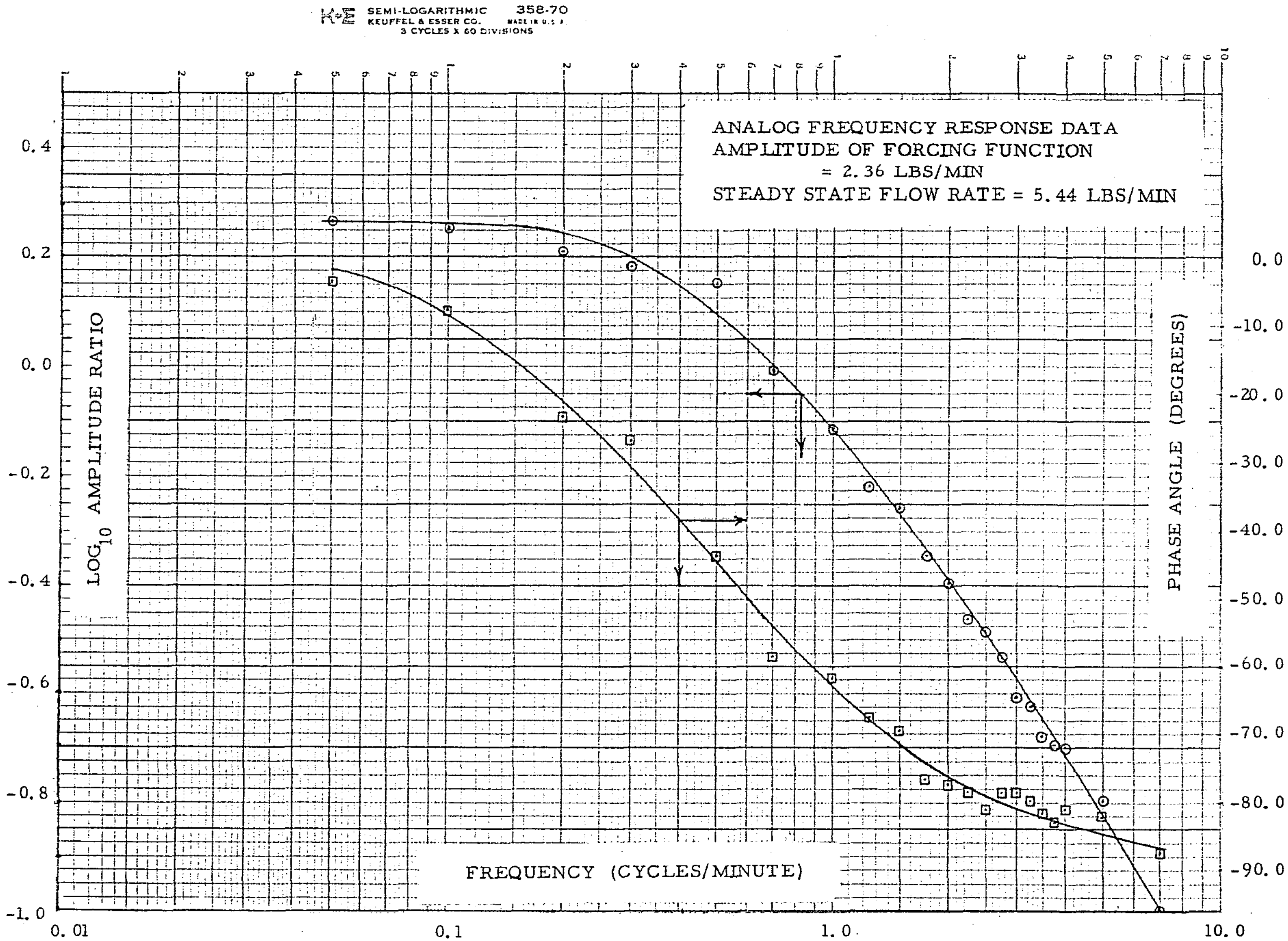

Figure 28. Bode Plot of Analog Frequency Response Data

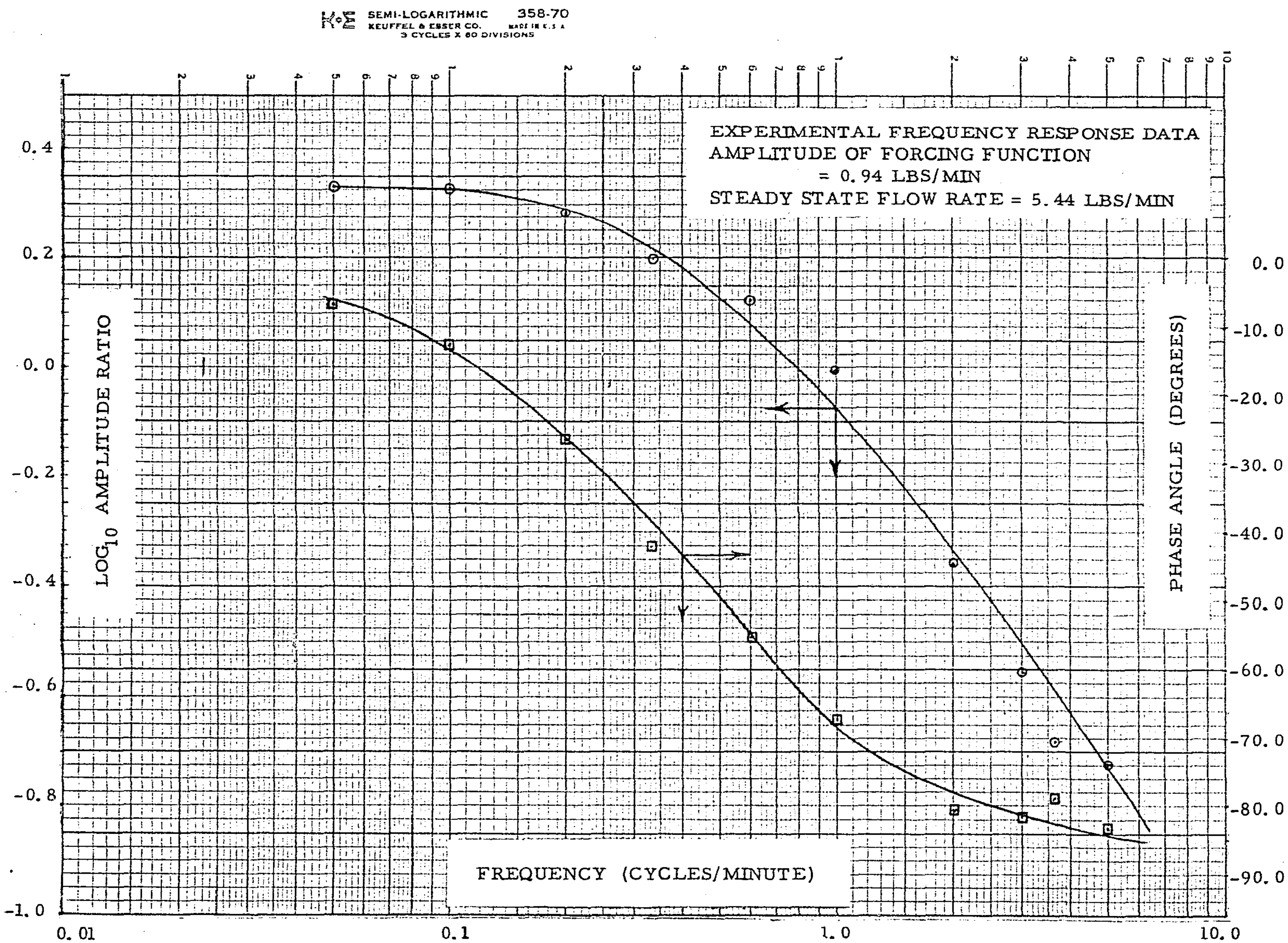

Figure 29. Bode Plot of Experimental Frequency Response Data

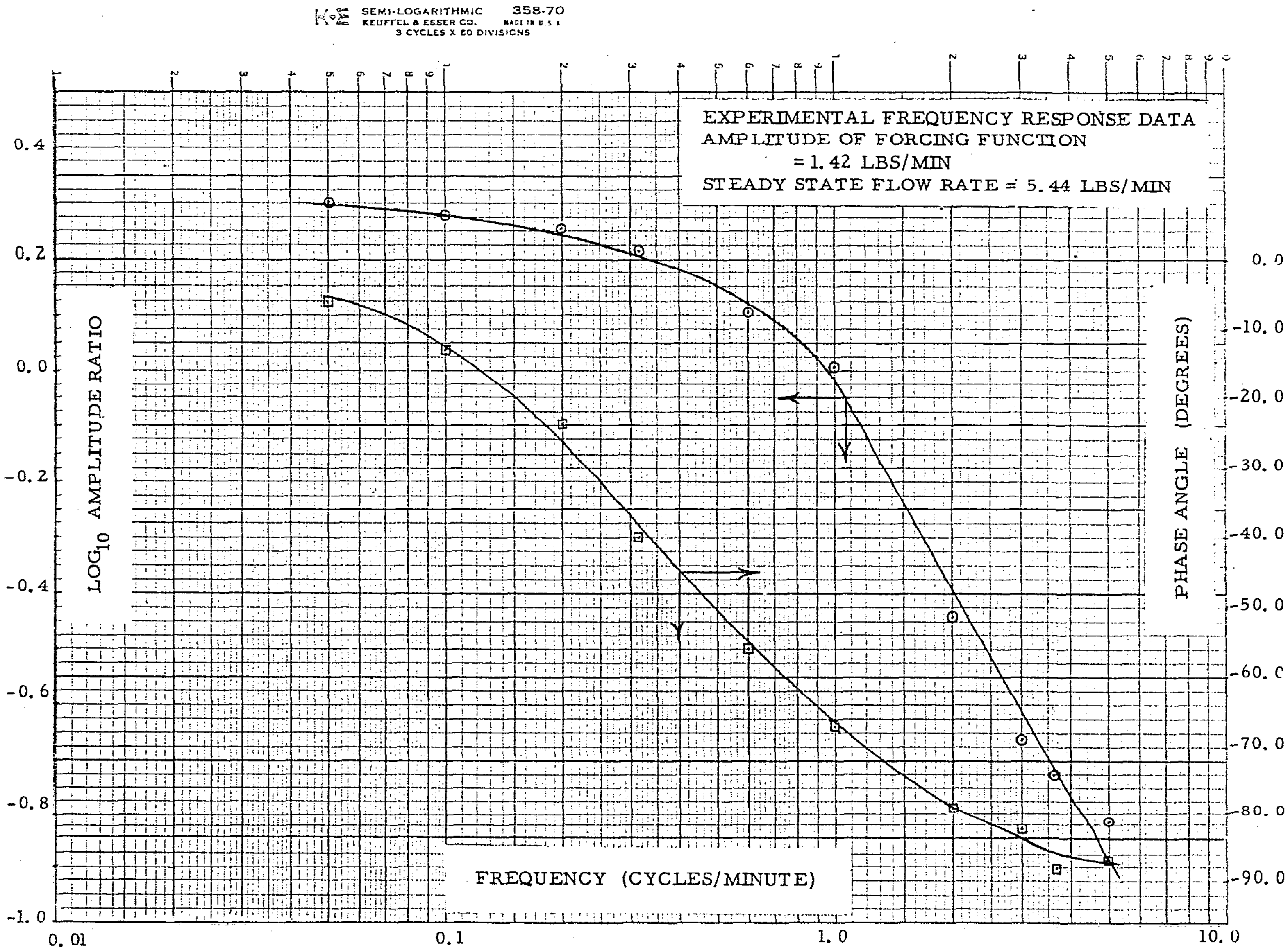

Figure 30. Bode Plot of Experimental Frequency Response Data

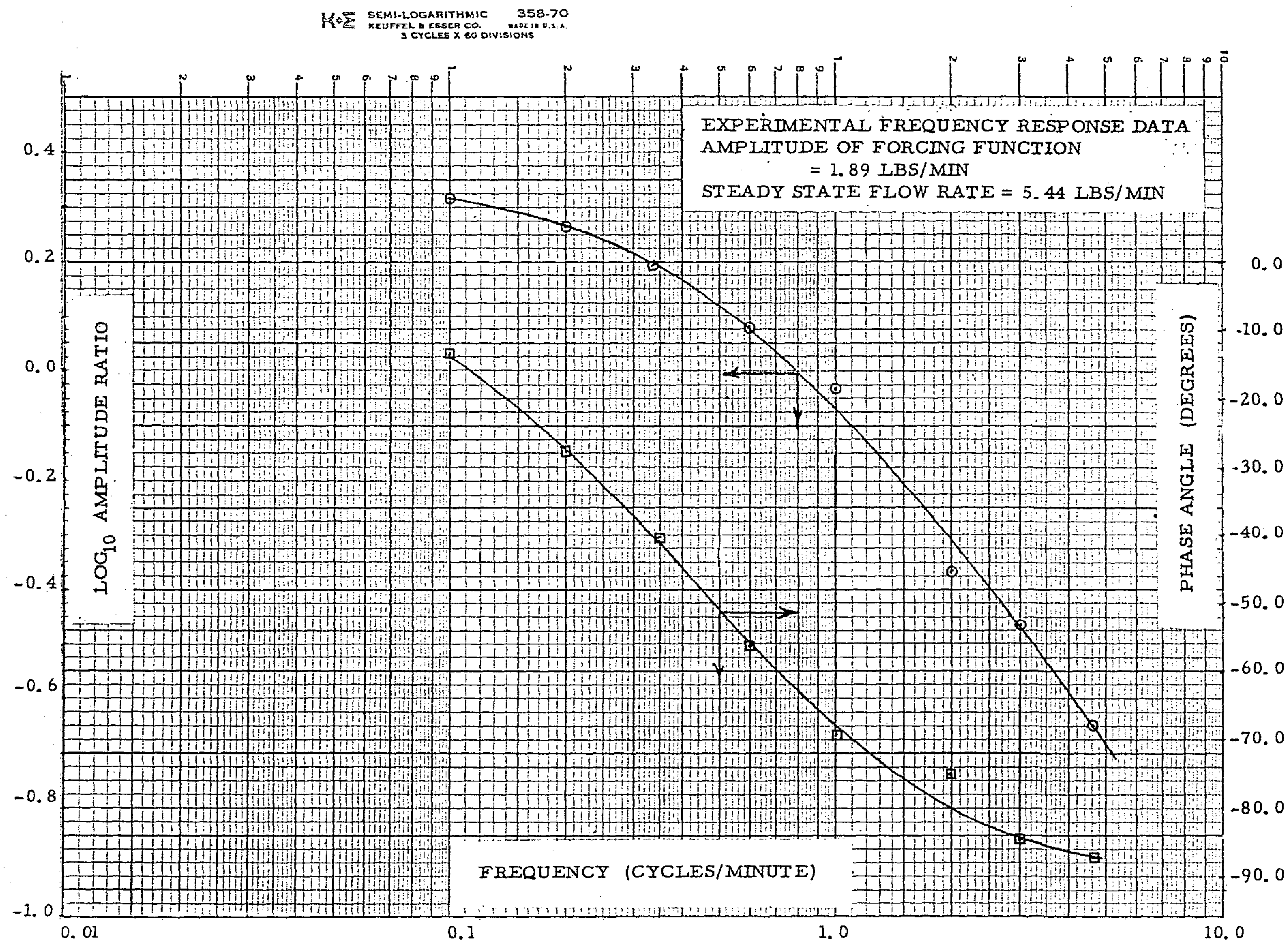

Figure 31. Bode Plot of Experimental Frequency Response Data